RESEARCH REPORT DOCUMENTATION PAGE

1. Report No.	2. Report Date	3. Contract No.	4. Project No.
NDSU 2017-01	July 2019	91171289 / 91171289A	

5. Title and Subtitle	6. Report Type	7. Project No.
Snow-Proof Marking System through Electrically Conductive Fly Ash-Based Geopolymer Mortar / Concrete	Work Plan ☐ Construction ☐ Evaluation ☐ **Final** ☒	8. Project No. 9. Project No. 10. Project No.

11. Author(s)/Principle Investigator(s)
Mijia Yang, Zhibin Lin, Shree Paudel

12. Performing Organization Name and Address	13. Sponsoring Agency Name and Address
NDDOT M+R ☐ NDDOT OTHER* ☐ NDSU ☒ UND ☐ UGPTI ☐ OTHER* ☐ *see supplementary notes North Dakota State University Department of Civil and Environmental Engineering Fargo, ND 58102	North Dakota DOT Materials and Research Division 300 Airport Road Bismarck ND 58504-6005

14. Supplementary Notes

15. Abstract

Purpose and Need
During winter weather conditions, highway pavement markings become snow-covered and create hazards to the traveling public. The resulting life and property losses could be mitigated by a system which could redisplay these marking using snow-melting techniques. The objective of this TRIP project is to develop a snow-proof pavement marking system through electrically conductive fly ash-based geopolymer concrete.

Objective
The objective of this research was to evaluate the feasibility of utilizing geopolymer concrete for heat transfer in order to eliminate snow on the surface of pavement markings.

Summary
The test results of this research show that the geopolymer concrete with incorporated steel fibers proves to be a viable option to conduct electricity and transfer heat to create a snow-proof pavement marking system. The high cost of this system is restrictive to its implementation compared to conventional markings. Also, workability concerns regarding the high early strength and low air-entrainment could be encountered in field applications and pose additional challenges.

16. Key Words	17. Distribution Statement	18. No. of Pages
Snow-Proof, Conductive, Geopolymer Concrete	No restrictions. This document is available from: North Dakota Department of Transportation Materials and Research Division: 300 Airport Road Bismarck ND 58504-6005 Office: (701) 328-6900 Fax: (701) 328-0310	75

SNOW PROOF MARKING SYSTEM THROUGH ELECTRICALLY CONDUCTIVE FLY ASH BASED GEOPOLYMER MORTAR/CONCRETE

ND Department of Transportation
Transportation Innovative Research Program

Final Report

Prepared for
North Dakota Department of Transportation

Prepared by
Mijia Yang, Associate Professor
Zhibin Lin, Assistant Professor
Shree Paudel, Research Assistant

Department of Civil and Environmental Engineering
North Dakota State University
Fargo, North Dakota

February 2019

Acknowledgement

We would like to thank NDDOT for the support to the project. We also thank the NDDOT project committee members for their valuable guidance and support during the course of conducting the research.

The contents are solely written based on the detailed experiment and calculation performed by the research team, which do not necessarily reflect the official views of the NDDOT or North Dakota State University at the time of publication.

Disclaimer

The contents of this report reflect the work of the authors, who are responsible for the facts and the accuracy of the information presented.

Table of Contents

Acknowledgement 2
Executive Summary 9
Chapter 1. Introduction 10
1.1 Project background and purpose 10
1.2 Literature review 10
1.3 Report organization 11
Chapter 2. Strength and Stiffness of Fly-ash Geopolymer Concrete and Its Mix Design 12
2.1 Mix of fly-ash geopolymer concrete 12
2.2 Specimen preparation 13
2.3 Strength and stiffness of fly-ash geopolymer concrete 15
2.3.1) Mix FGM1.0-3010.5: 16
2.3.2) Mix FGM1.2-30101: 16
2.3.3) Mix FGM1.2-30101.5: 18
2.3.4) Mix FGM1.4-3010.5: 19
2.3.5) Mix FGM1.4-30101: 20
2.3.6) Mix FGM1.4-30101.5: 21
2.3.7) Mix FGM1.4-3010.5: 22
2.3.8) Mix FGM1.0-30101: 23
2.3.9) Mix FGM1.2-30101.5: 24
2.3.10) Mix FGM1.4-301000: 25
Chapter 3. Strength and Stiffness of Geopolymer Mortar and Concrete with Elevated Curing 26
3.1 Stiffness and strength of fiber reinforced geopolymer mortar 26
3.1.1) 0.5% fibers content: 27
3.1.2) 1% fibers content: 29
3.1.3) 1.5% fibers content: 31
3.2 Stiffness and compressive strength of geopolymer concrete 33
3.2.1) 0.5% fiber content: 35
3.2.2) 1% fiber content: 35
3.2.3) 1.5% fiber content: 36
Chapter 4. Conductivity of Geopolymer Concrete Materials 37
4.1 Resistivity of geopolymer mortar 37

4.1.1) 0.5% fibers content: 38
4.1.2) 1.0% fibers content: 39
4.1.3) 1.5% fibers content: 40
4.2 Resistivity measurement of geopolymer concrete 40
4.2.1) 0.5% fiber content: 41
4.2.2) 1% fiber content: 42
4.2.3) 1.5 % fiber content: 43
Chapter 5. Freeze-thaw Test of the Suggested Geopolymer Concrete 44
5.1 Relative dynamic modulus of elasticity 45
5.2 Mass loss 46
Chapter 6. Pull-off Adhesion Test 48
Chapter 7. Maturity Test 50
7.1 Concrete cylinder maturity test 50
7.2 Concrete beam maturity test 51
Chapter 8. Air Content Test 53
Chapter 9. Conductivity of the Suggested System when Cracking 54
9.1 Resistivity measurement of longitudinally cracked specimens 54
9.1.1) 0.5% fiber content: 54
9.1.2) 1.0% fiber content 54
9.1.3) 1.5% fiber content 55
9.2 Resistivity measurement of transversely cracked specimens 55
9.2.1) 0.5% fiber content 55
9.2.2) 1.0% fiber content 56
9.2.3) 1.5% fiber content 56
Chapter 10. Melting Test for Marking Reveals Under Controlled Temperatures 57
Chapter 11. Alternative Power Sources and Cost-effectiveness Analysis of the Suggested Snow-Proof Marking System 66
Chapter 12. Conclusions and Future Research Needs 70
12.1 Project conclusions 70
12.2 Future research needs 72
References: 73

List of tables:

Table 1 Fly ash-based geopolymer mortar mix proportion 13
Table 2 Modified mix design for mix-2 in Table 1 with different fiber percentages and curing conditions 26
Table 3 Mix design for geopolymer concrete specimens 33
Table 4 Bond Strength between painted dolly and concrete surface 48
Table 5 Mix design used for snow melting test 57
Table 6 Energy and time required to melt 0.5 inch, 1 inch and 1.5 inch of snow at -20 °C 59
Table 7 Energy and time required to melt 0.5 inch, 1 inch and 1.5 inch of snow at -15 °C 60
Table 8 Energy and time required to melt 0.5 inch, 1 inch and 1.5 inch of snow at -10 °C 61
Table 9 Cost-Effectiveness Analysis Per 100 Feet Markings 66

List of figures:

Figure 1 Specimen notation 13
Figure 2 Mixing, molding and demolding 14
Figure 3 MTS machine (a) and test scheme (b) 15
Figure 4 Load displacement curve of mix FGM1.0-3010.5 (a) 1 day, (b) 3 day, (c) 14 day, and (d) 28 day 16
Figure 5 Stiffness and Strength versus time of Mix FGM1.0-3010.5 16
Figure 6 Load displacement curve of mix FGM1.2-30101 (a) 1 day, (b) 3 day, (c) 14 day, and (d) 28 day 17
Figure 7 Stiffness and strength versus time of Mix FGM1.2-30101 17
Figure 8 Load displacement curve of mix FGM1.2-30101.5 (a) 1 day, (b) 3 day, (c) 14 day, and (d) 28 day 18
Figure 9 Stiffness and strength versus time of Mix FGM1.2-30101.5 18
Figure 10 Load displacement curve of mix FGM1.4-3510.5 (a) 1 day, (b) 3 day, (c) 14 day, and (d) 28 day 19
Figure 11 Stiffness and strength versus time of Mix FGM1.4-3510.5 19
Figure 12 Load displacement curve of mix FGM1.4-40101 (a) 1 day, (b) 3 day, (c) 14 day, and (d) 28 day 20
Figure 13 Stiffness and strength versus time of Mix FGM1.4-40101 20
Figure 14 Load displacement curve of mix FGM1.4-45101.5 (a) 1 day, (b) 3 day, (c) 14 day, and (d) 28 day 21
Figure 15 Stiffness and strength versus time of Mix FGM1.4-45101.5 21
Figure 16 Load displacement curve of mix FGM1.4-5010.5 (a) 1 day, (b) 3 day, (c) 14 day, and (d) 28 day 22
.Figure 17 Stiffness and strength versus time of Mix FGM1.4-5010.5 22
Figure 18 Load displacement curve of mix FGM1.0-30101. (a) 1 day, (b) 3 day, (c) 14 day, and (d) 28 day 23
Figure 19 Stiffness and strength versus time of Mix FGM1.0-30101 23
Figure 20 Load displacement curve of mix FGM1.2-30101.5 (a) 1 day, (b) 3 day, (c) 14 day, and (d) 28 24
Figure 21 Stiffness and strength versus time of Mix FGM1.2-30101.5 24
Figure 22 Load displacement curve of mix FGM1.4-301000. (a) 1 day, (b) 3 day, (c) 14 day, and (d) 28 25
Figure 23 Stiffness and strength versus time of Mix FGM1.4-301000 25
Figure 24 Specimen notation for stiffness, strength and resistivity measurement of geopolymer mortars 27
Figure 25 Load displacement curve of mix FGM1.2-0.5. (a) 1 day, (b) 7 day, (c) 14 day, and (d) 28 27
Figure 26 Stiffness (Ksi) versus time of Mix FGM1.2-0.5 28
Figure 27 Strength versus time of Mix FGM1.2-0.5 28
Figure 28 Load displacement curve of mix FGM1.2-1.0. (a) 1 day, (b) 7 day, (c) 14 day, and (d) 28 29
Figure 29 Stiffness (Ksi) versus time of Mix FGM1.2-1.0 30
Figure 30 Strength versus time of Mix FGM1.2-1.0 30
Figure 31 Load displacement curve of mix FGM1.2-1.5. (a) 1 day, (b) 7 day, (c) 14 day, and (d) 28 31
Figure 32 Stiffness (Ksi) versus time of Mix FGM1.2-1.5 32
Figure 33 Strength versus time of Mix FGM1.2-1.5 32
Figure 34 Specimen notation for stiffness, strength and resistivity measurement of geopolymer concrete. 33

Figure 35 Compressive strength testing scheme (a) and Specimen after failure (b)..... 34
Figure 36 Compressive strength of geopolymer concrete mix FGC1.2-0.5 at different curing temperatures 35
Figure 37 Compressive strength of geopolymer concrete mix FGC1.2-1.0 at different curing temperatures 35
Figure 38 Compressive strength of geopolymer concrete mix FGC1.2-1.5 at different curing temperatures 36
Figure 39 Electrical circuit used for resistivity measurement of mortar samples..... 37
Figure 40 (a) Sample used for resistivity resting (b) Resistivity testing setup 38
Figure 41 Resistivity of mix FGM1.2-0.5. (a) 14 days, and (b) 28 days 38
Figure 42 Resistivity of mix FGM1.2-1.0. (a) 14 days, and (b) 28 days 39
Figure 43 Resistivity of mix FGM1.2-1.5. (a) 14 days, and (b) 28 days 40
Figure 44 (a) Sample used for resistivity resting (b) Resistivity testing instrument setup 41
Figure 45 Resistivity of mix FGC1.2-0.5. (a) 14 days, and (b) 28 days 41
Figure 46 Resistivity of mix FGC1.2-1.0. (a) 14 days, and (b) 28 days 42
Figure 47 Resistivity of mix FGC1.2-1.5. (a) 14 days, and (b) 28 days 43
Figure 48 Freeze-thaw chamber (a) and testing scheme of concrete specimen (b) 44
Figure 49 Variation of relative dynamic elasticity modulus with the number of freeze-thaw cycles. (a) Longitudinal (b) Transverse (c) Torsional direction testing 46
Figure 50 Variation of mass loss (%) with the number of freeze-thaw cycles. 46
Figure 51 Placing dolly on painted concrete surface (a) and testing instrument set up (b) 49
Figure 52 Dollies after pull-off adhesion test; (a) OPC based concrete and (b) Geopolymer concrete..... 49
Figure 53 Testing set up for real time maturity measurement 50
Figure 54 Relationship between compressive strength and the temperature-time factor for different percentage of fiber inclusions, (a) 0%, (b) 0.5%, (c) 1%, and (d) 1.5% steel fiber. 51
Figure 55 Relationship between flexural strength and temperature-time factor, (a) 0.5%, and (b) 1.5%, steel fiber..... 51
Figure 56 Air content measurement of the fresh geopolymer concrete per ASTM 321, (a) Fill the container of the air meter, (b) Air content measurement result after pressure releasing 53
Figure 57 Resistivity measurement of specimens with longitudinal crack (a) and transverse crack (b) 54
Figure 58 Resistivity of mix longitudinally cracked specimen with 0.5% steel fiber (a) 14 days, and (b) 28 days 54
Figure 59 Resistivity of mix longitudinally cracked specimen with 1.0% steel fiber (a) 14 days, and (b) 28 days 55
Figure 60 Resistivity of mix longitudinally cracked specimen with 1.5% steel fiber (a) 14 days, and (b) 28 days 55
Figure 61 Resistivity of mix transversely cracked specimen with 0.5% steel fiber (a) 14 days, and (b) 28 days 55
Figure 62 Resistivity of mix transversely cracked specimen with 1.0% steel fiber (a) 14 days, and (b) 28 days 56
Figure 63 Resistivity of mix transversely cracked specimen with 1.5% steel fiber (a) 14 days, and (b) 28 days 56
Figure 64 Energy meter (a) and circuit diagram (b) used for the melting test experiment..... 58
Figure 65 Beam specimen (a) and Epoxy based Painted beam specimen to mimic the road pavement (b)58

Figure 66 Melting process of Specimen with 1.5 % fiber content for 1 inch heavy snow at -15°C (a) Initial condition, (b) after 30 minutes, (c) after 1 hour, and (d) after 1 hour 10 minutes 62
Figure 67 Melting process of Specimen with 1% fiber content for 1 inch fluffy snow at -15°C (a) Initial condition, (b) after 15 minutes, (c) after 30 minutes, and (d) after 1 hour 20 minutes 63
Figure 68 Melting process of Specimen with 1% fiber content for 1.5 inch fluffy snow at -20°C (a) Initial condition, (b) after 1 hour, (c) after 2 hours, and (d) after 2 hours 15 minutes 64
Figure 69 Melting process of Specimen with 1.5 % fiber content for 1.5 inch fluffy snow at -20°C (a) Initial condition, (b) after 40 minutes, (c) after 1 hour 20 minutes, and (d) after 1 hour 35 minutes 65
Figure 70 Customized Power Conversion and Storage System through Solar Panels..... 66

Executive Summary

Project Background

NDDOT is interested in pavement marking reveal in winter times. Even though there are some documents in literature on conductive concrete and its application in snow and ice melting, it is the first time to develop a conductive fly ash geopolymer concrete for pavement marking reveal.

What the Researchers Did

Researchers utilized the fly ash waste in North Dakota and performed a systematic study on compressive, flexural strength of the geopolymer concrete formed with and without steel fiber inclusions and found a suitable mix for pavement implementation. Based on the selected mix design, the research team also performed series tests on effect of curing conditions, freeze and thaw resistance of the new material, electrical conductivity, its strength monitoring through maturity tests, and effect of cracks on the performance of the geopolymer concrete in terms of its electrical conductivity. Finally the research team conducted a mimic marking reveal testing in a temperature controlled environment, and revealed the marking in an excellent time period with reasonable energy consumption.

What They Found

Researchers found a suitable conductive steel fiber reinforced geopolymer concrete. The developed new material has excellent electrical conductivity and long-term durability and could reveal markings in a timely and cost-effective fashion.

What This Means

Based upon findings from the study and guidance from the Project Advisory Committee, the research team recommends implementing the outcomes through a 2nd phase of the project. The extension of the project could look into the following issues and make it ready for adoption of the material in NDDOT:

A. Effect of marking patching sizes on the long-term overall performance of pavements.

B. Cost effectiveness of extending the conductive steel fiber reinforced geopolymer concrete to the whole pavement surface.

C. Wear resistance of the suggested steel fiber reinforced geopolymer concrete under traffic.

Chapter 1. Introduction

1.1 Project background and purpose

When snow covers highways, highway markings are buried and invisible to drivers, which has caused many travel accidents, including property and life losses. A highway that could melt the snow and redisplay disappeared markings could solve this problem. Based on this idea, the objective of the NDDOT TRIP project is to develop a snow-proofing marking system through electrically conductive fly ash geopolymer concrete.

The electrically conductive geopolymer concrete will be adopted either as base material or pavement material, connected with power sources generated through solar panels or existing power grid, to melt the ice and snow covered the markings. In this project, a systematic lab study has been conducted to validate the idea, refine the mix design, develop the connection circuit, and estimate the cost efficiency of the electrical conductive geopolymer concrete for marking snow and ice melting.

1.2 Literature review

Many deicing strategies exist in the past decades. However these methods have disadvantages ranging from being destructive to the road structure itself to being cost ineffective (Yehia et al., 2016). Deicing salt is one of the most commonly used methods to remove snow and ice, however, it has been reported to be the cause of corrosion of the reinforcing bar in concrete and environmental pollution.

An electrical conductive concrete system is another approach that has been drawing attention. This system uses electrically resistive heating elements to heat concrete structures and melt surface ice or snow. The carbon black mortar slabs (CBMS) developed by Sun et al. were able to be used for the application of electrical conductive concrete flooring material (Sun et al., 2008). It has been reported that carbon black (CB) or carbon nano-fibers can improve the conductivity capable in the electrical heating of cement-based composite (Baldwin, 1998; Feng et al., 2009). The addition of conductive admixtures transforms concrete into a good electrical conductor (Chung, 2002). The self-heating application is directly related to the increase of the composite's thermal and electrical conductivities. Just like any electrical resistance, if a constant electrical current is applied to multifunctional cement composites (which electrical resistivity has been diminished due to conductive admixtures) a part of the energy is transformed into heat; hence the specimen's temperature increases due to the Joule effect (Chung, 2002). This property would be very useful if these conductive composites were used as heating or deicing elements.

However, since the production of conventional concrete is causing many problems, such as carbon dioxide emission and high energy cost, the application Portland cement concrete is limited by its low durability, low heat resistance, and so on. Research has been developed to find alternatives to replace conventional concrete, among which, geopolymer is drawing most of the attention. The term geopolymer was first introduced by Davidovits (1979) to represent the amorphous alumino-silicate binder materials, which is also termed as "inorganic polymers", "alkali-activated cements" (Palomo & Lopez dela Fuente, 2003), "geocement", "alkali-bonded

ceramic", and "hydroceramic" etc. Geopolymers are formed when an alkali solution and an Al or Si rich material react and are defined as "an alkali aluminosilicate binder" (Saravananet al., 2013). The structural strength of the Geopolymer comes from the "three dimensional framework of SiO_4 and AlO_4 tetrahedra interlinked by shared O atoms" (Saravanan et al., 2013).

In this project, the geopolymer was developed using fly ash as the source material. Fly ash is the by-product of coal burning power plants, and causes both ecological and financial problems. Fly-ash is classified into two classes, Class C and Class F. The classification is based on the sum of silicon oxide (SiO_2), aluminum oxide (Al_2O_3), and iron oxide Fe_2O_3 contents, expressed as a percentage. Class F fly-ash has a minimum sum of 70%, and Class C fly-ash has a sum less than 70%, but greater than 50% (Du, Lukefahr, & Naranjo, 2013). Each class of fly-ash offers different utilizations in the construction industry. The fly-ash used in this study was Class C fly-ash. The power plants of North Dakota produce an abundant supply of this type of fly ash, the majority of which is treated as waste and placed in landfills.

1.3 Report organization

This project evaluated the potential of developing self-heating concrete system using fly ash based geopolymer as a snow-proof marking system, which has many aspects that needed to be evaluated. The most critical aspects are posed below as questions that will be answered in each following chapters.

- What is the right mix that could be used as pavement materials with sufficient electrical conductivity?
- Do the curing conditions affect the mix strength and stiffness?
- Does the developed mix have sufficient freeze and thaw resistance? Could the mix serve the intended service life if used as a pavement material?
- Does the new pavement material have adequate bonding strength with marking paints?
- How do field engineers monitor and control the mix quality? How does the electrical conductivity change when the pavement cracks?
- Does the suggested system consume a lot of energy to perform the function? Is it cost-effective to implement such a system in roadways?

Chapter 2. Strength and Stiffness of Fly-ash Geopolymer Concrete and Its Mix Design

2.1 Mix of fly-ash geopolymer concrete

The purpose of this phase of the project is to develop a conductive geopolymer mortar with good strength, which could be used to reveal roadway marking in the late stages of the project. The main constituents of the conventional geopolymer mortar are fly ash, sand, water, and alkaline activator, which make them weak in strength and stiffness and require special curing conditions. In order to overcome this shortcoming, steel fibers were used as additive to enhance the strength and conductivity of mortar samples. Please note, the fly ash adopted in this project was supplied from Minnkota Power Cooperative and could be classified as Class C type. The commercially available river sand with size less than 4.75 μm has been used. Sodium based alkaline solution was used as alkaline activator for this project, which is a mixture of NaOH and Na_2SiO_3. The sodium hydroxide flake with a purity of 98% and the sodium silicate solution were supplied by the science company. The sodium silicate solution (Na_2SiO_3) consisted of 9% Na_2O, 28% SiO_2, and 63% water, by mass.

The alkaline solution was prepared by dissolving NaOH flakes into Na_2SiO_3 solution that was proportioned to the desired SiO_2/Na_2O molar ratio. The solution was prepared 24 hours prior to mixing due to heat generation when dissolving NaOH.

The major difference in ordinary Portland cement (OPC) mortar and geopolymer mortar is the binder material (Hardjito & Rangan, 2005). In case of the ordinary Portland cement mortar, the cement and water are considered as binder but in case of geopolymer mortar there are fly ash and the alkaline activators.

For the fly ash based geopolymer mortar mix design, the variables used for this project were as follows:

- Activator modulus (Ms), this is the molar ratio of SiO_2/Na_2O in the alkaline solution. The Na_2O in the alkaline solution includes both the Na_2O content in the Na_2SiO_3 and the Na_2O content in the NaOH;
- Dosage of Na_2O (%Na_2O), which is mass ratio of the Na_2O content for the alkaline solution to the fly ash mass;
- The water to binder ratio (w/b); the water's mass consists of the water in the Na_2SiO_3 solution and extra water added to the alkaline solution. This extra water was added to make sure the water to binder ratio as per needed. The binder's mass included the mass of fly ash and the solid content in the alkaline solution;
- Doses of steel fiber (%S), which is the volume percentage of the steel fiber to the total volume of the sample.

The mix notation for the fly ash based geopolymer mortar is given in Figure 1.

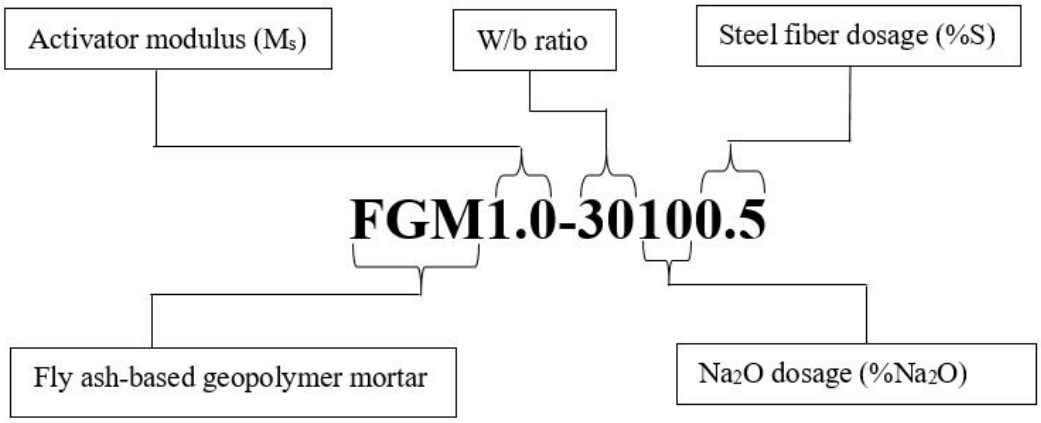

Figure 1 Specimen notation

2.2 Specimen preparation

Table 1 Fly ash-based geopolymer mortar mix proportion

S/N	Mix	M_s	W/b	F-A/S	%Na_2O	%S
1	FGM1.0-3010.5	1.0	0.3	2.75	10%	0.5%
2	FGM1.2-30101	1.2	0.3	2.75	10%	1%
3	FGM1.2-30101.5	1.4	0.3	2.75	10%	1.5%
4	FGM1.4-3510.5	1.4	0.35	2.75	10%	0.5%
5	FGM1.4-40101	1.4	0.40	2.75	10%	1%
6	FGM1.4-45101.5	1.4	0.45	2.75	10%	1.5%
7	FGM1.4-5010.5	1.4	0.50	2.75	10%	0.5%
8	FGM1.0-30101	1.0	0.3	2.75	12%	1%
9	FGM1.2-30101.5	1.2	0.3	2.75	12%	1.5%
10	FGM1.4-301000	1.4	0.3	2.75	12%	0%

According to ASTM C109 (ASTM Standard C109, 2016), 2 in cube specimens were prepared with a fixed fly ash to sand (F-A/S) mass ratio of 2.75. The detailed mixing proportions are shown in Table 1. For each mix, 3 samples are prepared.

A Hobart table mixer was used to prepare the geopolymer mortar for all specimens. The following process of mixing was followed:

1) The fly ash and alkaline solution were mixed for 30 seconds at low speed using the table mixer;
2) The sand and steel fiber were slowly added to the mixing bowl within the 30 second period, while mixing at low speed.
3) The mixer was stopped, and the speed was switched to medium; then, the mixer was re-run for another 30 seconds.
4) The mixer was stopped for another 90 seconds and then run for the last 60 seconds at a medium speed.

The mortar was then casted into each 2 inch cubic mold in two layers. Each layer was followed by 32 times of rodding. After 24 hours of curing in ambient condition, the specimens were demolded and continued curing in ambient conditions (Figure 2).

Figure 2 Mixing, molding and demolding

The load displacement curve of each specimen was obtained through the MTS machine (Figure 3). The strength and stiffness of these specimens were measured after 1, 3, 14, and 28 days of

curing based on the derived load displacement curve. The recorded load displacement and stiffness for each testing period was the average of three testing results.

Figure 3 MTS machine (a) and test scheme (b)

2.3 Strength and stiffness of fly-ash geopolymer concrete

The graph between load applied and the displacement measured by using MTS machine was plotted for each type of mixes in different days (Figures 4, 6, 8, 10, 12, 14, 16, 18, 20, and 22). The slope and the peak strength of the stress strain curve are calculated and plotted for the different mixes in different days (Figures 5, 7, 9, 11, 13, 15, 17, 19, 21, and 23).

2.3.1) Mix FGM1.0-3010.5:

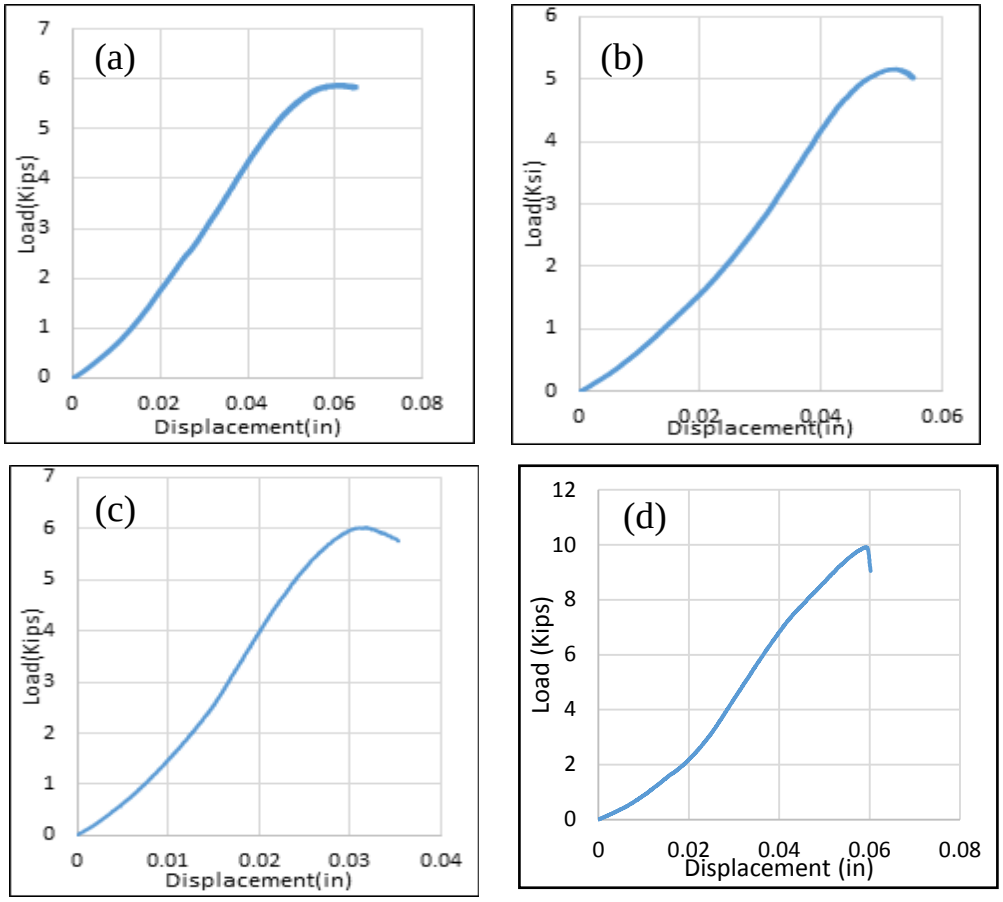

Figure 4 Load displacement curve of mix FGM1.0-3010.5 (a) 1 day, (b) 3 day, (c) 14 day, and (d) 28 day

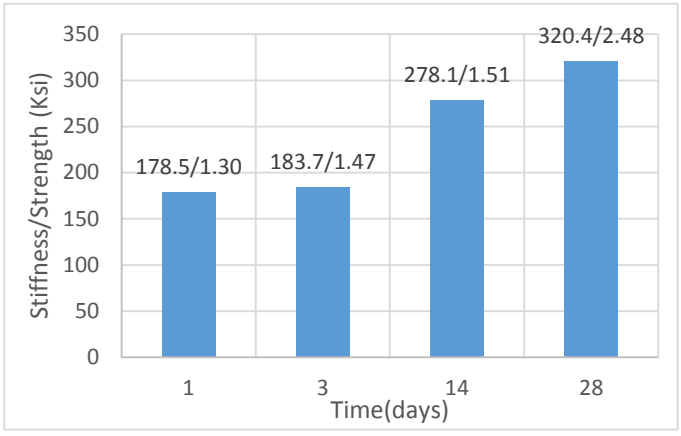

Figure 5 Stiffness and Strength versus time of Mix FGM1.0-3010.5

2.3.2) Mix FGM1.2-30101:

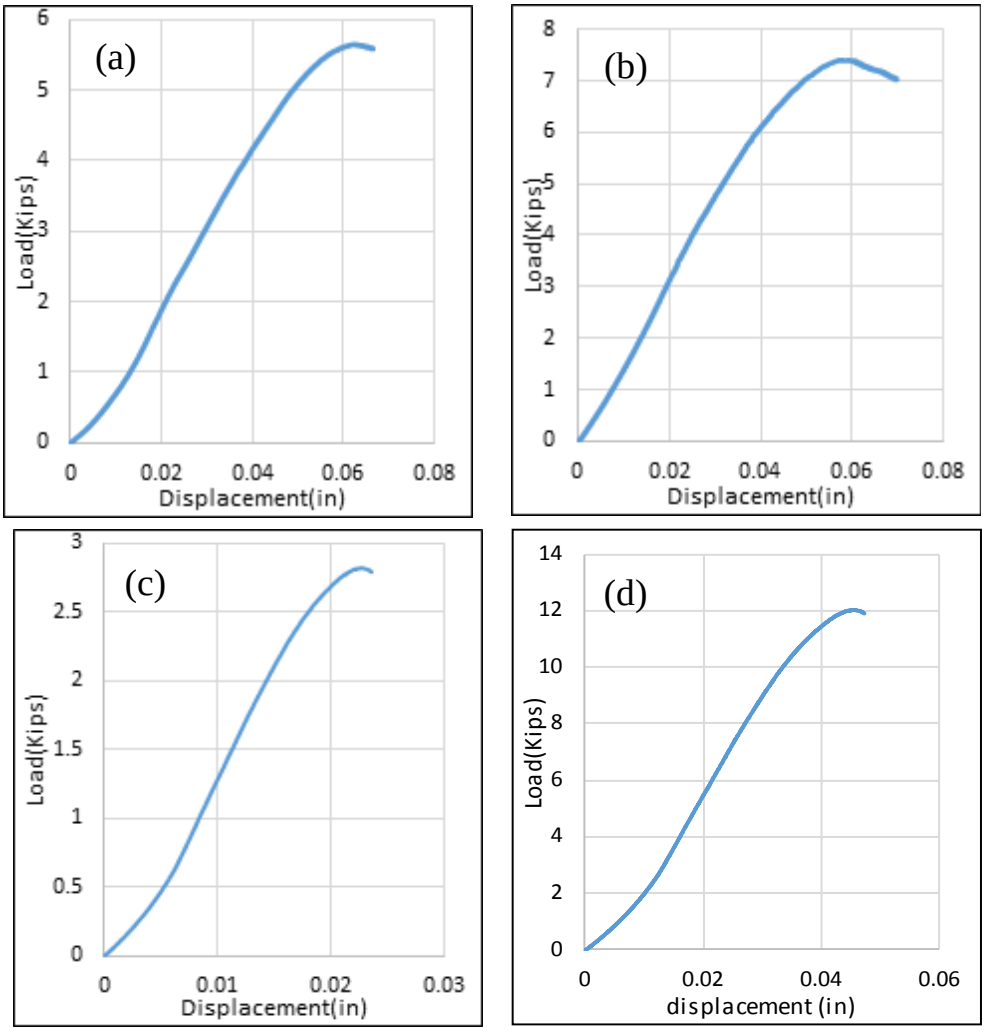

Figure 6 Load displacement curve of mix FGM1.2-30101 (a) 1 day, (b) 3 day, (c) 14 day, and (d) 28 day

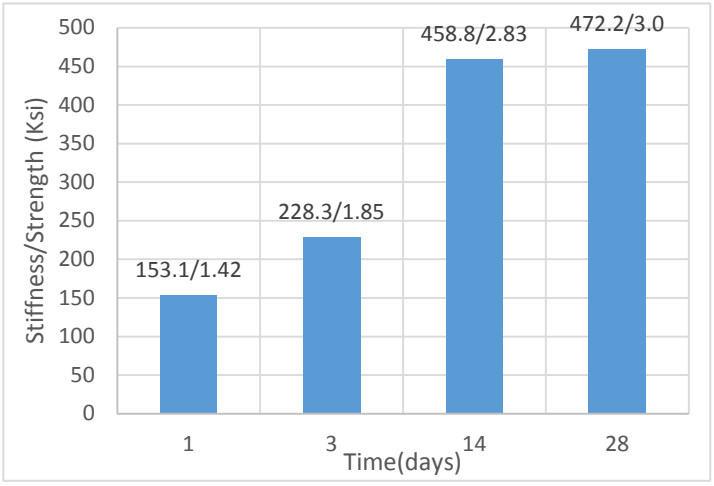

Figure 7 Stiffness and strength versus time of Mix FGM1.2-30101

2.3.3) Mix FGM1.2-30101.5:

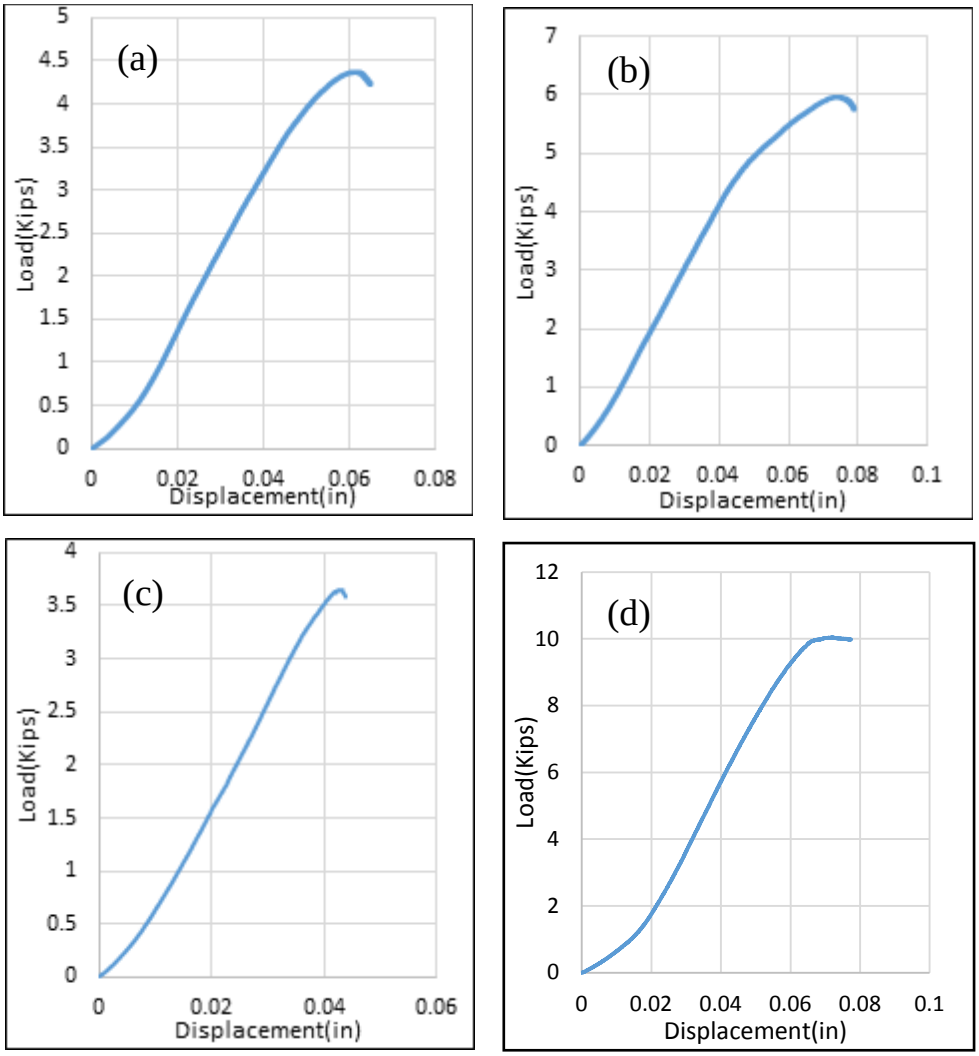

Figure 8 Load displacement curve of mix FGM1.2-30101.5 (a) 1 day, (b) 3 day, (c) 14 day, and (d) 28 day

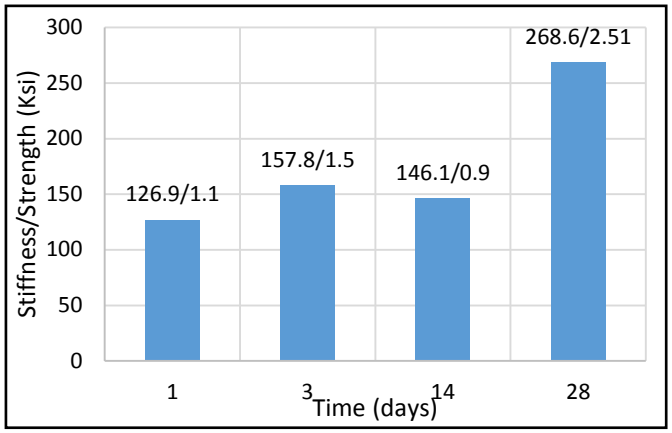

Figure 9 Stiffness and strength versus time of Mix FGM1.2-30101.5

2.3.4) Mix FGM1.4-3010.5:

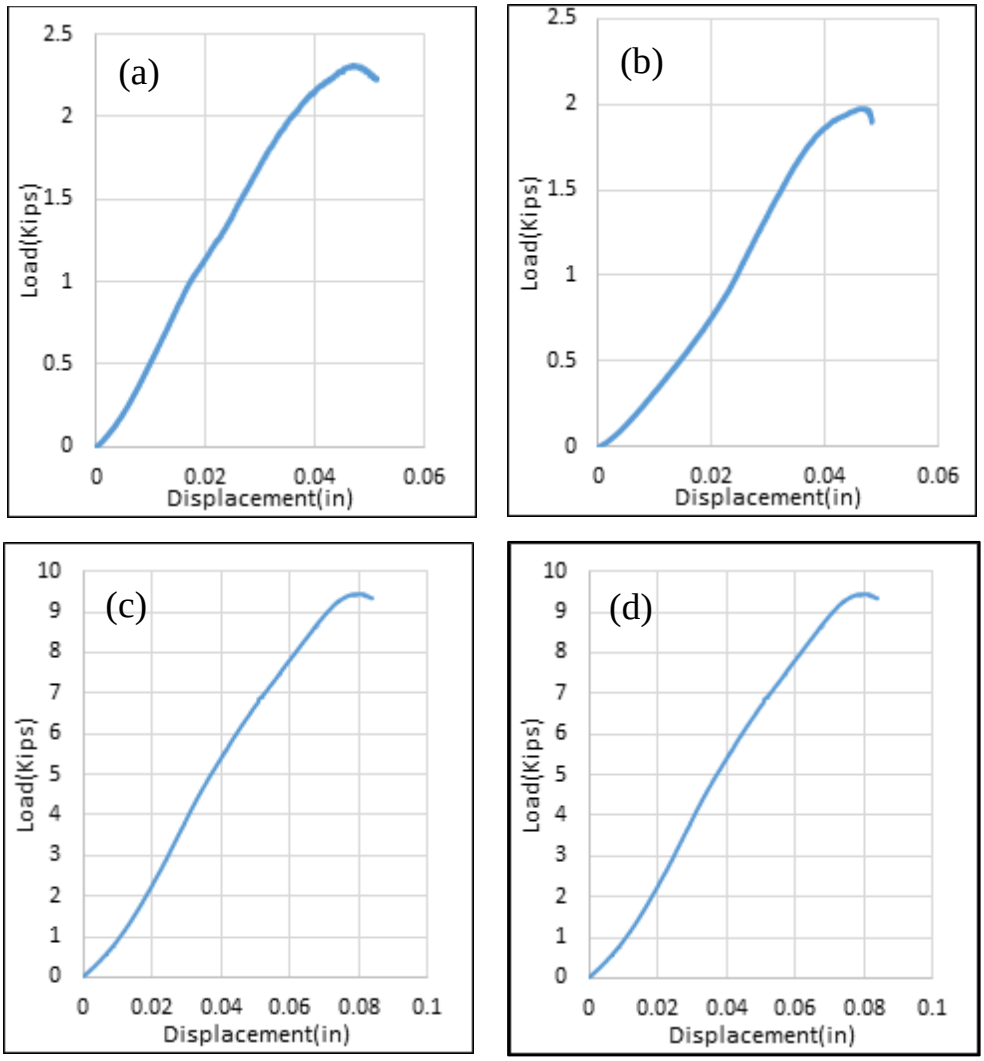

Figure 10 Load displacement curve of mix FGM1.4-3510.5 (a) 1 day, (b) 3 day, (c) 14 day, and (d) 28 day

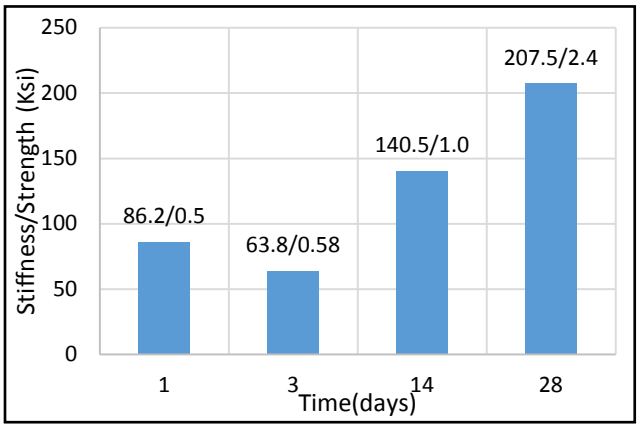

Figure 11 Stiffness and strength versus time of Mix FGM1.4-3510.5

2.3.5) Mix FGM1.4-30101:

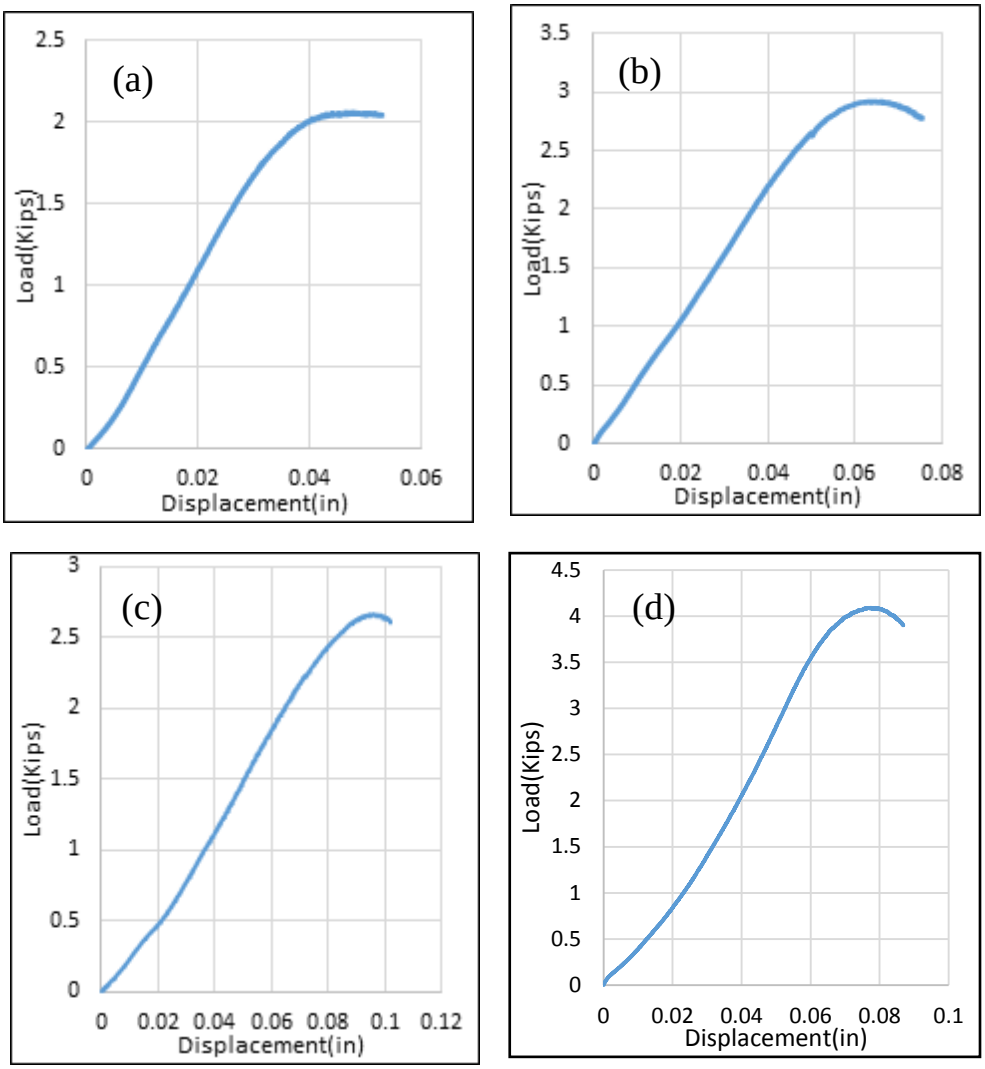

Figure 12 Load displacement curve of mix FGM1.4-40101 (a) 1 day, (b) 3 day, (c) 14 day, and (d) 28 day

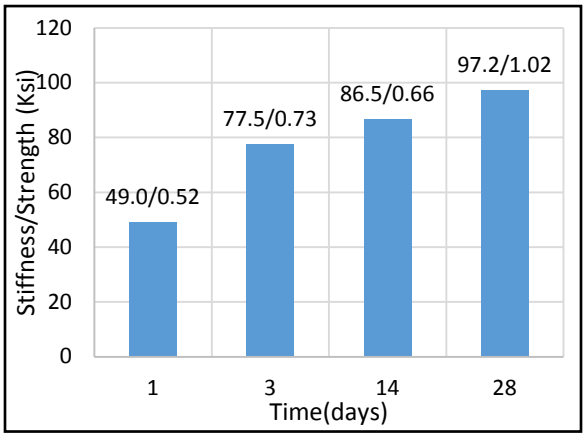

Figure 13 Stiffness and strength versus time of Mix FGM1.4-40101

2.3.6) Mix FGM1.4-30101.5:

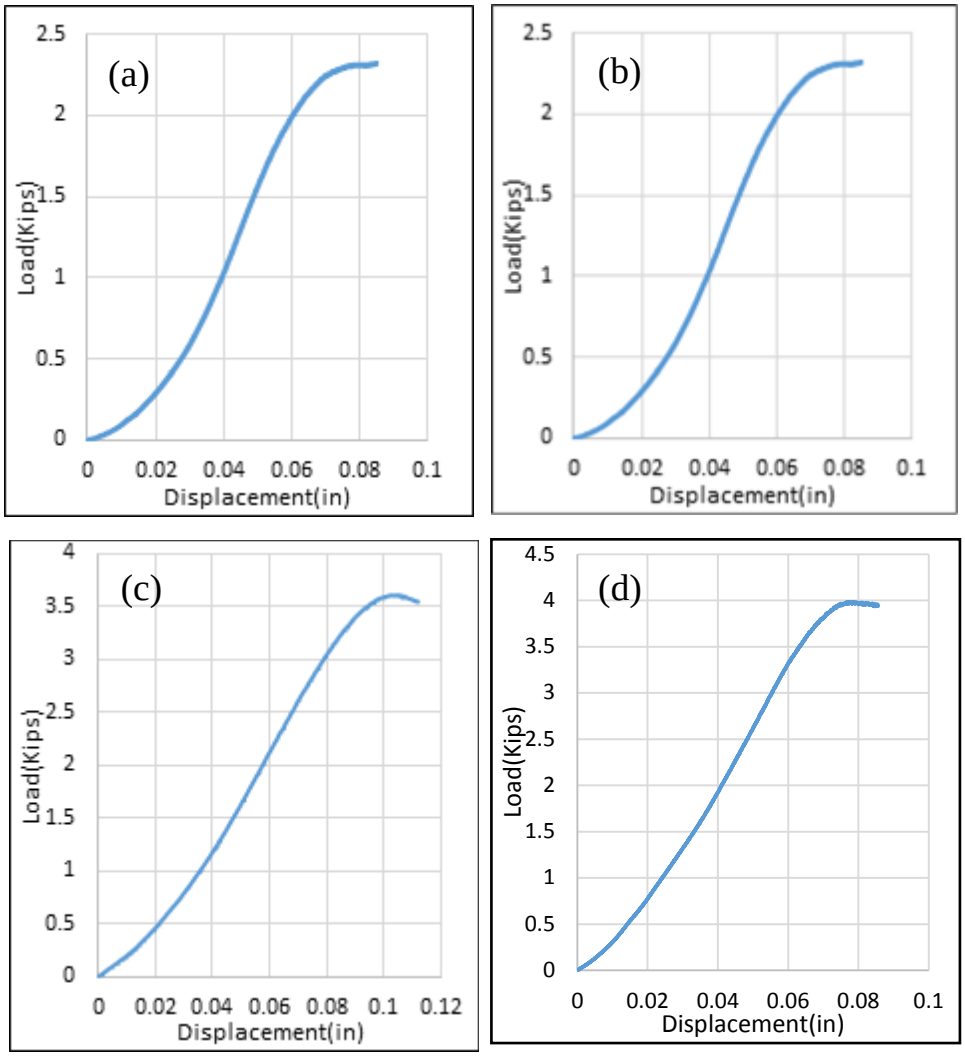

Figure 14 Load displacement curve of mix FGM1.4-45101.5 (a) 1 day, (b) 3 day, (c) 14 day, and (d) 28 day

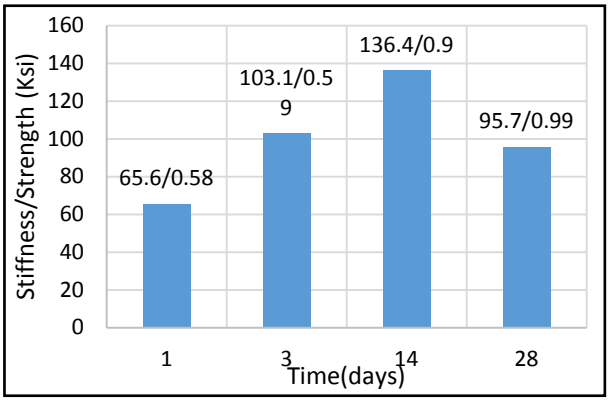

Figure 15 Stiffness and strength versus time of Mix FGM1.4-45101.5

2.3.7) Mix FGM1.4-3010.5:

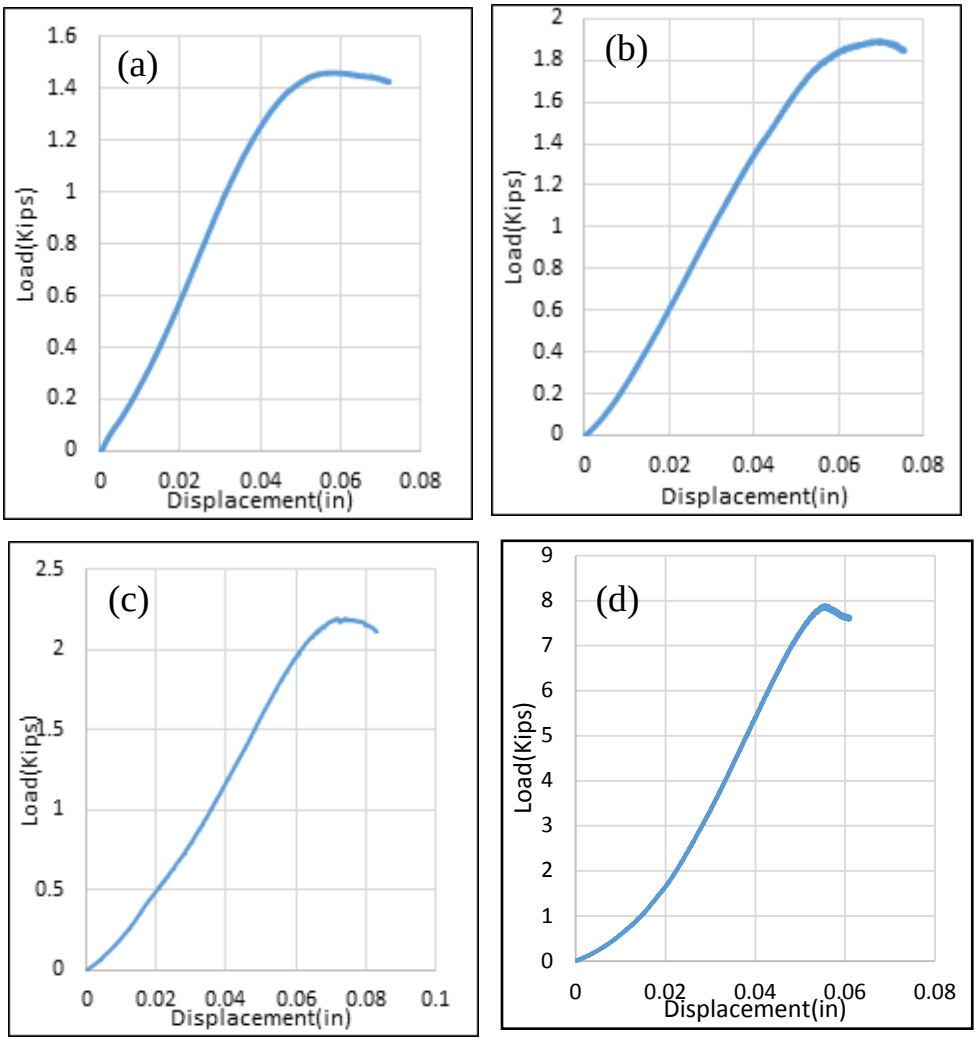

Figure 16 Load displacement curve of mix FGM1.4-5010.5 (a) 1 day, (b) 3 day, (c) 14 day, and (d) 28 day

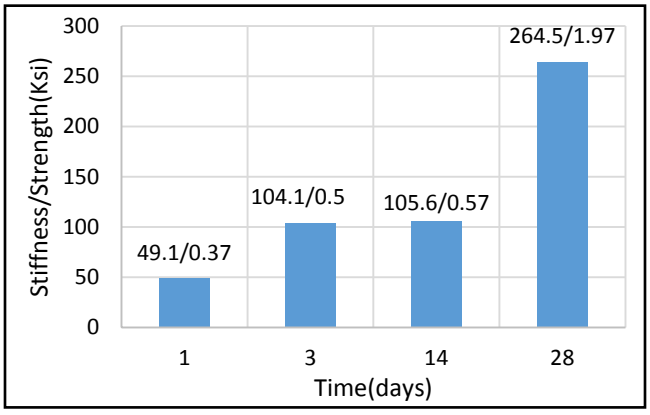

.Figure 17 Stiffness and strength versus time of Mix FGM1.4-5010.5

2.3.8) Mix FGM1.0-30101:

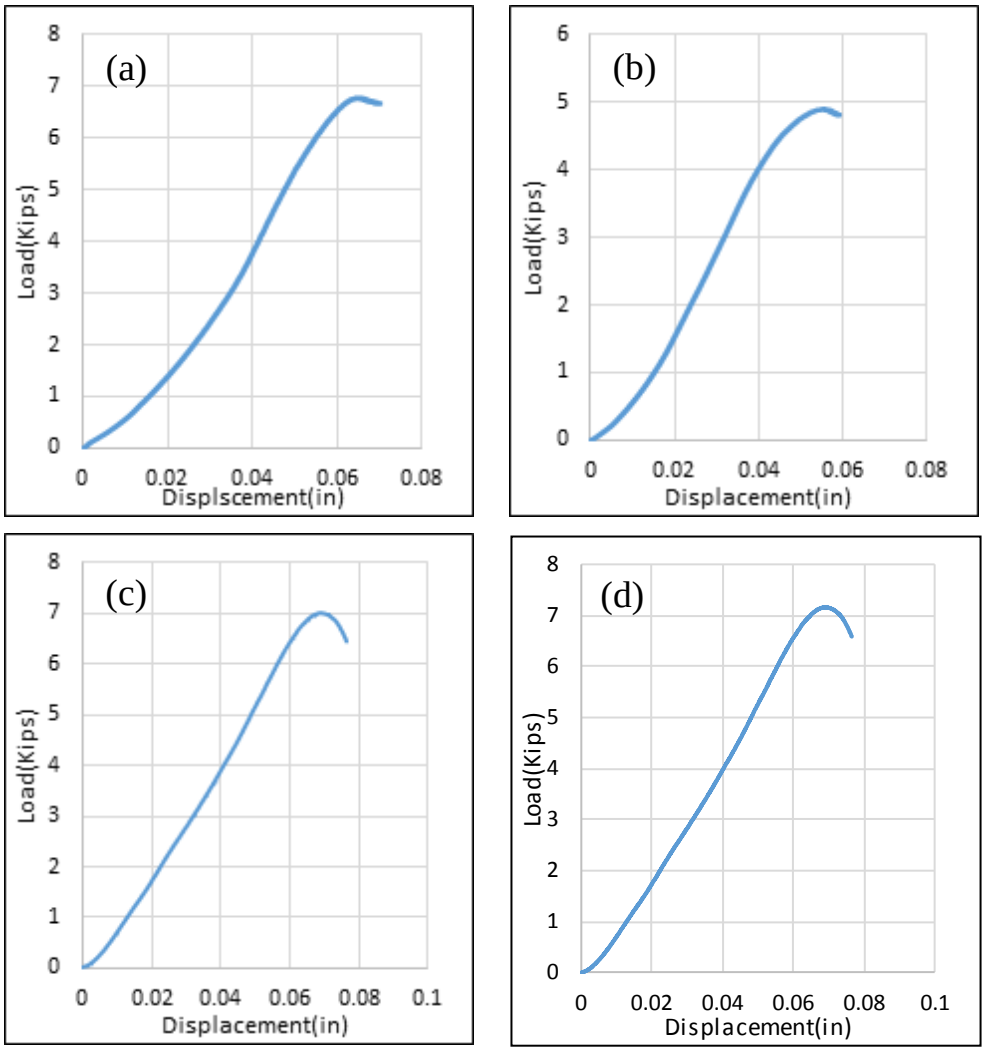

Figure 18 Load displacement curve of mix FGM1.0-30101. (a) 1 day, (b) 3 day, (c) 14 day, and (d) 28 day

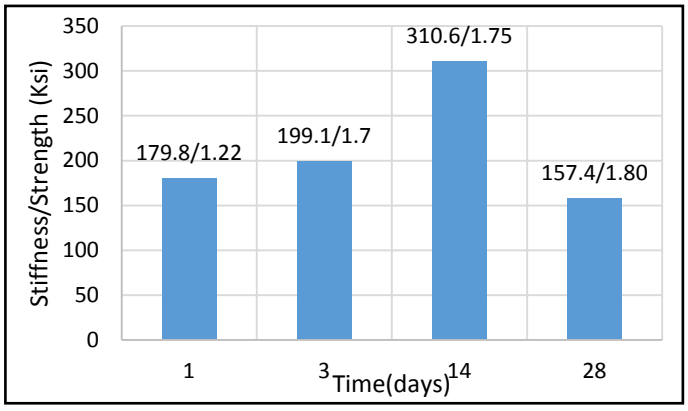

Figure 19 Stiffness and strength versus time of Mix FGM1.0-30101

2.3.9) Mix FGM1.2-30101.5:

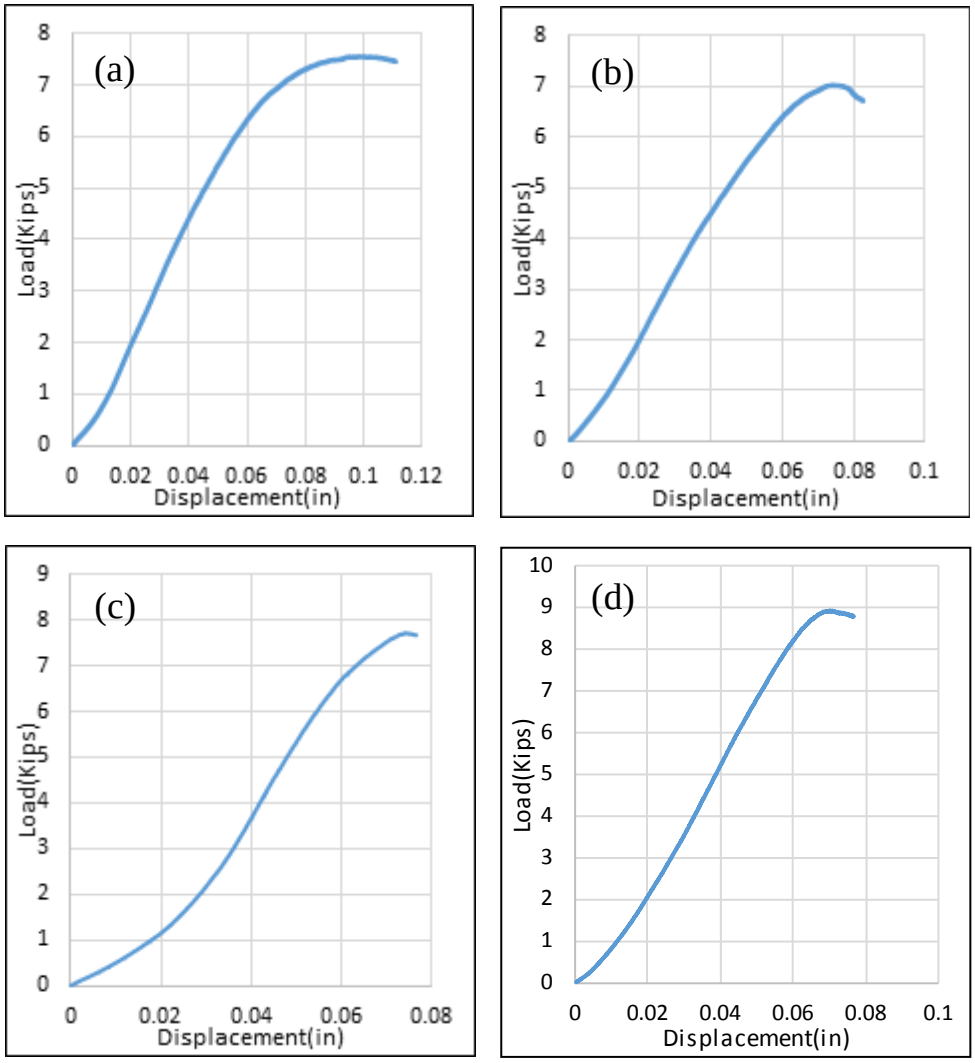

Figure 20 Load displacement curve of mix FGM1.2-30101.5 (a) 1 day, (b) 3 day, (c) 14 day, and (d) 28

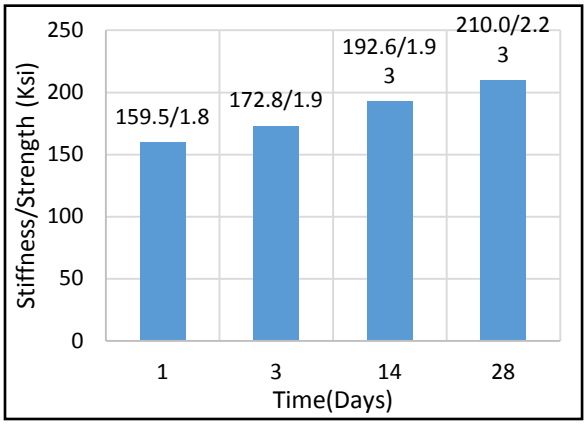

Figure 21 Stiffness and strength versus time of Mix FGM1.2-30101.5

2.3.10) Mix FGM1.4-301000:

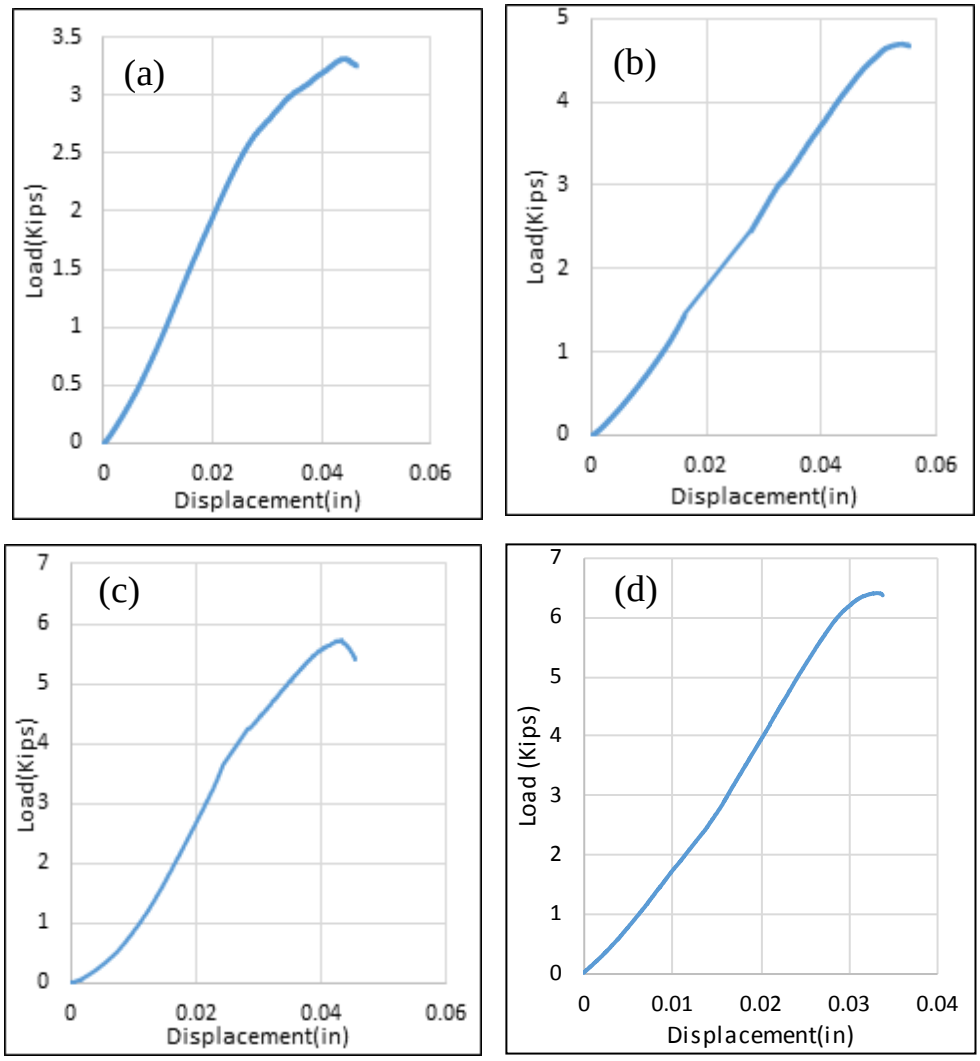

Figure 22 Load displacement curve of mix FGM1.4-301000. (a) 1 day, (b) 3 day, (c) 14 day, and (d) 28

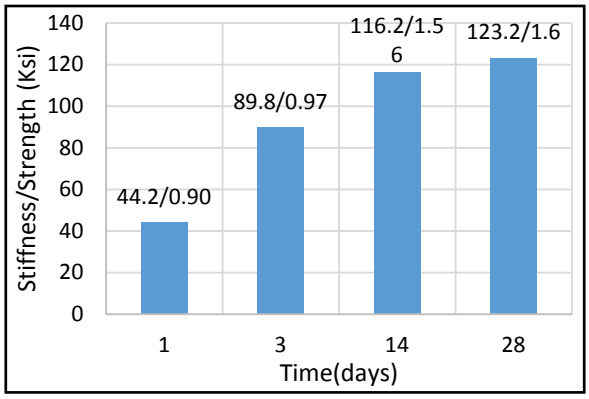

Figure 23 Stiffness and strength versus time of Mix FGM1.4-301000

Chapter 3. Strength and Stiffness of Geopolymer Mortar and Concrete with Elevated Curing

3.1 Stiffness and strength of fiber reinforced geopolymer mortar

From the mixes mentioned in Table-1, only mix 2 has reached 3 ksi in strength. More tests on mix 2 were conducted by varying the percentage of the steel fiber and curing temperature. 0.5 %, 1%, and 1.5 % volume percentage of the fiber (compared to the total volume of the specimen) was added respectively and four different curing temperatures (ambient, 80 °F, 100 °F and 120 °F) were chosen. The load displacement, stiffness and strength were obtained for all the 12 mixes given in Table 2 below. Except the percentage of fiber inclusion and curing temperature, all other variables are kept constant as in mix 2 in Table 1. The notation used for this set of experiments is shown in Figure 24. Different testing results are shown in Figures 25-33.

Table 2 Modified mix design for mix-2 in Table 1 with different fiber percentages and curing conditions

Mix	Activator modulus (M_s)	W/b	Steel fiber percentage	Curing condition
FGM1.2-0.5	1.2	0.3	0.5	Ambient
FGM1.2-0.5	1.2	0.3	0.5	80 °F
FGM1.2-0.5	1.2	0.3	0.5	100 °F
FGM1.2-0.5	1.2	0.3	0.5	120 °F
FGM1.2-1.0	1.2	0.3	1.0	Ambient
FGM1.2-1.0	1.2	0.3	1.0	80 °F
FGM1.2-1.0	1.2	0.3	1.0	100 °F
FGM1.2-1.0	1.2	0.3	1.0	120 °F
FGM1.2-1.5	1.2	0.3	1.5	Ambient
FGM1.2-1.5	1.2	0.3	1.5	80 °F
FGM1.2-1.5	1.2	0.3	1.5	100 °F
FGM1.2-1.5	1.2	0.3	1.5	120 °F

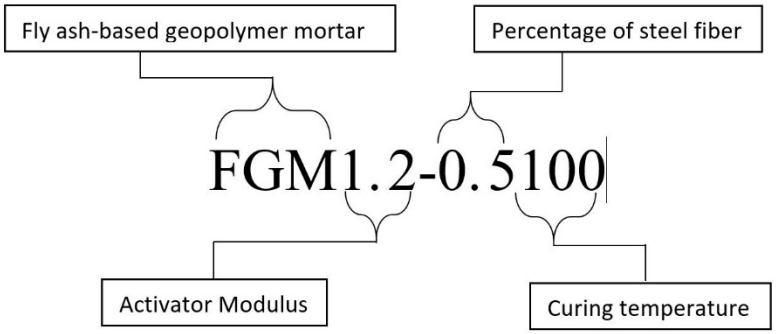

Figure 24 Specimen notation for stiffness, strength and resistivity measurement of geopolymer mortars

3.1.1) 0.5% fibers content:

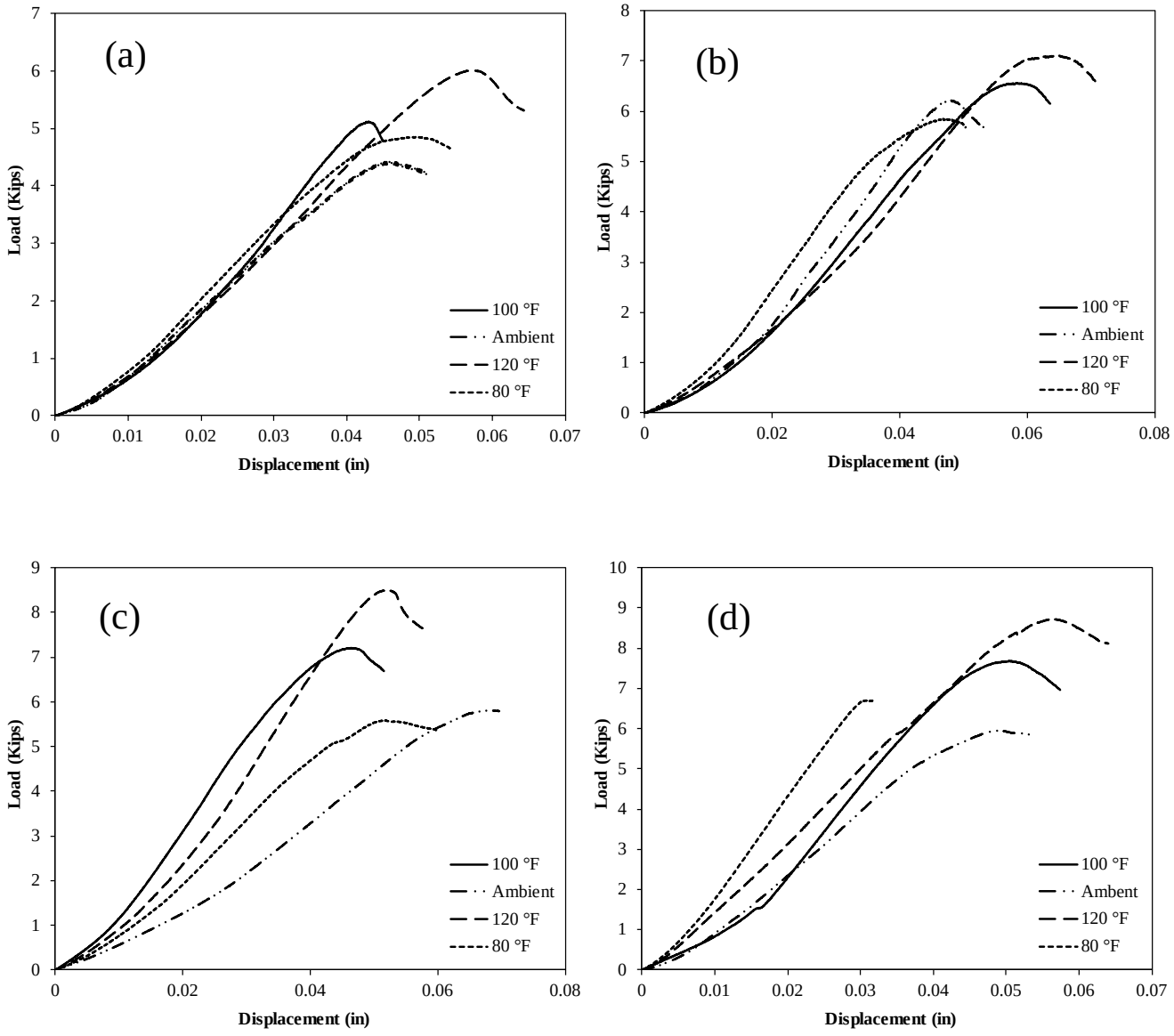

Figure 25 Load displacement curve of mix FGM1.2-0.5. (a) 1 day, (b) 7 day, (c) 14 day, and (d) 28

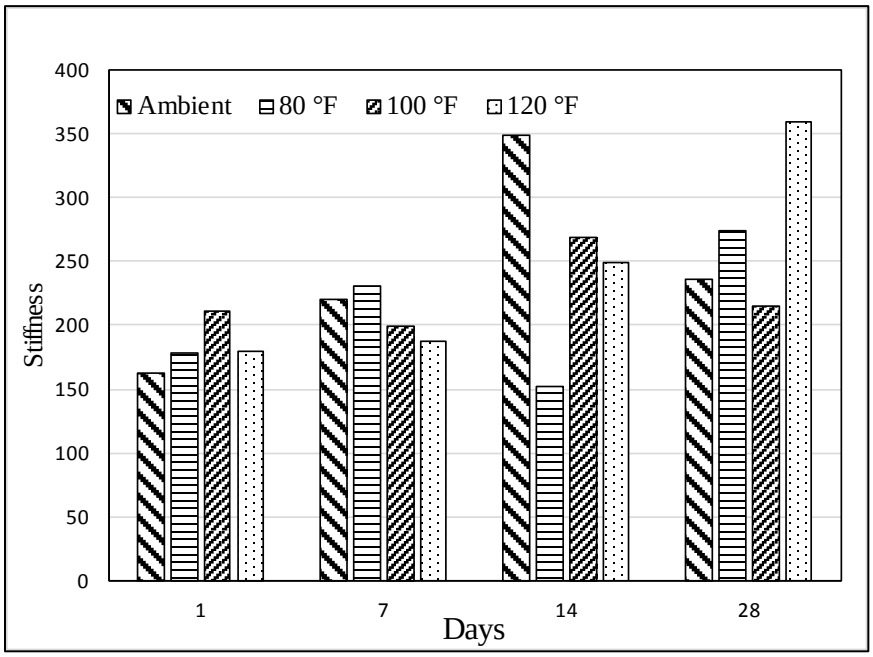

Figure 26 Stiffness (Ksi) versus time of Mix FGM1.2-0.5

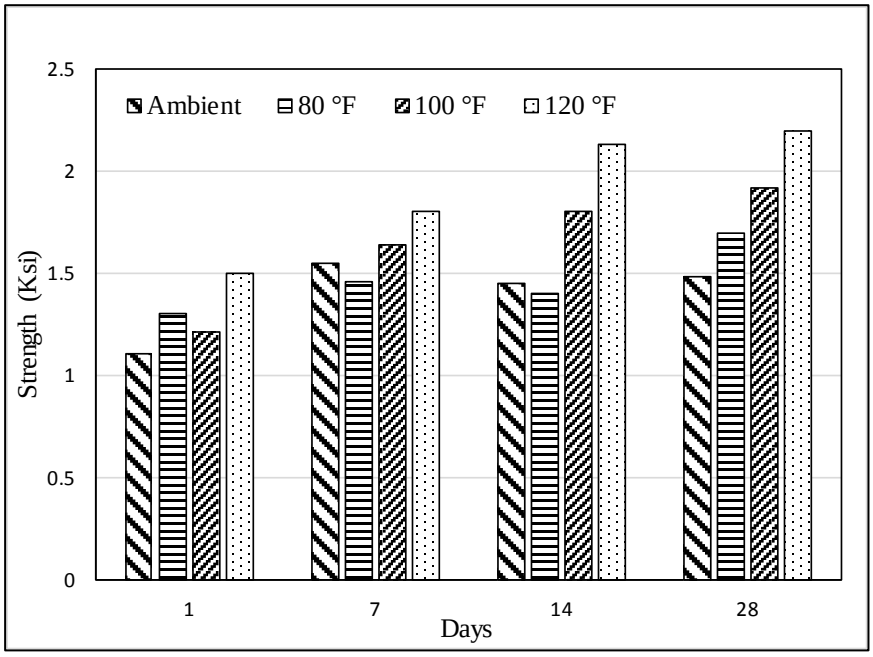

Figure 27 Strength versus time of Mix FGM1.2-0.5

3.1.2) 1% fibers content:

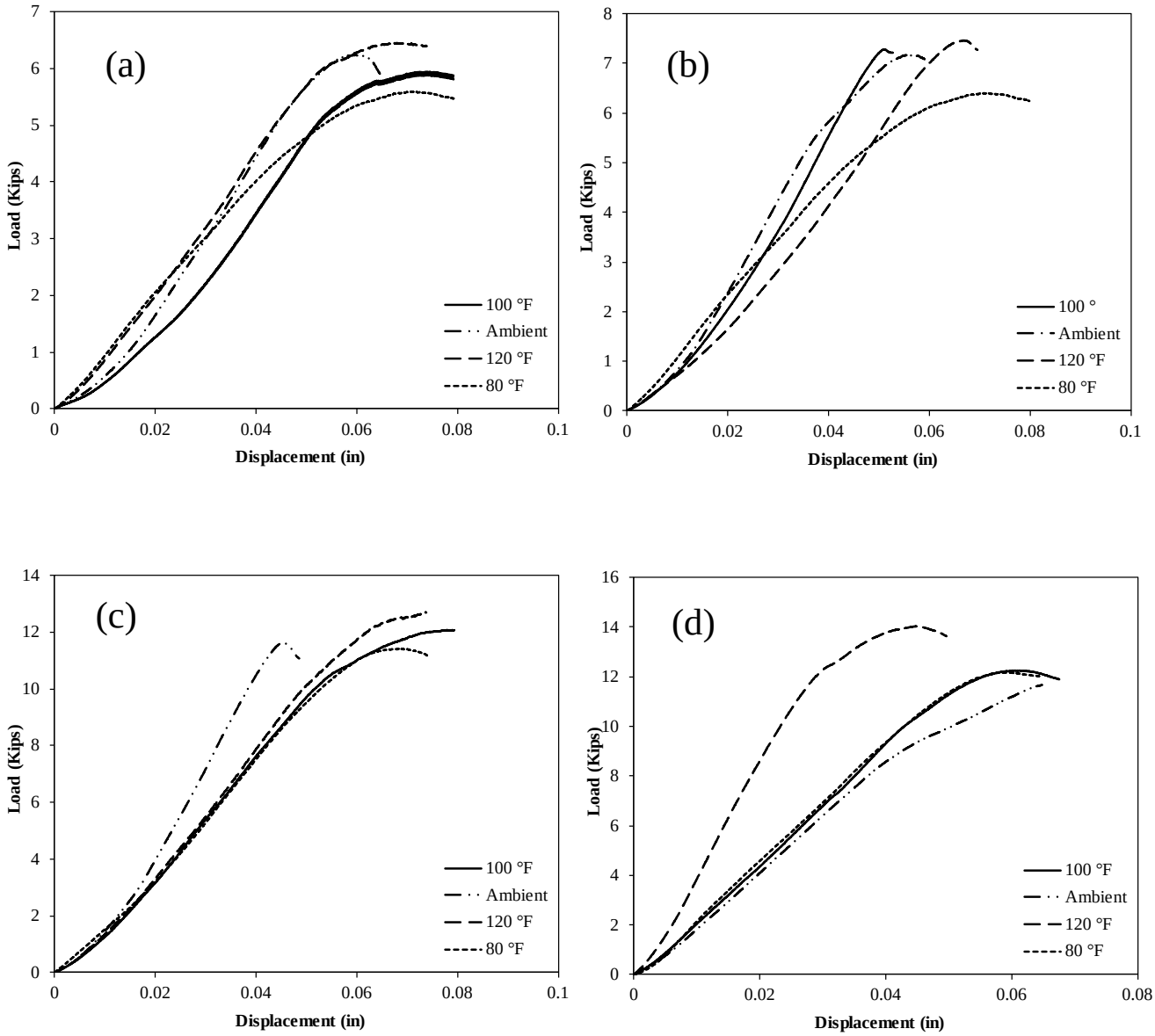

Figure 28 Load displacement curve of mix FGM1.2-1.0. (a) 1 day, (b) 7 day, (c) 14 day, and (d) 28

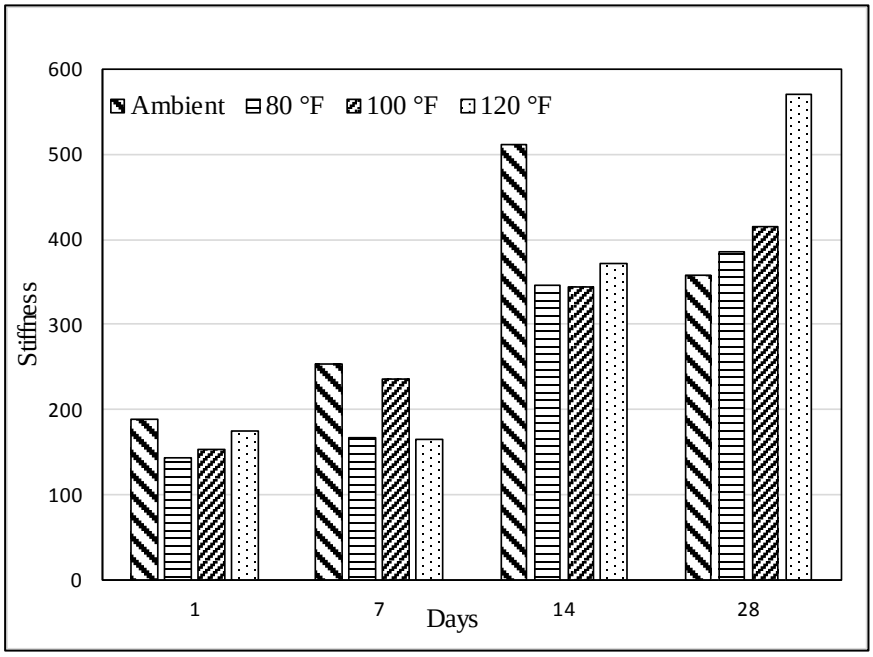

Figure 29 Stiffness (Ksi) versus time of Mix FGM1.2-1.0

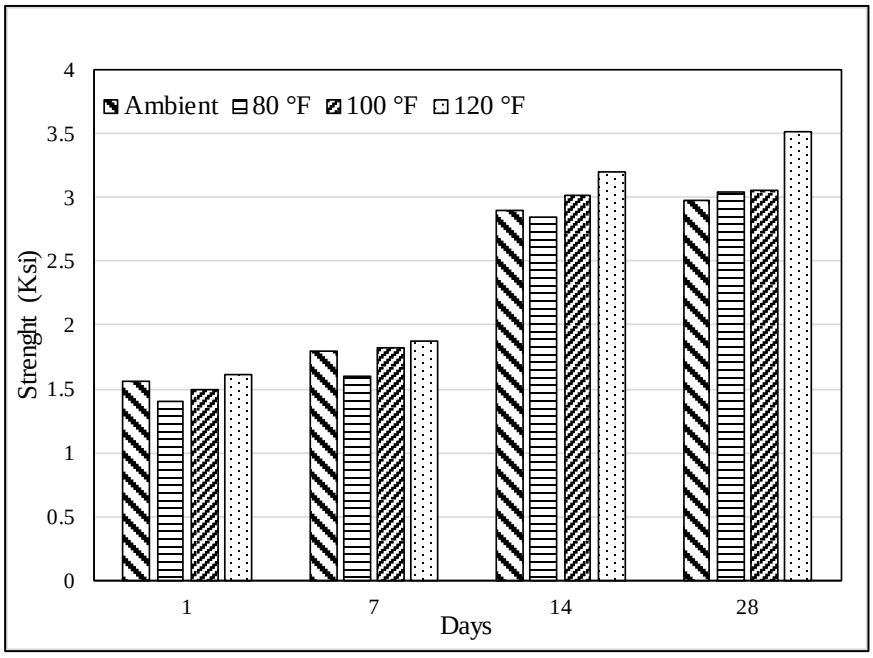

Figure 30 Strength versus time of Mix FGM1.2-1.0

3.1.3) 1.5% fibers content:

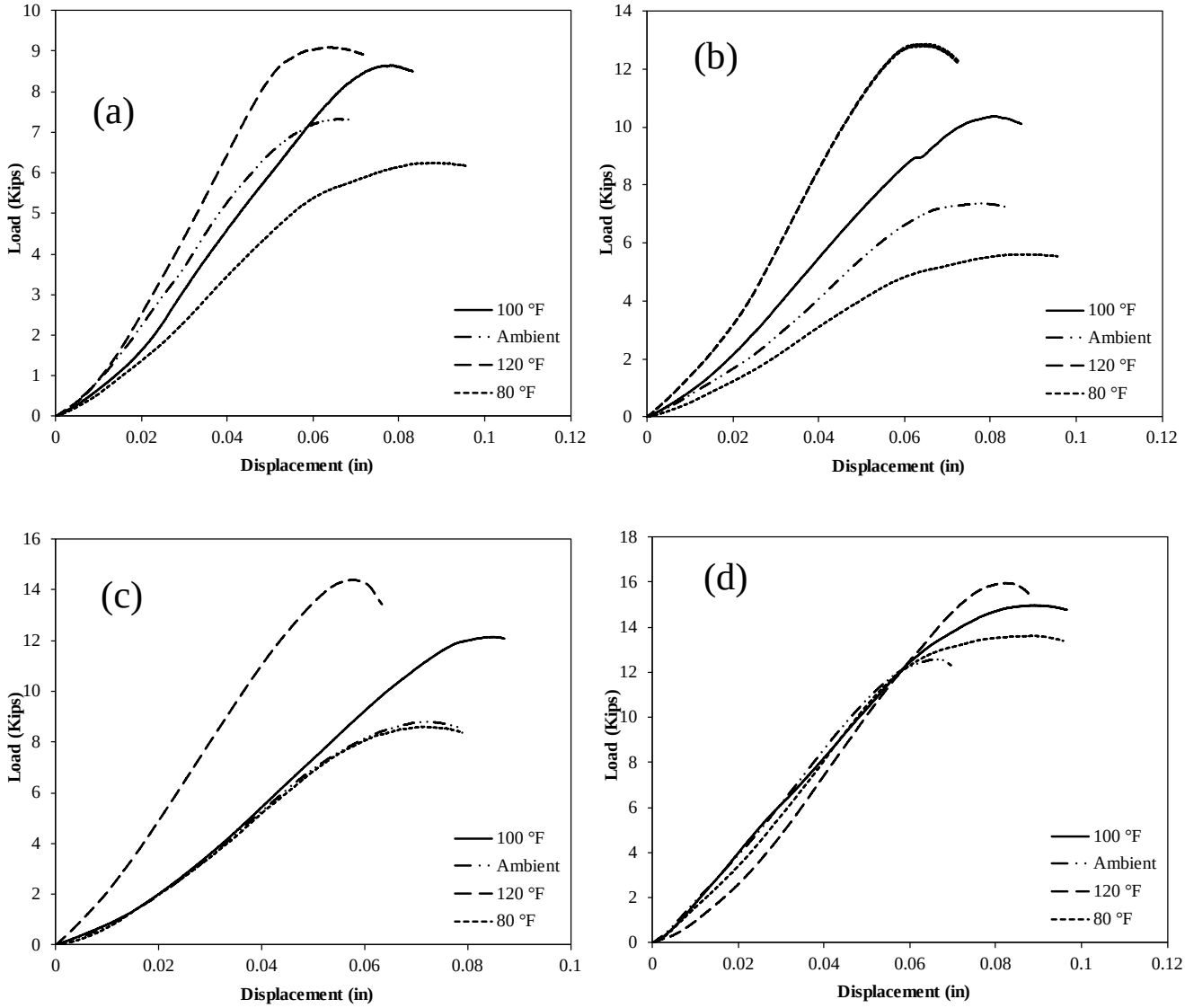

Figure 31 Load displacement curve of mix FGM1.2-1.5. (a) 1 day, (b) 7 day, (c) 14 day, and (d) 28

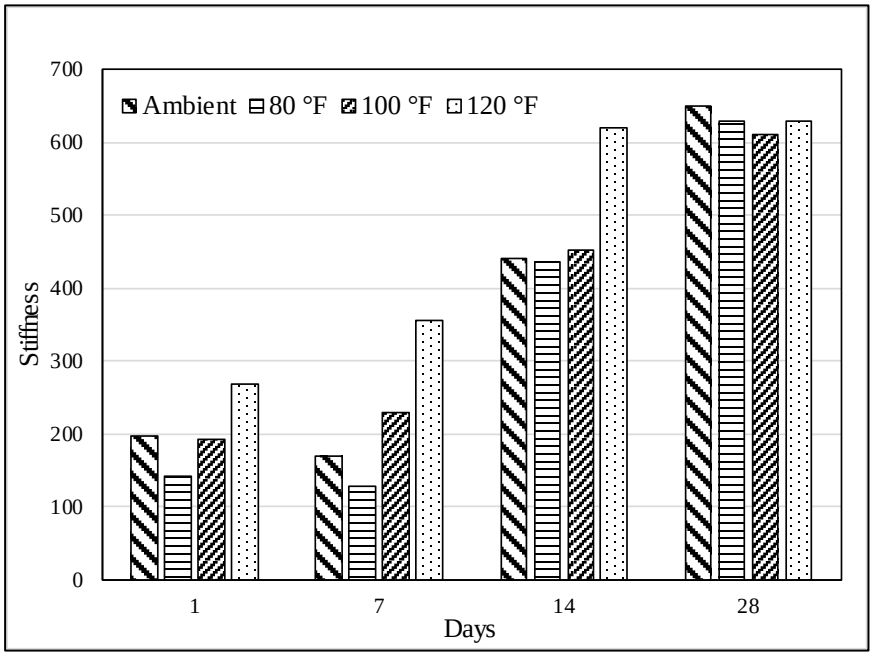

Figure 32 Stiffness (Ksi) versus time of Mix FGM1.2-1.5

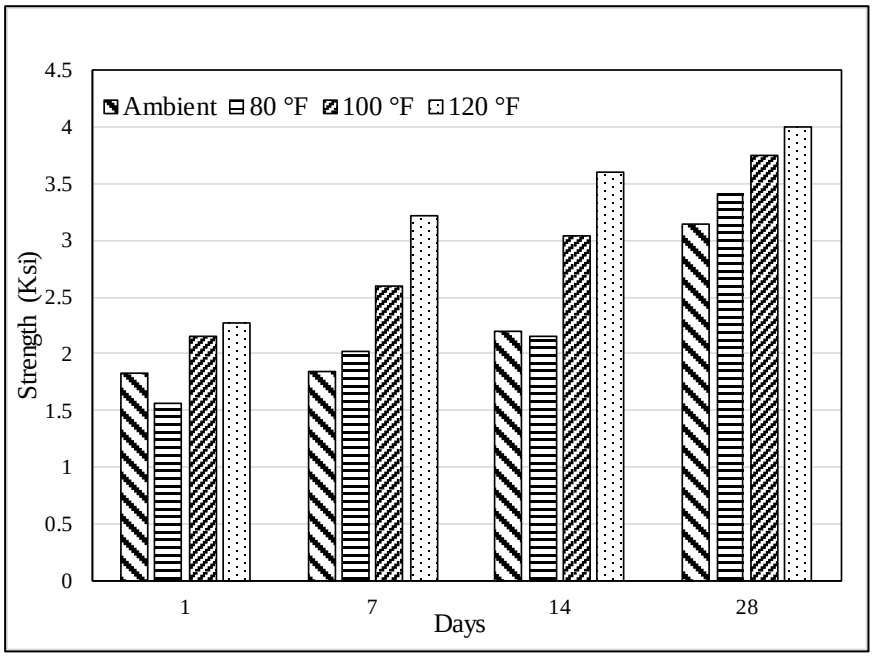

Figure 33 Strength versus time of Mix FGM1.2-1.5

3.2 Stiffness and compressive strength of geopolymer concrete

Concrete cylinders of 4 inch in diameter and 8 inch in height were prepared for the measurement of compressive strength of geopolymer concrete. Three different percentages (0.5%, 1% and 1.5%) of steel fiber were used and four different curing conditions (Ambient, 80°F, 100°F and 120°F) were selected as shown in Table 3. The notation for this set of the experiments is shown in Figure 34. The testing setup of the concrete cylinders and one of the failed specimens are shown in Figure 35. Testing results of the different mixes are shown in Figures 36-38.

Table 3 Mix design for geopolymer concrete specimens

Mix	Activator modulus (M_s)	W/b	Steel fiber percentage	Curing condition
FGC1.2-0.5	1.2	0.3	0.5	Ambient
FGC1.2-0.5	1.2	0.3	0.5	80 °F
FGC1.2-0.5	1.2	0.3	0.5	100 °F
FGC1.2-0.5	1.2	0.3	0.5	120 °F
FGC1.2-1.0	1.2	0.3	1.0	Ambient
FGC1.2-1.0	1.2	0.3	1.0	80 °F
FGC1.2-1.0	1.2	0.3	1.0	100 °F
FGC1.2-1.0	1.2	0.3	1.0	120 °F
FGC1.2-1.5	1.2	0.3	1.5	Ambient
FGC1.2-1.5	1.2	0.3	1.5	80 °F
FGC1.2-1.5	1.2	0.3	1.5	100 °F
FGC1.2-1.5	1.2	0.3	1.5	120 °F

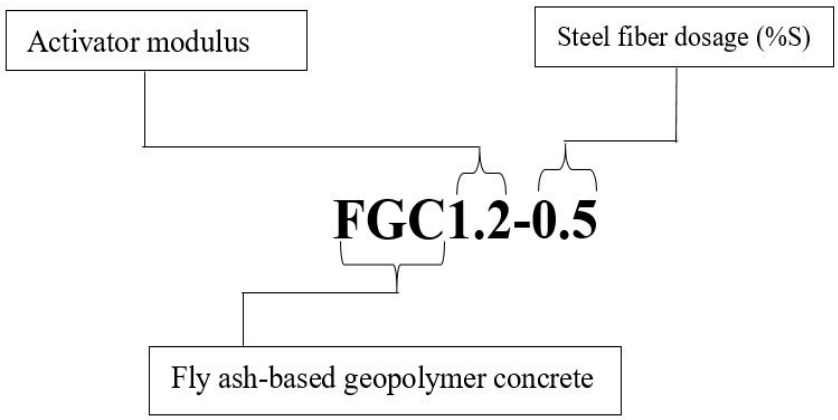

Figure 34 Specimen notation for stiffness, strength and resistivity measurement of geopolymer concrete.

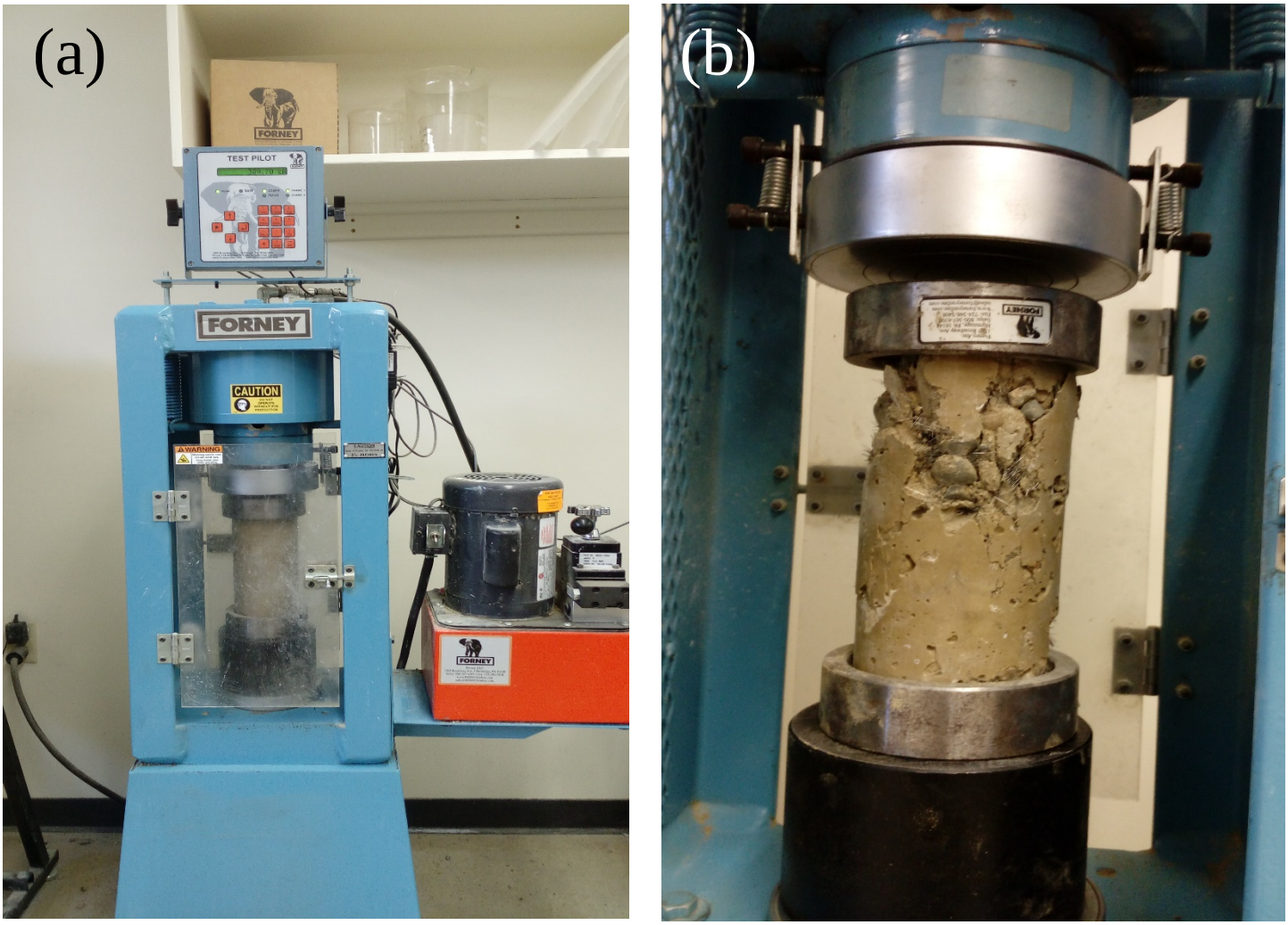

Figure 35 Compressive strength testing scheme (a) and Specimen after failure (b)

3.2.1) 0.5% fiber content:

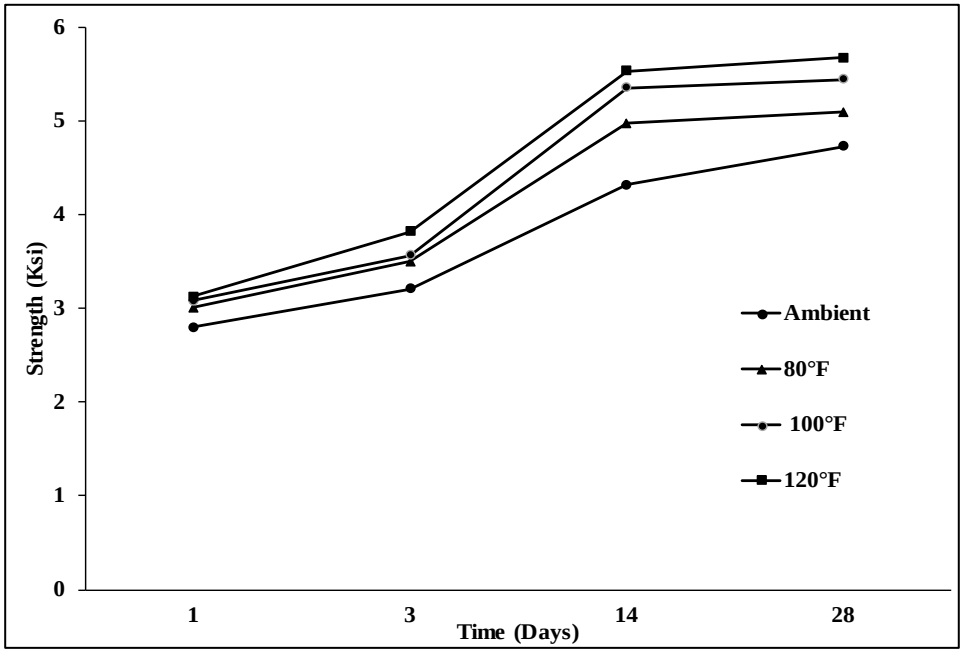

Figure 36 Compressive strength of geopolymer concrete mix FGC1.2-0.5 at different curing temperatures

3.2.2) 1% fiber content:

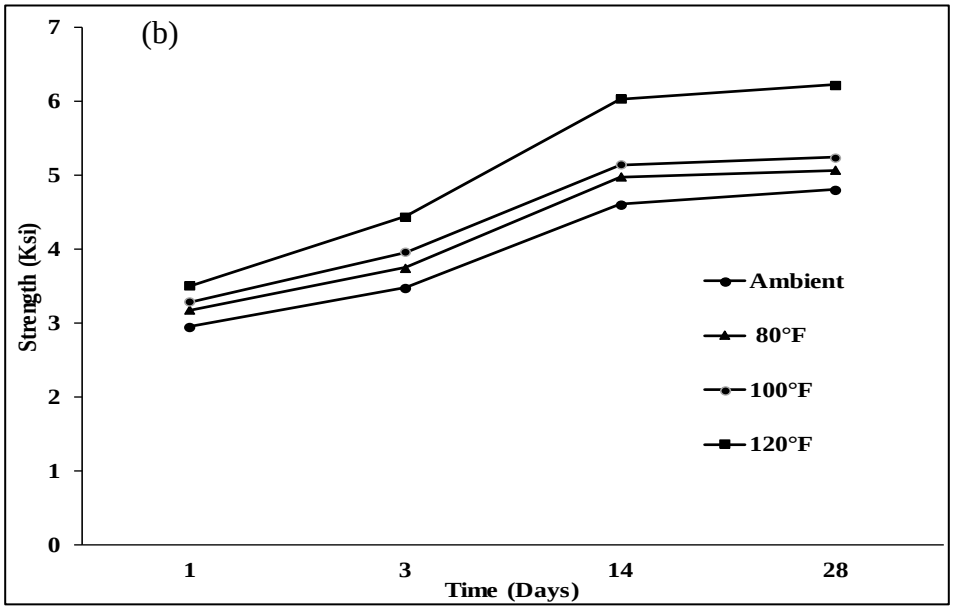

Figure 37 Compressive strength of geopolymer concrete mix FGC1.2-1.0 at different curing temperatures

3.2.3) 1.5% fiber content:

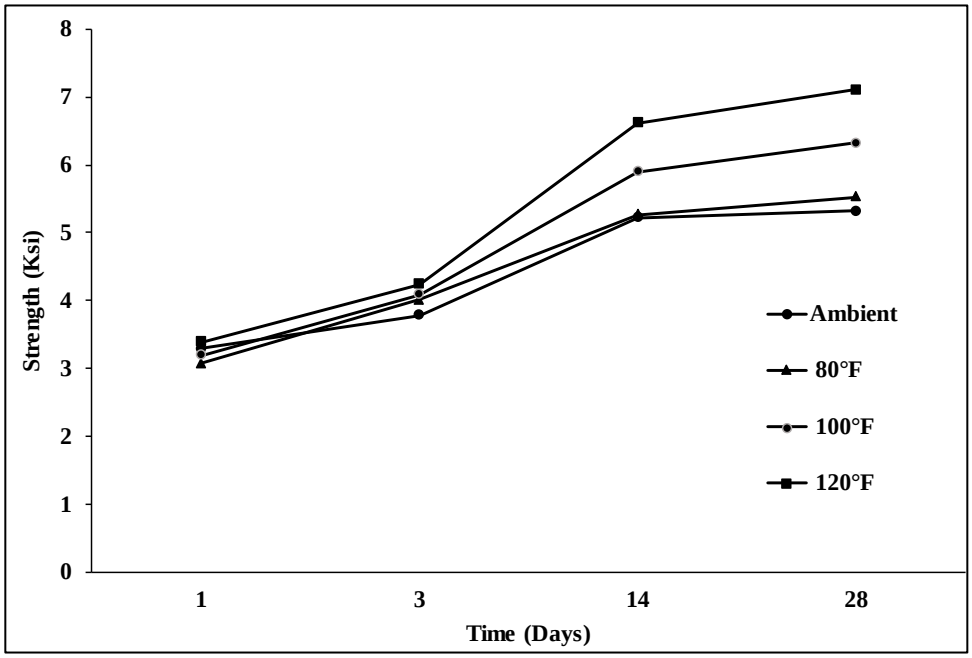

Figure 38 Compressive strength of geopolymer concrete mix FGC1.2-1.5 at different curing temperatures

Chapter 4. Conductivity of Geopolymer Concrete Materials

4.1 Resistivity of geopolymer mortar

Many studies have been conducted on electrical conductivity of ordinary and geopolymer mortar and concrete. W.J McCarter et al. (2000) studied electrical conductivity of Portland cement based mortar and found that electrical conductivity of the cement mortar keeps decreasing until 450 days after curing. Sakonwan Hanjitsuwan et al. (2010) studied electrical conductivity and dielectric properties of the fly ash based geopolymer mortars by using different ratio of alkaline liquid to fly ash (L/A) and found that geopolymer mortar with a high L/A ratio of 0.7 is a highly porous structure and gives lower values of conductivity and dielectric constant comparing to those of the geopolymer mortars with lower L/A ratios of 0.4, 0.5, and 0.6. The geopolymer paste with a L/A ratio of 0.6 gives relatively higher conductivity and dielectric constant. However there is no comprehensive study on the electrical conductivity of geopolymer mortar and concrete, such as what effects of curing temperatures and mix designs will have on this property?

2x2x2 in. geopolymer mortar cubes with different steel fiber percentage (0.5%, 1% and 1.5%) and cured at different curing temperatures (Ambient, 80 °F, 100 °F and 120 °F) were prepared. Electrical resistivity of the geopolymer mortar cubes were measured on the 14^{th} day and 28^{th} day using the two probe method (Figure 40). The measured electrical resistivity for different mixes is shown in Figures 41-43.

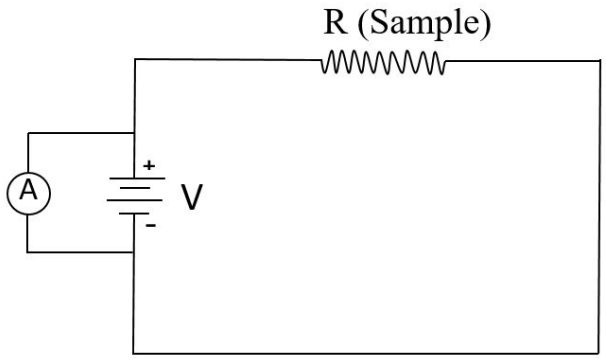

Figure 39 Electrical circuit used for resistivity measurement of mortar samples

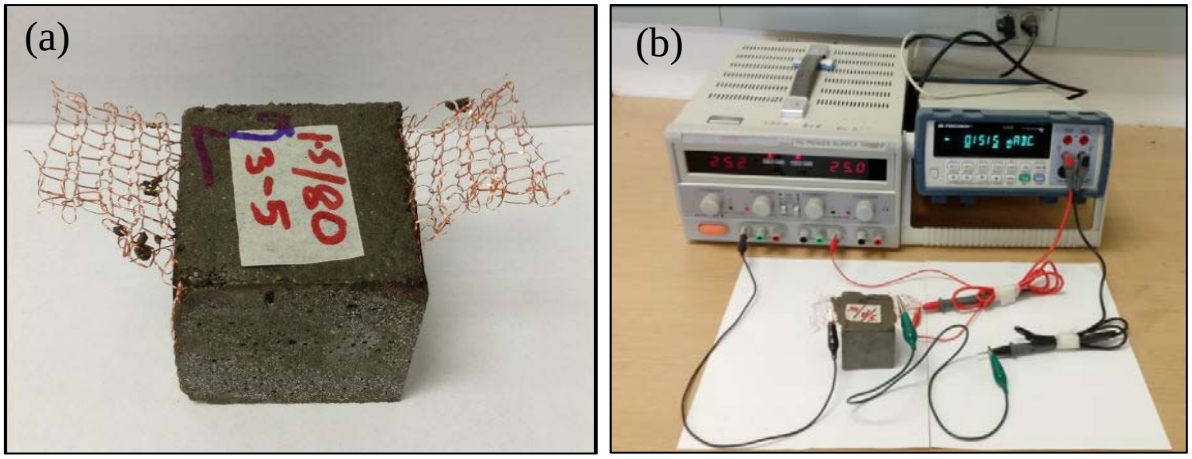

Figure 40 (a) Sample used for resistivity resting (b) Resistivity testing setup

4.1.1) 0.5% fibers content:

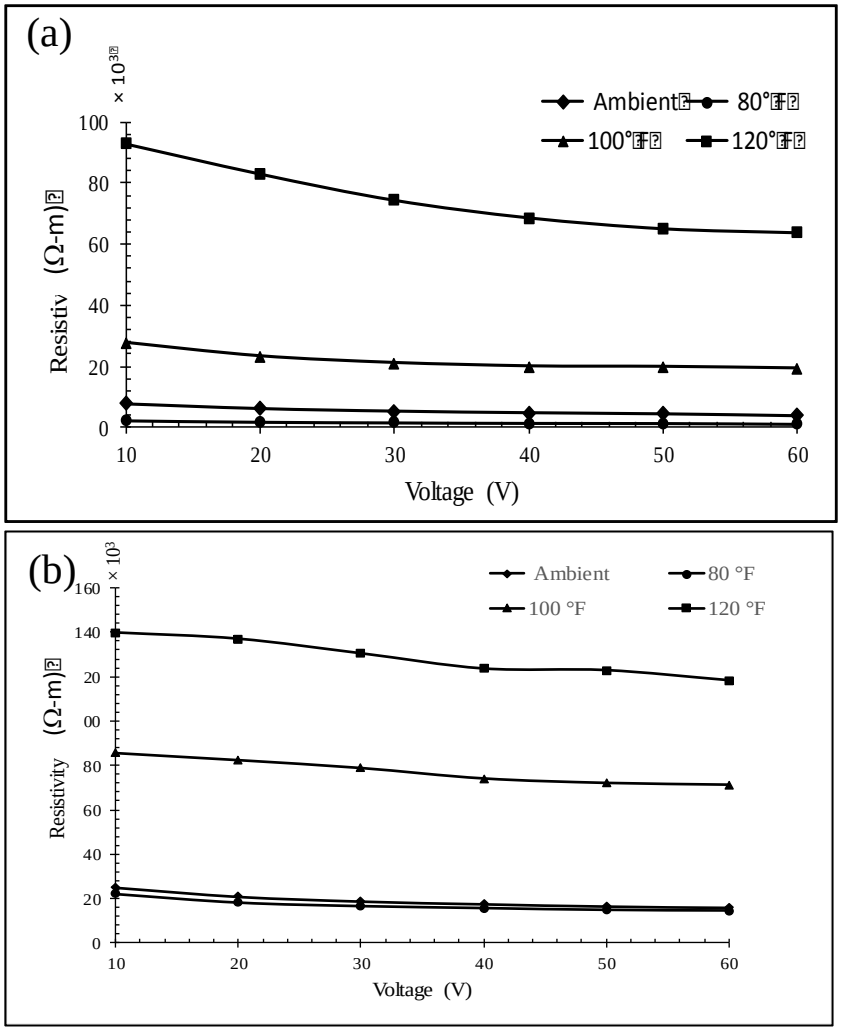

Figure 41 Resistivity of mix FGM1.2-0.5. (a) 14 days, and (b) 28 days

4.1.2) 1.0% fibers content:

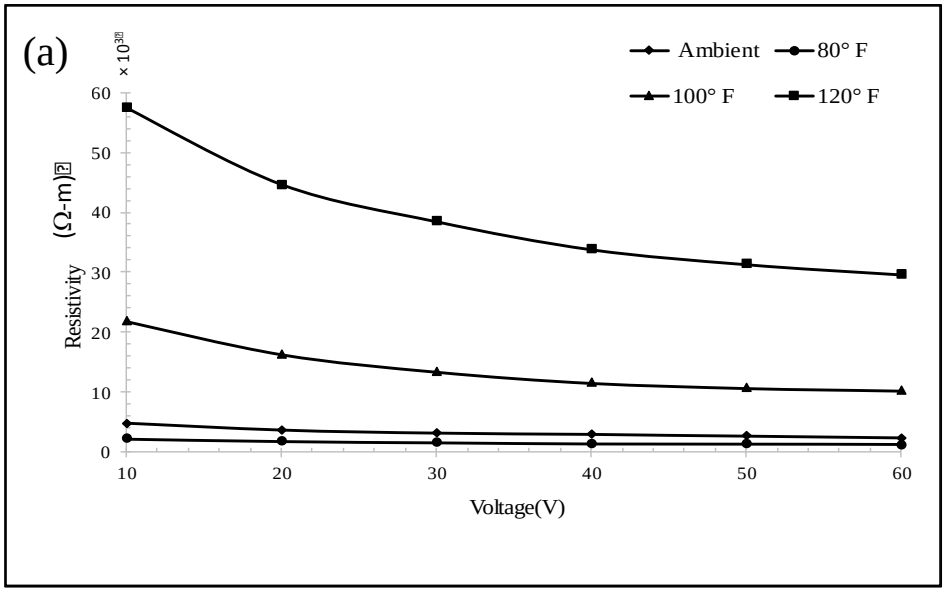

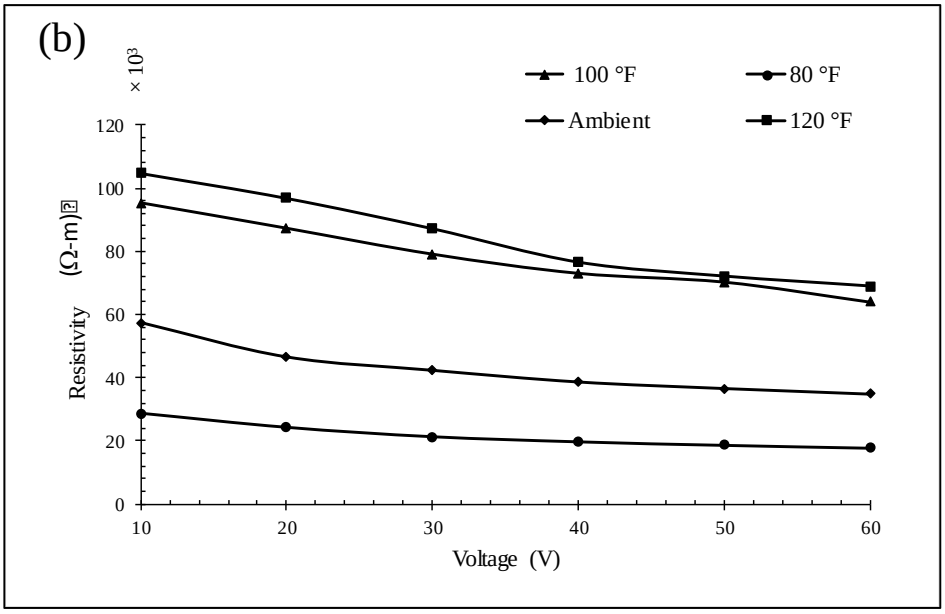

Figure 42 Resistivity of mix FGM1.2-1.0. (a) 14 days, and (b) 28 days

4.1.3) 1.5% fibers content:

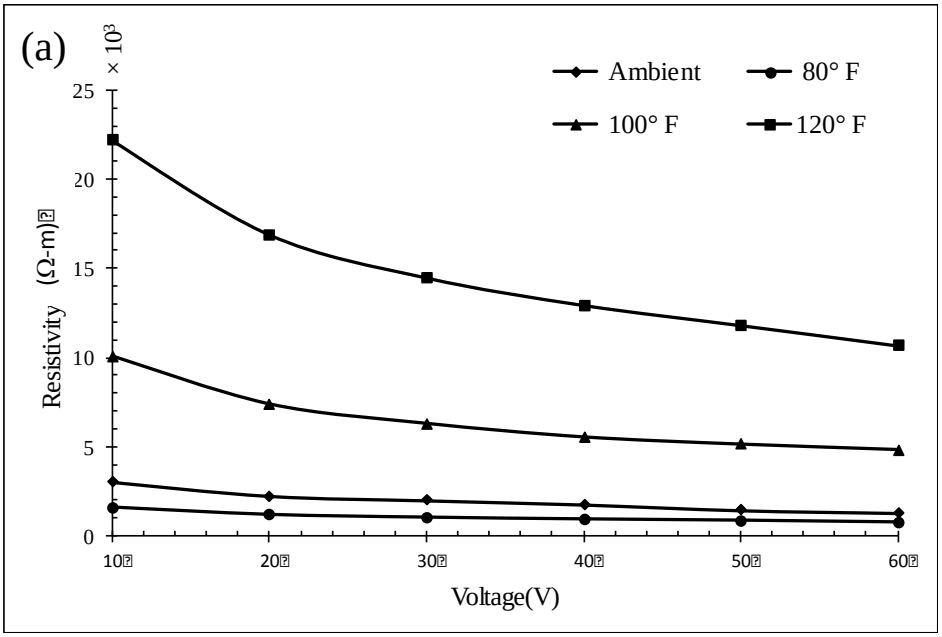

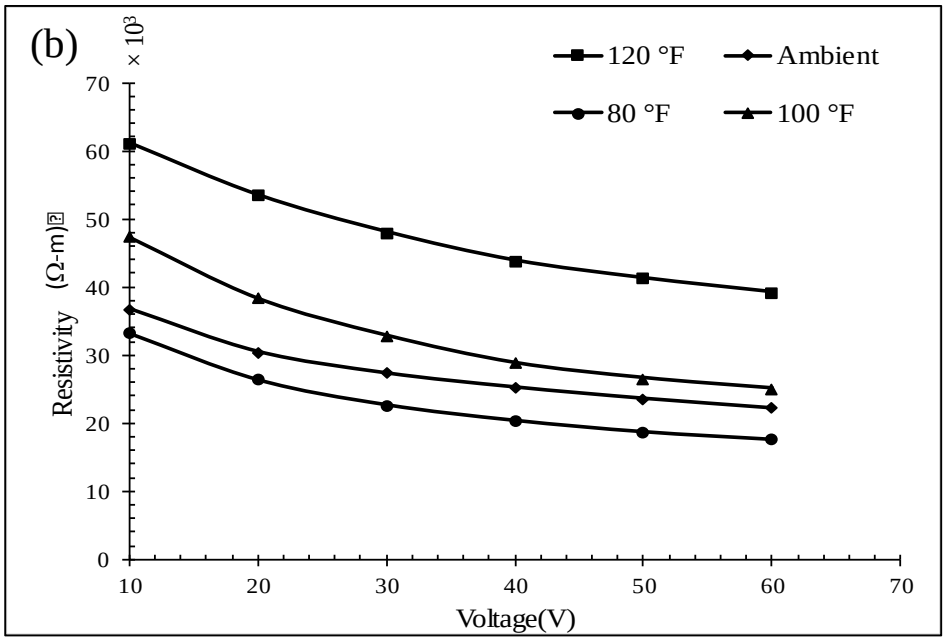

Figure 43 Resistivity of mix FGM1.2-1.5. (a) 14 days, and (b) 28 days

4.2 Resistivity measurement of geopolymer concrete

In section 5.1, resistivity of geopolymer mortar cubes was measured. In this section, concrete cylinders with 4 inch in diameter and 8 inch in height were prepared to characterize the

resistivity of geopolymer based concrete. Three different percentages of steel fiber and four different curing conditions (Ambient, 80°F, 100°F and 120°F) were used for comparison purpose. The electrical circuit adopted for resistivity measurement is the same as Figure 39, and the experiment setup is shown in Figure 44. The measured resistivity is shown in Figures 45-47.

Figure 44 (a) Sample used for resistivity resting (b) Resistivity testing instrument setup

4.2.1) 0.5% fiber content:

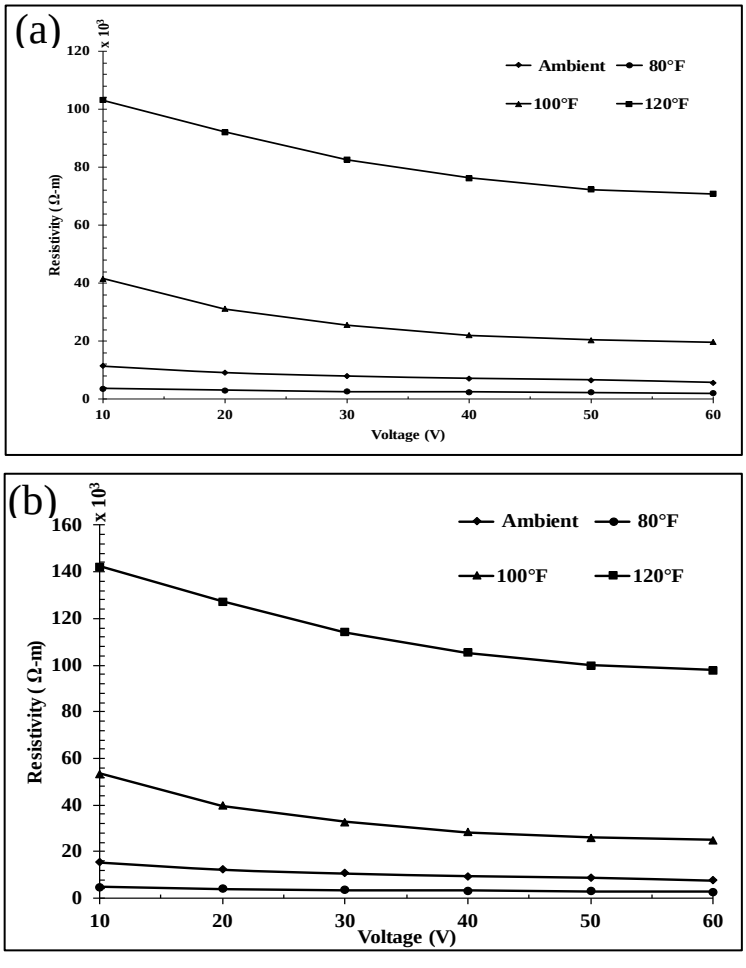

Figure 45 Resistivity of mix FGC1.2-0.5. (a) 14 days, and (b) 28 days

4.2.2) 1% fiber content:

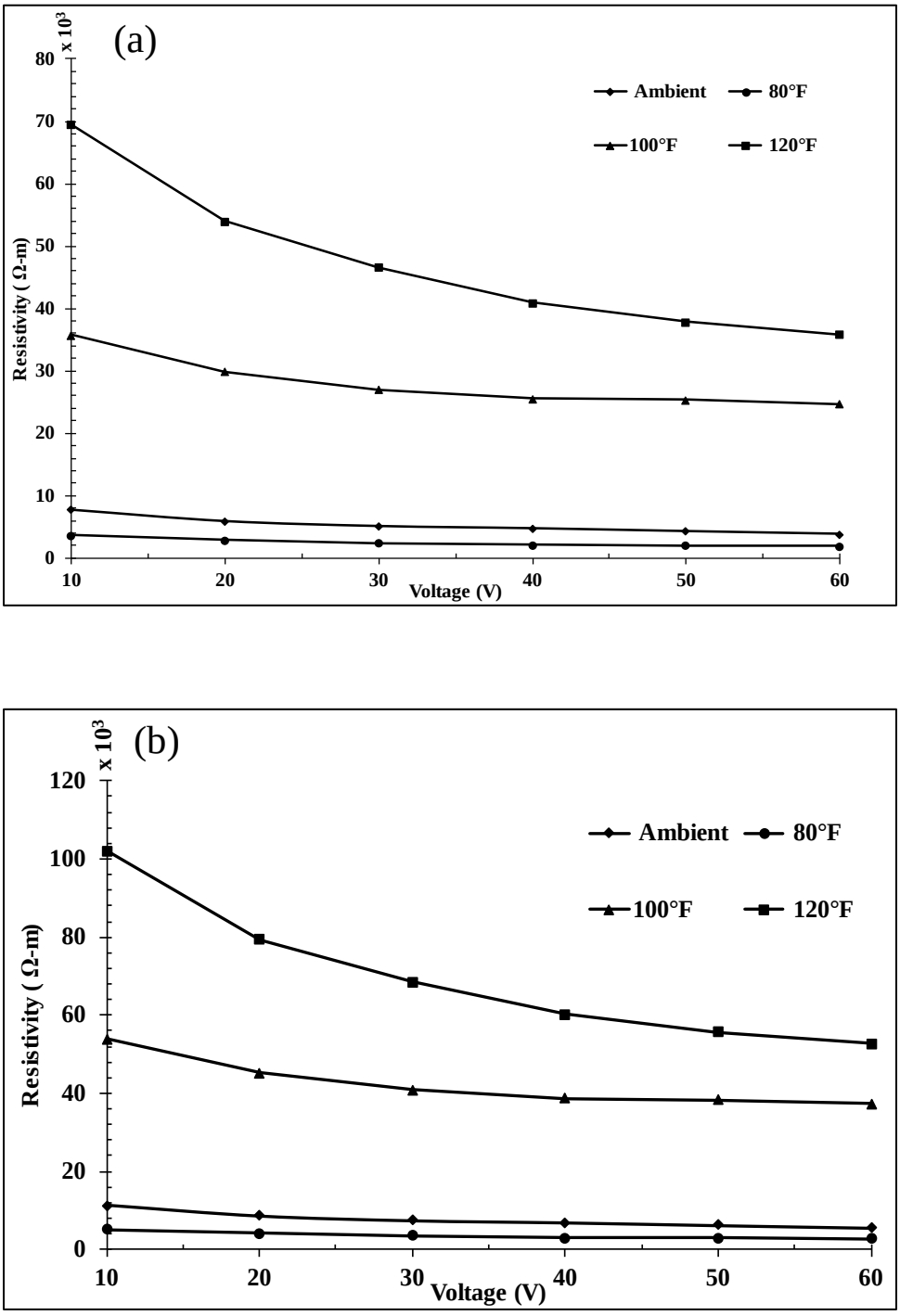

Figure 46 Resistivity of mix FGC1.2-1.0. (a) 14 days, and (b) 28 days

4.2.3) 1.5 % fiber content:

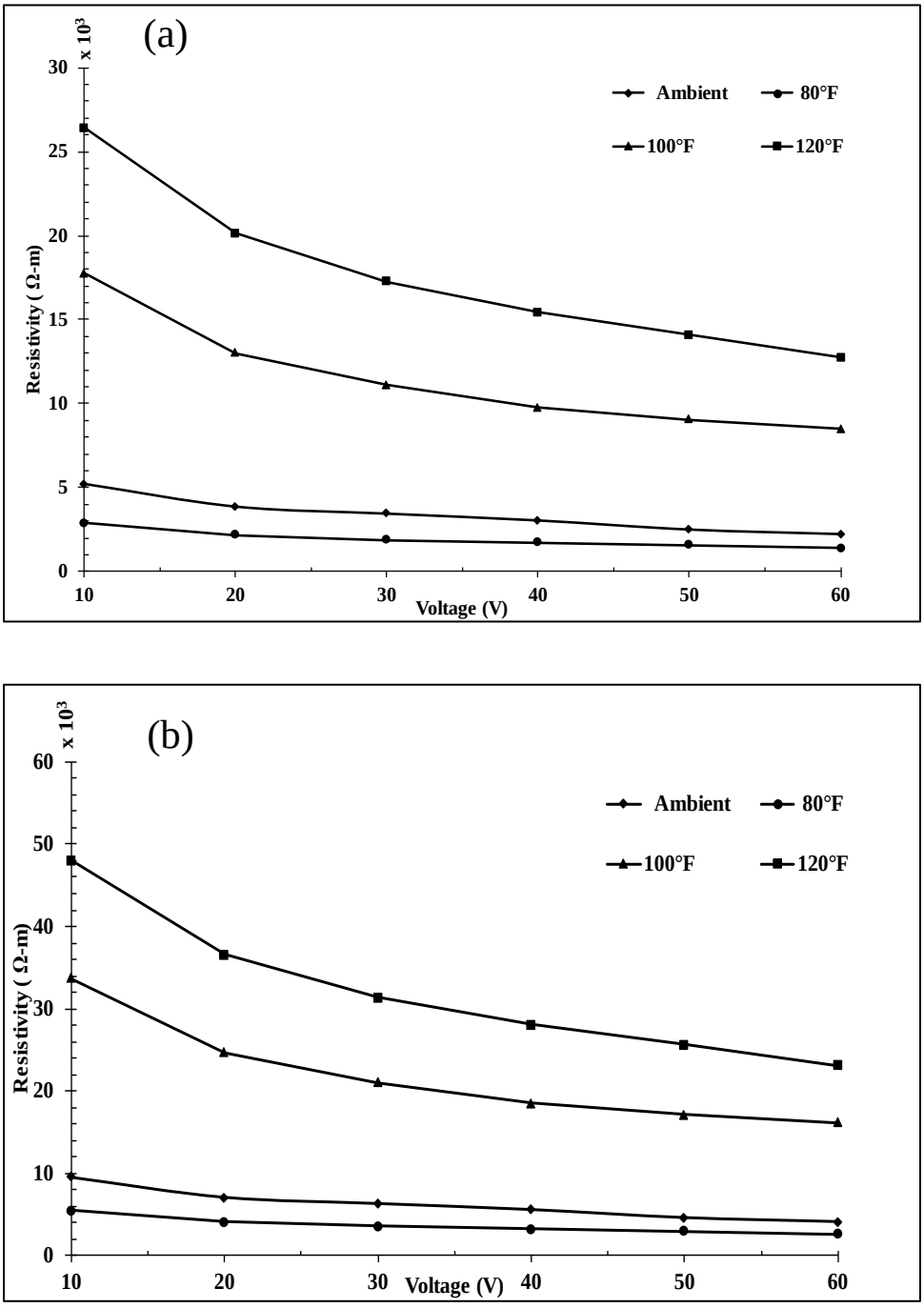

Figure 47 Resistivity of mix FGC1.2-1.5. (a) 14 days, and (b) 28 days

From the electrical conductivity experiment results, less than $5x10^3$ Ω*m resistivity is reached. To apply this material in pavement, it takes about 10 minutes to melt 1g ice on 1 in^2 surface (about 0.07 in thick ice over the surface). For a case of 1'' ice on surface, it takes about 2.4 hours to fully melt it.

Chapter 5. Freeze-thaw Test of the Suggested Geopolymer Concrete

The freeze and thaw test was carried out according to ASTM C666. Concrete beams of size 4" x 3" x 16" were prepared. According to the ASTM standard, the specimens were prepared 14 days before the starting of freeze and thaw testing. Three different percentages (0.5%, 1%, and 1.5%) of steel fiber were used in the mixture and one control mix of without steel fiber was also prepared for comparison purpose. On the 14th day, the specimens were placed into the freezer to make sure that the test is starting from the origin (0°C). After the specimens were placed into the freeze and thaw chamber as shown in Figure 48(a), the temperature on the chamber was set up according to the ASTM standard. The temperature ran from 4.44°C to -17.8°C over 1.5 hours, followed by a temperature hold at -17.8°C for 0.5 hour, and then increased from -17.8°C to 4.44°C for 1.5 hours and held at 4.44°C for 0.5 hours. Total 240 cycles were conducted and the remaining dynamic modulus of elasticity and the weight loss at each 30 cycles were measured.

Figure 48 Freeze-thaw chamber (a) and testing scheme of concrete specimen (b)

5.1 Relative dynamic modulus of elasticity

Relative dynamic modulus of different mixes is measured and shown in Figure 48. From Figure 48, we could see that the relative dynamic modulus did not change much with the number of freeze and thaw cycles and is much higher than the qualification residual dynamic modulus of elasticity (60%) for construction materials.

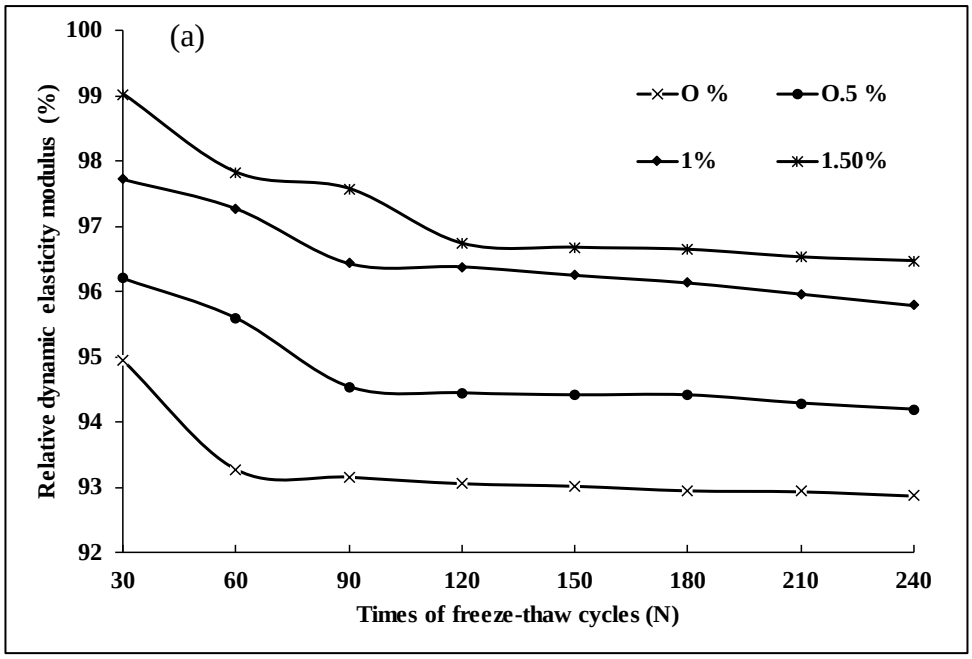

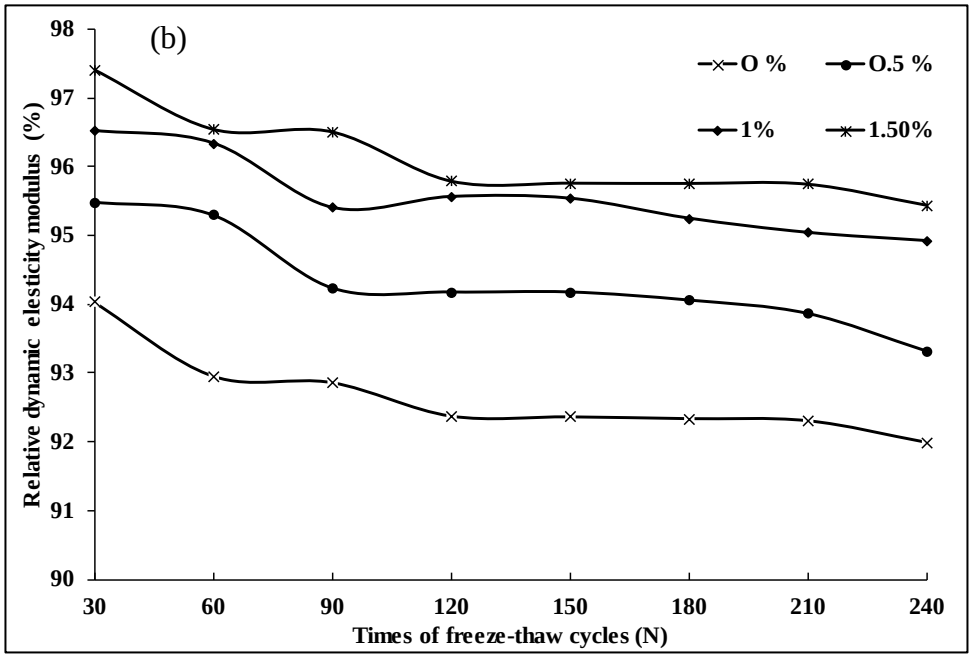

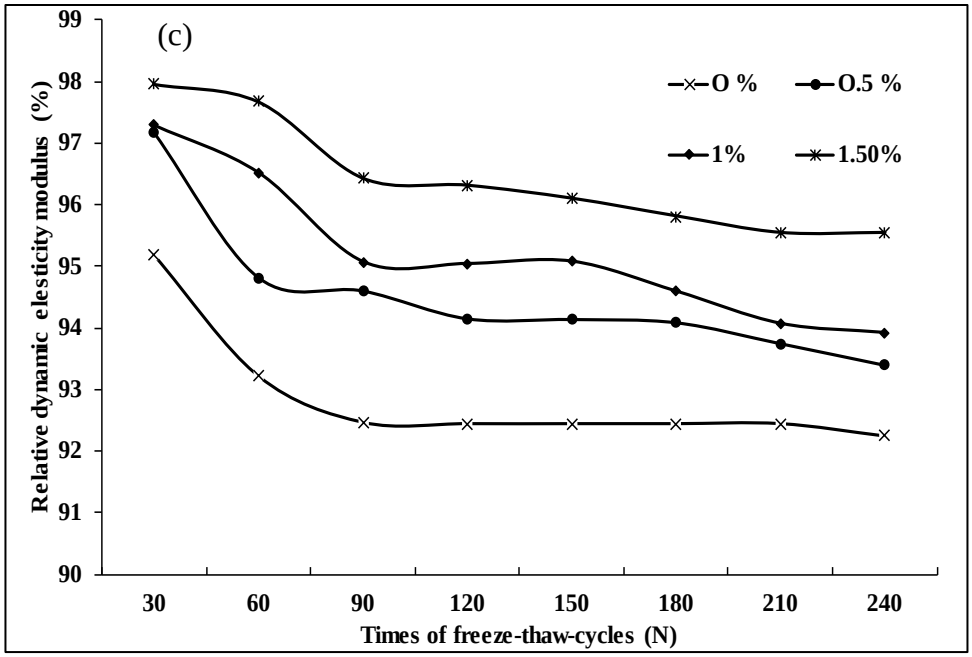

Figure 49 Variation of relative dynamic elasticity modulus with the number of freeze-thaw cycles. (a) Longitudinal (b) Transverse (c) Torsional direction testing

5.2 Mass loss

Material loss is also measured for all the mixes, which are shown in Figure 49. The suggested mixes show less than 0.3% mass loss, which qualifies them to be used in road constructions (1%).

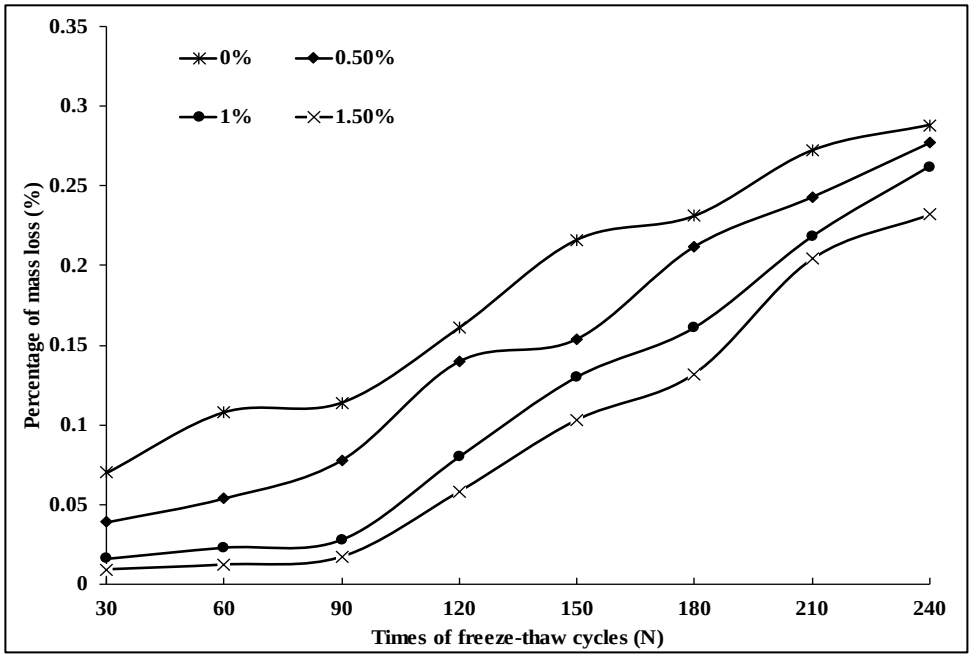

Figure 50 Variation of mass loss (%) with the number of freeze-thaw cycles.

From Figure 49, the mass loss of all candidate mixes is very small (about 0.3%), much less than the conventional concrete does (around 0.6-0.7%). The current mass loss of the geopolymer concrete also fulfills the ASTM durability requirement of concrete materials in construction, which is 1%.

Chapter 6. Pull-off Adhesion Test

The pull-off adhesion test was performed according to ASTM D4541 through a portable pull-off adhesion testing device. The geopolymer concrete beams of size 4” x 4” x 12” were prepared. Similar sizes of OPC based concrete were also prepared and tested for the comparison purpose. Four different percentages of steel fibers (0%, 0.5%, 1% and 1.5%) were used. On the 28th day of sample preparation, the surface of beam was cleaned using sand paper and wiped using wet wipes. The epoxy based paint permitted by NDDOT was applied on the concrete beam surface and left for 48 hours.

In order to permit the use of geopolymer concrete for roadway constructions along the roadway markings, how the markings bond with the new geopolymer concrete needs to be measured. For measuring this, epoxy glue was first applied to the 20 mm dolly and then the dolly was pressed tightly to the painted concrete surface until initially cured (Figure 50(a)). For each beam surface three dollies were used and the average value of the pull-off strength was calculated. Once the dolly was attached, the sample was left for curing for 24 hours. After 24 hours, the pull-off test was performed by securing the loading fixture normal to the surface of the painted beam. Tensile load was applied to the pull-off adhesion testing device and continuously increased until a piece of material is detached from the surface. The load at which the paint came off was recorded. Figure 50(b) showed the testing set up for the pull-off adhesion test, while the bond strengths recorded were given in Table 4.

Figure 51 shows the dollies after test. In case of geopolymer concrete, we can see that some pieces of concrete were detached from the surface and came out with dolly when the maximum pull-off forces were reached. In case of OPC based concrete, only the painting and dolly were detached from the concrete surface. The tensile pull-off strength is slightly more in case of OPC based concrete compared to these of geopolymer concrete, which is reasonable since the tensile strength of geopolymer concrete is lower than that of conventional concrete but the bond between the paint and geopolymer concrete is very good.

Table 4 Bond Strength between painted dolly and concrete surface

Mix	Bond Strength(psi)	Mix	Bond Strength (psi)
OPC with 0% fibers	434.67	FGC1.2-0.0	332.47
OPC with 0.5% fibers	467.51	FGC1.2-0.5	401.42
OPC with 1.0% fibers	521.43	FGC1.2-1.0	451.71
OPC with 0.5% fibers	535.20	FGC1.2-1.5	492.34

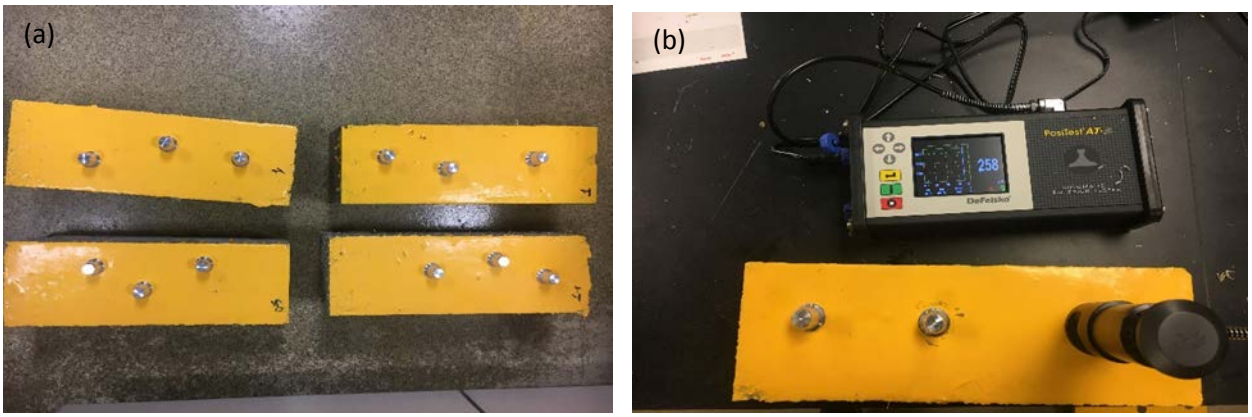

Figure 51 Placing dolly on painted concrete surface (a) and testing instrument set up (b)

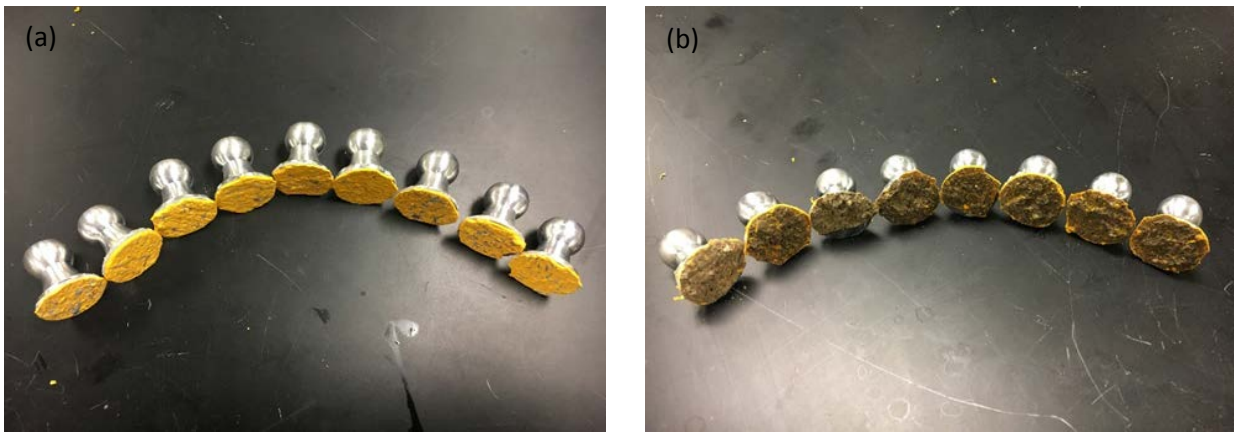

Figure 52 Dollies after pull-off adhesion test; (a) OPC based concrete and (b) Geopolymer concrete

Chapter 7. Maturity Test

Geopolymer concrete maturity test was conducted according to ASTM C1074.

7.1 Concrete cylinder maturity test

Six 6” in diameter with 12” in height geopolymer concrete cylinders were prepared for the maturity test. The real time maturity index (temperature-time factor) was measured using the maturity meter shown in Figure 52. The purpose of the maturity test is to know about the time when the concrete reaches the desirable amount of strength. The maturity test starts when the sample was made, correspondingly the compressive strength testing of similar samples on 1, 3, 7, 14 and 28 days was conducted. For this experiment we prepared the geopolymer concrete samples with 0%, 0.5%, 1%, and 1.5% fiber content.

Figure 53 Testing set up for real time maturity measurement

Figure 52 shows the testing set up for maturity measurement, which records the change in temperature inside the geopolymer concrete specimens automatically. After 28 days, the data from the maturity meter were imported into the computer and a relationship between the maturity index and the compressive strength was plotted. Figure 53 shows the plot between the temperature time factor measured by the maturity meter and the compressive strength of the geopolymer concrete specimens.

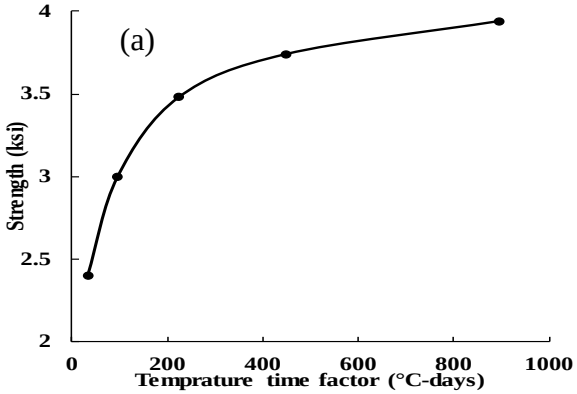

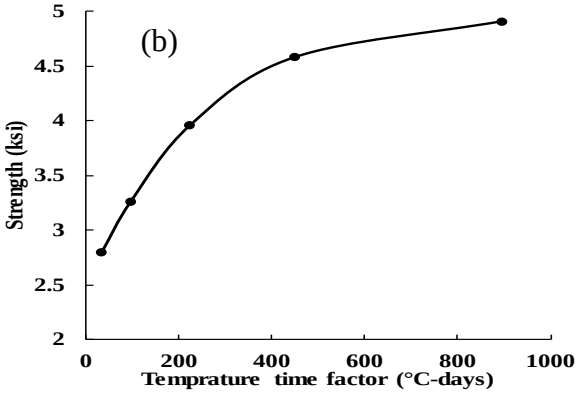

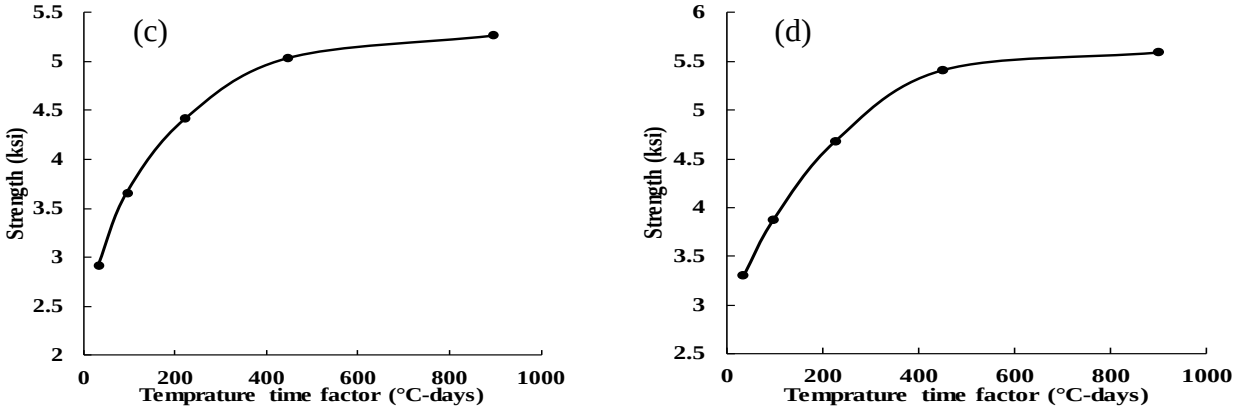

Figure 54 Relationship between compressive strength and the temperature-time factor for different percentage of fiber inclusions, (a) 0%, (b) 0.5%, (c) 1%, and (d) 1.5% steel fiber.

From Figure 53, we can see that the time required for the geopolymer concrete to become mature depends upon the percentage of the fibers on the concrete specimens. However, the geopolymer concrete with zero percentage of fibers (without fibers content) achieved the 3 ksi compressive strength within 6 hours of curing, while other mixes reached the 3 ksi strength even earlier, which qualifies all these mixes for accelerated pavement repairs.

7.2 Concrete beam maturity test

As similar in concrete cylinder maturity test, the geopolymer concrete beam of size 3" x 4" x 18" beam were prepared. The maturity meter sensor was connected in a similar way as shown for the cylinder in Figure 53. Along with the real time temperature change measurement using the maturity meter, the flexural strength of the similar mix specimens were carried out on 1, 3, 7, 14, and 28 days. After 28 days the temperature time factor data was extracted from the maturity meter and plotted with the flexural strength of the beams. Figure 54 shows the plots between the temperature time factor and flexural strength of the geopolymer concrete beams.

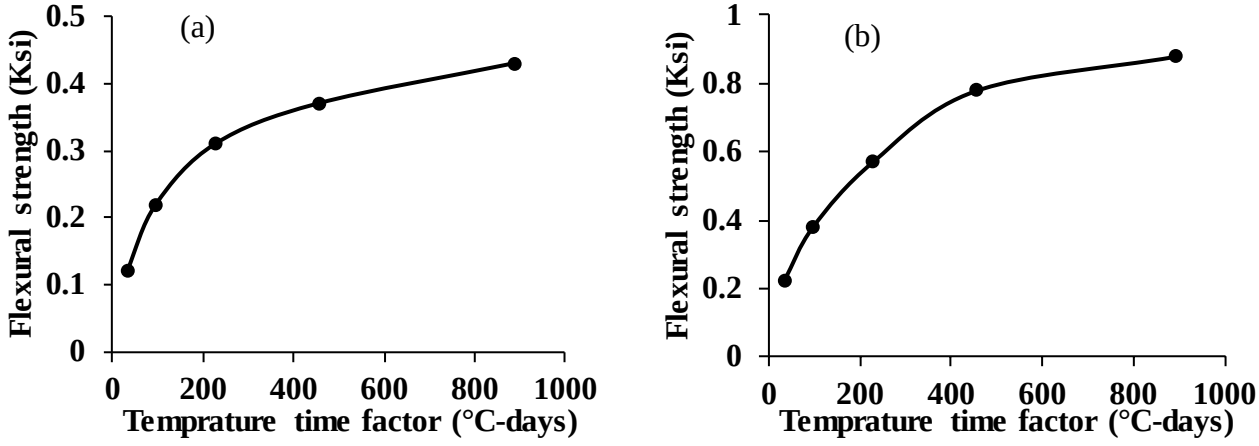

Figure 55 Relationship between flexural strength and temperature-time factor, (a) 0.5%, and (b) 1.5%, steel fiber.

From Figure 54, we can see that the flexural strength of the geopolymer concrete beam increased with increase in the curing time. The flexural strength of the concrete beam with 0.5% steel fiber was found to be 0.12 at 1 day and 0.43 Ksi at 28 days. Similarly the flexural strength of the concrete with 1.5% of steel fiber was found 0.22 Ksi on 1 day and 0.88 after 28 days of curing. The change on the temperature inside the specimen was found to be varied more at the initial days of the curing. After 14 days of curing, the temperature was found to be remaining almost constant. In both cases of the fiber percentage, the flexural strength of the geopolymer concrete beam was found to be above 350 psi (0.35 Ksi) in between 7 to 14 days of curing. This result seems not consistent with the cylinder compression test conclusion. Further tests are suggested to calibrate this test outcome.

Chapter 8. Air Content Test

Air content test of the fresh geopolymer concrete was carried out per ASTM C231. Forney LA-0316 Air meter/Press-Aire meter was used to measure the air content. Before starting the test, the fresh concrete mix was prepared. The 0.25 ft^3 of bucket was filled by freshly prepared geopolymer concrete in three layers. Each layer was rodded by using a tamping rod for 25 times, followed by striking the outside of the bucket using rubber mallet. When the bucket was filled out, the top surface was levelled and made smooth, and the surface of the bucket was cleaned. Then the upper part of the instrument was attached and clamped (Figure 55). The main valve was kept closed and water was placed from one of the branch valve using syringe. Once the water was filled and started to come out from another side of the branch valve, both branch valve were closed. The device was the pressurized by using the built-in hand pump until zeroed out (or as calibrated). After a stabilization period of 5 seconds, the pressure was released from the main valve gradually and the dial on the top of the meter was recorded as the air content of the fly ash geopolymer concrete. From the test results, the air content of the geopolymer concrete was found to be 0.8%.

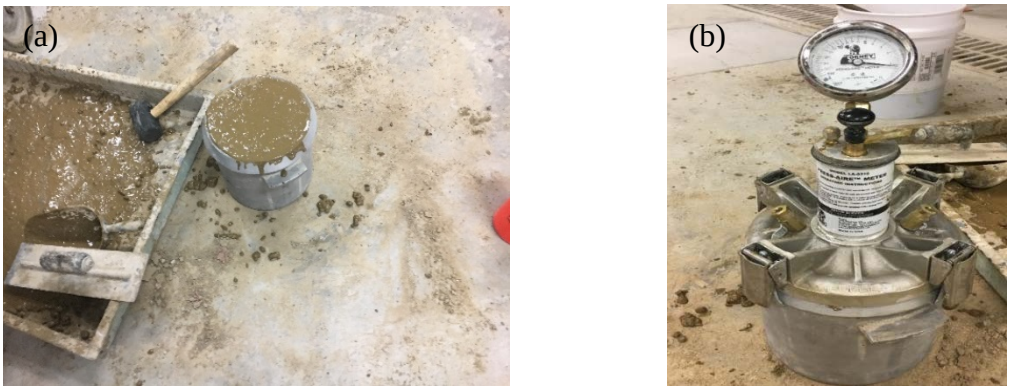

Figure 56 Air content measurement of the fresh geopolymer concrete per ASTM 321, (a) Fill the container of the air meter, (b) Air content measurement result after pressure releasing

Chapter 9. Conductivity of the Suggested System when Cracking

Beam specimens of 3 x 4 x 16 inches were prepared with man-made longitudinal and transverse cracking. The thickness of the cracks was set to be 1/8 inch and the depth was 1.33 inch. The samples were prepared by using three percentages of the steel fibers i.e. 0.5%, 1%, and 1.5% as before. Four different curing conditions were applied by varying the curing temperature from ambient to 80°F, 100°F, and 120°F. The samples were put on the elevated temperature for initial 24 hours and left to be cured in ambient conditions. The test setup is shown in Figure 56. The resistivity of both longitudinal and transverse cracked samples was measured at 14 and 28 days of curing.

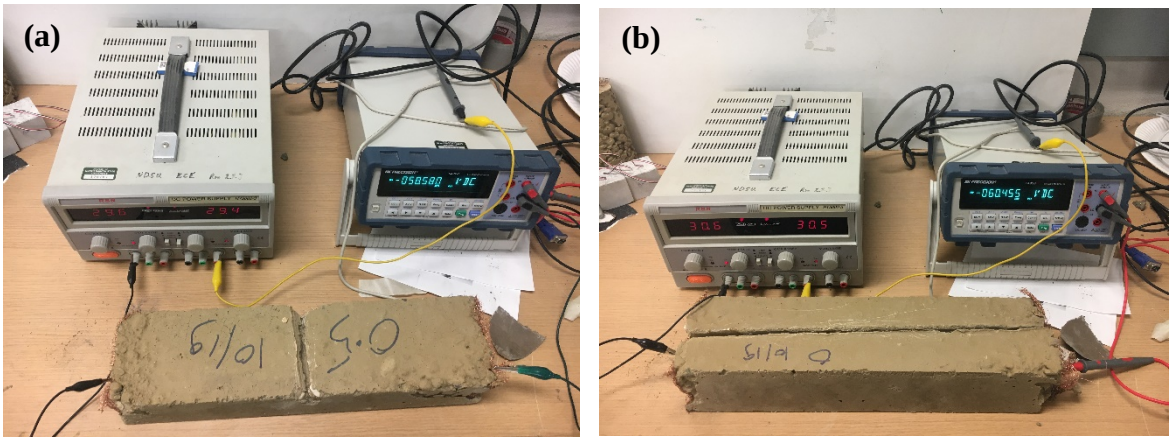

Figure 57 Resistivity measurement of specimens with longitudinal crack (a) and transverse crack (b)

9.1 Resistivity measurement of longitudinally cracked specimens

9.1.1) 0.5% fiber content:

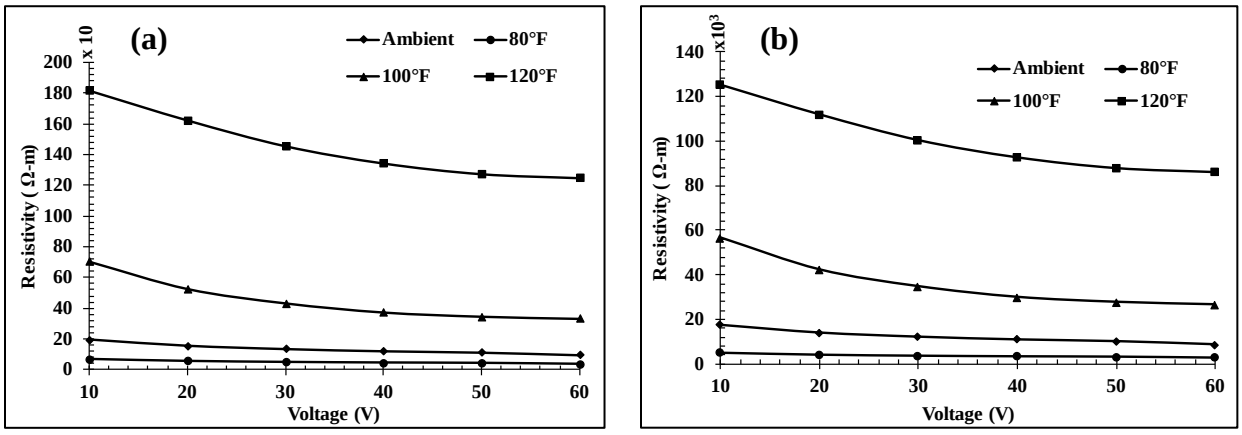

Figure 58 Resistivity of mix longitudinally cracked specimen with 0.5% steel fiber (a) 14 days, and (b) 28 days

9.1.2) 1.0% fiber content

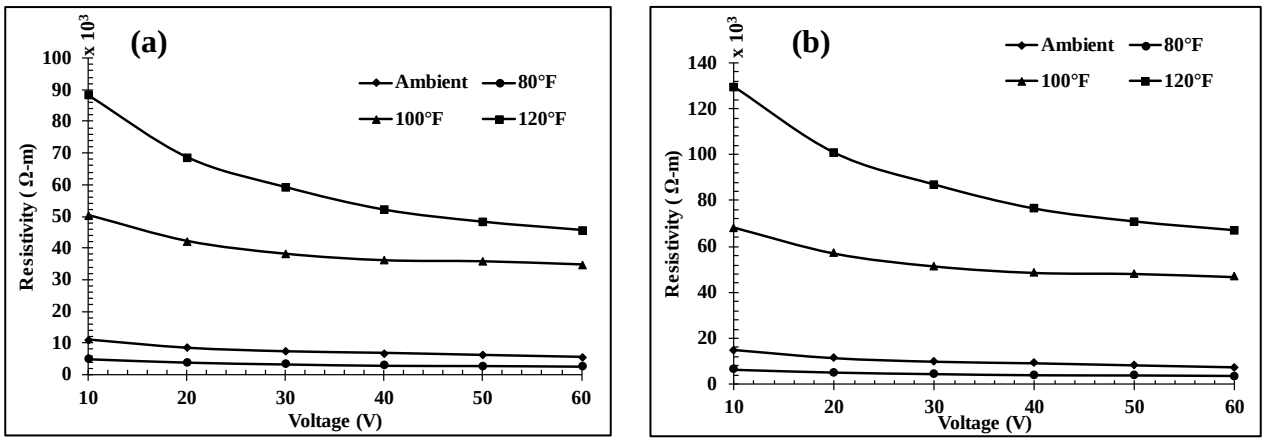

Figure 59 Resistivity of mix longitudinally cracked specimen with 1.0% steel fiber (a) 14 days, and (b) 28 days

9.1.3) 1.5% fiber content

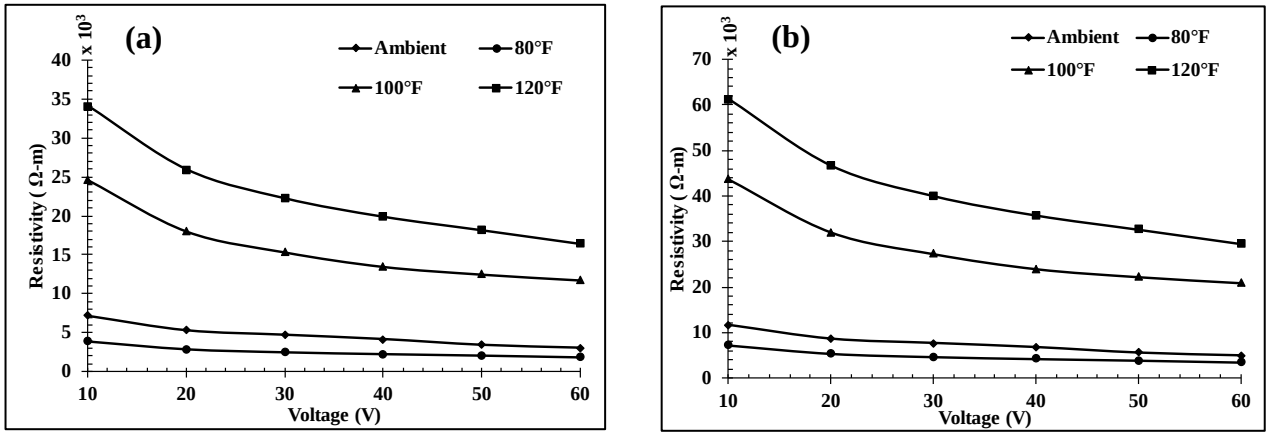

Figure 60 Resistivity of mix longitudinally cracked specimen with 1.5% steel fiber (a) 14 days, and (b) 28 days

9.2 Resistivity measurement of transversely cracked specimens

9.2.1) 0.5% fiber content

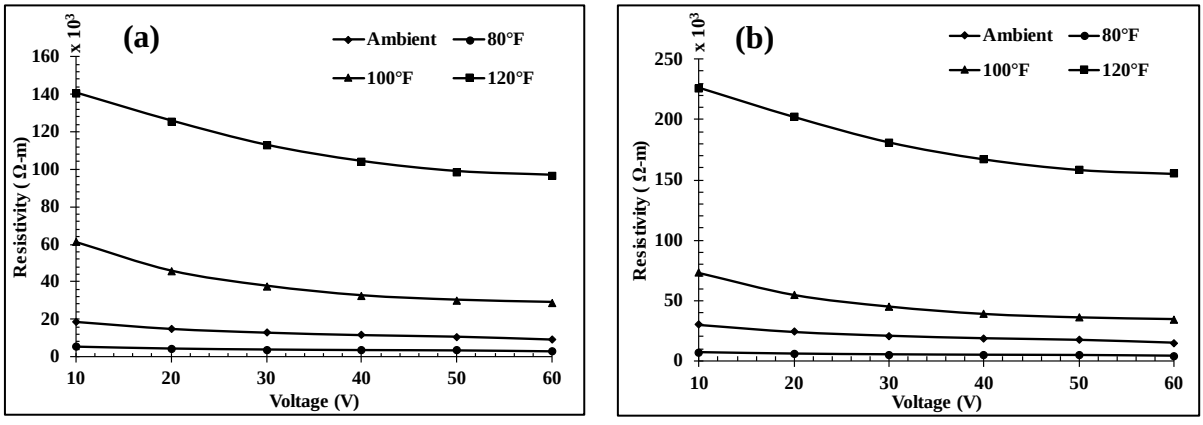

Figure 61 Resistivity of mix transversely cracked specimen with 0.5% steel fiber (a) 14 days, and (b) 28 days

9.2.2) 1.0% fiber content

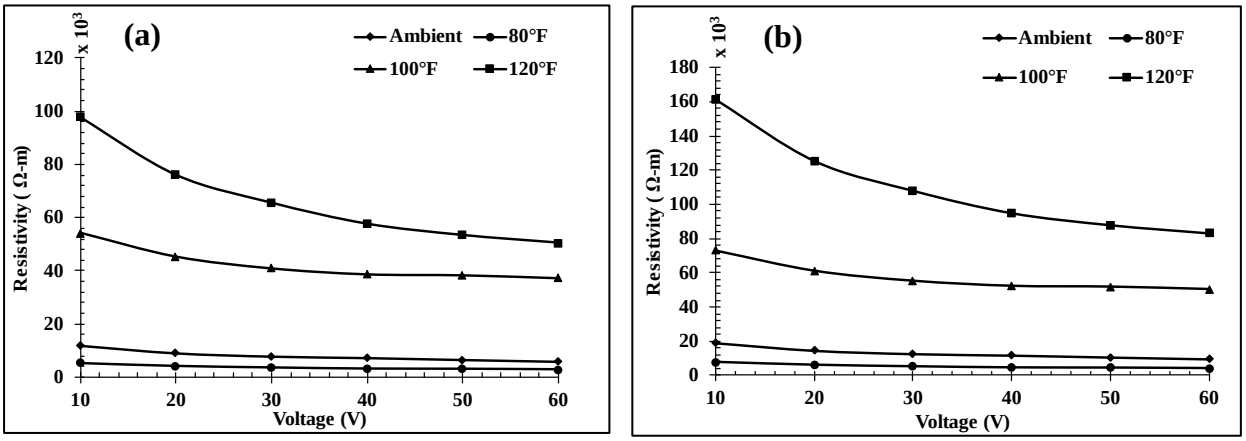

Figure 62 Resistivity of mix transversely cracked specimen with 1.0% steel fiber (a) 14 days, and (b) 28 days

9.2.3) 1.5% fiber content

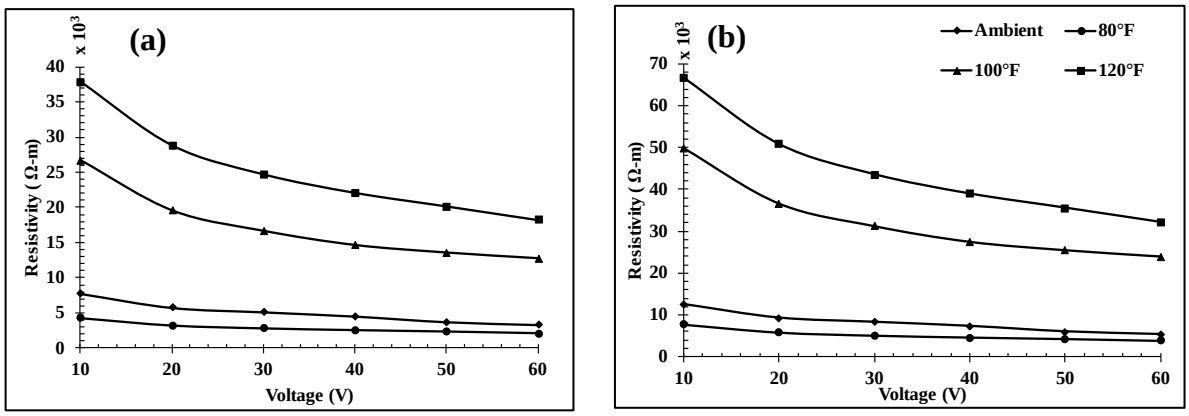

Figure 63 Resistivity of mix transversely cracked specimen with 1.5% steel fiber (a) 14 days, and (b) 28 days

From Figures 57-62, one can see that the resistivity of the specimen with longitudinal crack is less as compared to the transverse crack. It also shows that the resistivity of specimen with longitudinal crack is 1.5 to 2 times more as compared to healthy specimen whereas the resistivity of specimen with transverse crack is 1.7 to 2.5 times more as compared to the healthy specimen. However cracks in these cracks do not break the existing circuit and the reasonable electric conductivity could still provide a viable approach to melt snow and ice on its surface.

Chapter 10. Melting Test for Marking Reveals Under Controlled Temperatures

The selected three mixes were poured and cured using the room temperature curing, with an additional benchmark specimen (Table 5). The NDDOT Epoxy based pavement markings with standard glass beads and Epoxy pavement markings are deployed on the top of the specimens. The formed base and marking system is stored in a freezer and kept in different control temperatures. The setup was then subjected to power supplied heating through the geopolymer concrete. Their corresponding energy consumptions to melt different thickness snow are measured and compared with the theoretical calculations.

The power supply is provided through the outlet in the material laboratory and connected through the power connectors embedded in the fly ash geopolymer concrete as shown in Figure 64(b).

Table 5 Mix design used for snow melting test

Melting test mix design								
NO #	Steel Fiber %	Fly Ash (g)	Sand (g)	Aggregate (g)	Na_2SiO_3 (g)	NaOH (g)	Extra Water (g)	Steel Fiber (g)
3	0%	1700	3400	5100	705.07	140.3	145.2	0
3	0.50%	1700	3400	5100	705.07	140.3	145.2	184
3	1%	1700	3400	5100	705.07	140.3	145.2	368
3	1.50%	1700	3400	5100	705.07	140.3	145.2	552.2

Three beams of 4x3x16 in. were prepared for each mixes and three different thickness of snow depth was used. Two types of snow with density 0.46 g/ml (heavy) and 0.23 g/ml (fluffy) were used for the experiment. P3 international P4460 Kill A Watt EZ electricity usage meter as shown in Figure 64(a) was used to measure the total amount of energy used to melt the specific thickness of the snow. The snow was placed on the surface of section 4 in x 16 in and the specimen was put inside a refrigerator to maintain the temperature. Three temperatures of -10°C, -15°C, and -20°C were used to perform this test. Figure 64 illustrates the circuit used in this experiment.

Table 6 shows the total energy and time required to melt 0.5 in., 1 in., and 1.5 in. snow for the different mixes used for this experiment. Let's assume pure water, which enthalpy of fusion is 334 J/g. So, a cubic inch of ice is 16.4 mL, or 14.8 g. Therefore, to melt a cubic foot of snow (equivalent to a cubic inch of ice, considering the densification ratio from snow to ice is 12) at 32^oF degrees, it consumes nearly 4,943 J. This can come in the form of sunlight or elevated the temperatures above 32^oF. If melting it over a time of 1 hour, this is a power of 1.37 Watts. Considering the specimen with an 1 in snow on top of the surface, the snow volume needs to be melted is 64 in^3, which will consume 0.0507 watt * hour in energy. From the experiment data in

Tables 6-8, the suggested geopolymer is a very good pavement material that could convert the electrical power energy efficiently and perform the desired functions successfully.

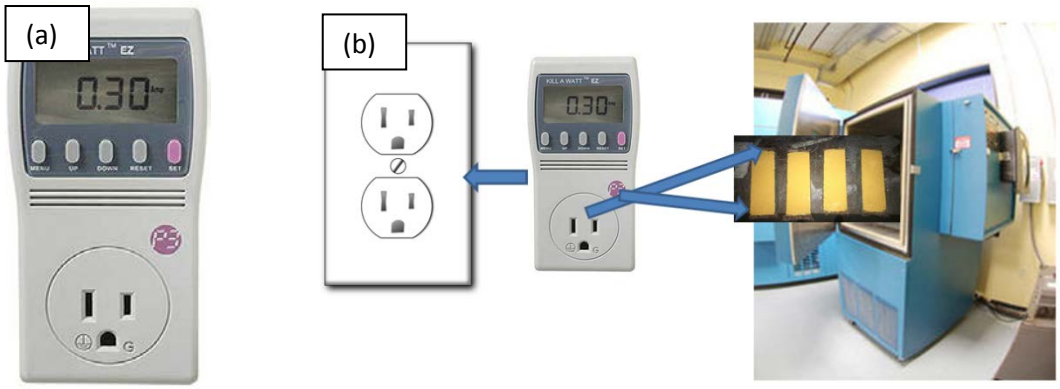

Figure 64 Energy meter (a) and circuit diagram (b) used for the melting test experiment

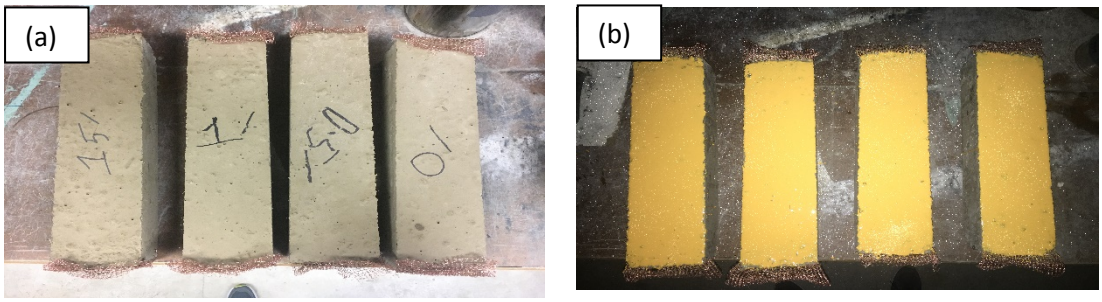

Figure 65 Beam specimen (a) and Epoxy based Painted beam specimen to mimic the road pavement (b)

Table 6 Energy and time required to melt 0.5 inch, 1 inch and 1.5 inch of snow at -20 °C

Mix	Snow Type	Snow Depth	Time taken for complete melting	Total Energy consumed (Watt)
0% Fiber	Heavy	0.5 inch	1 hour 15 minutes	0.16
0% Fiber	Heavy	1 inch	1 hour 40 minutes	0.23
0% Fiber	Heavy	1.5 inch	2 hours 30 minutes	0.25
0.5% Fiber	Heavy	0.5 inch	1 hour 30 minutes	0.18
0.5% Fiber	Heavy	1 inch	1 hour 50 minutes	0.19
0.5% Fiber	Heavy	1.5 inch	2 hours 25 minutes	0.17
1% Fiber	Heavy	0.5 inch	1 hour 10 minutes	0.18
1% Fiber	Heavy	1 inch	1 hour 25 minutes	0.18
1% Fiber	Heavy	1.5 inch	2 hours 15 minute	0.19
1.5% Fiber	Heavy	0.5 inch	1 hour	0.12
1.5% Fiber	Heavy	1 inch	1 hour 20 minutes	0.17
1.5% Fiber	Heavy	1.5 inch	1 hour 35 minutes	0.25
0% Fiber	Fluffy	0.5 inch	55 minutes	0.12
0% Fiber	Fluffy	1 inch	1 hour 25 minutes	0.15
0% Fiber	Fluffy	1.5 inch	1 hour 40 minute	0.21
0.5% Fiber	Fluffy	0.5 inch	55 minutes	0.14
0.5% Fiber	Fluffy	1 inch	1 hour 10 minutes	0.15
0.5% Fiber	Fluffy	1.5 inch	1 hour 20 minutes	0.17
1% Fiber	Fluffy	0.5 inch	35 minutes	0.05
1% Fiber	Fluffy	1 inch	1 hour	0.04
1% Fiber	Fluffy	1.5 inch	1 hour 20 minutes	0.08
1.5% Fiber	Fluffy	0.5 inch	40 minutes	0.04
1.5% Fiber	Fluffy	1 inch	50 minutes	0.04
1.5% Fiber	Fluffy	1.5 inch	55 minutes	0.07

Table 7 Energy and time required to melt 0.5 inch, 1 inch and 1.5 inch of snow at -15 °C

Mix	Snow Type	Snow Depth	Time taken for complete melting	Total Energy consumed (Watt)
0% Fiber	Heavy	0.5 inch	1 hour 10 minutes	0.13
0% Fiber	Heavy	1 inch	1 hour 40 minutes	0.23
0% Fiber	Heavy	1.5 inch	2 hours 15 minutes	0.22
0.5% Fiber	Heavy	0.5 inch	1 hour 10 minutes	0.16
0.5% Fiber	Heavy	1 inch	1 hour 35 minutes	0.18
0.5% Fiber	Heavy	1.5 inch	2 hours 15 minutes	0.18
1% Fiber	Heavy	0.5 inch	1 hour	0.18
1% Fiber	Heavy	1 inch	1 hour 20 minutes	0.17
1% Fiber	Heavy	1.5 inch	1 hour 50 minute	0.19
1.5% Fiber	Heavy	0.5 inch	50 minutes	0.10
1.5% Fiber	Heavy	1 inch	1 hour 10 minutes	0.18
1.5% Fiber	Heavy	1.5 inch	1 hour 25 minutes	0.21
0% Fiber	Fluffy	0.5 inch	50 minutes	0.10
0% Fiber	Fluffy	1 inch	1 hour 15 minutes	0.13
0% Fiber	Fluffy	1.5 inch	1 hour 30 minutes	0.18
0.5% Fiber	Fluffy	0.5 inch	45 minutes	0.13
0.5% Fiber	Fluffy	1 inch	1 hour 10 minutes	0.16
0.5% Fiber	Fluffy	1.5 inch	1 hour 15 minutes	0.18
1% Fiber	Fluffy	0.5 inch	30 minutes	0.04
1% Fiber	Fluffy	1 inch	55 minutes	0.06
1% Fiber	Fluffy	1.5 inch	1 hour 10 minutes	0.07
1.5% Fiber	Fluffy	0.5 inch	35 minutes	0.02
1.5% Fiber	Fluffy	1 inch	40 minutes	0.03
1.5% Fiber	Fluffy	1.5 inch	55 minutes	0.04

Table 8 Energy and time required to melt 0.5 inch, 1 inch and 1.5 inch of snow at -10 °C

Mix	Snow Type	Snow Depth	Time taken for complete melting	Total Energy consumed (Watt)
0% Fiber	Heavy	0.5 inch	1 hour 20 minutes	0.12
0% Fiber	Heavy	1 inch	1 hour 35 minutes	0.20
0% Fiber	Heavy	1.5 inch	2 hours 10 minutes	0.21
0.5% Fiber	Heavy	0.5 inch	1 hour	0.16
0.5% Fiber	Heavy	1 inch	1 hour 30 minutes	0.19
0.5% Fiber	Heavy	1.5 inch	2 hours 15 minutes	0.18
1% Fiber	Heavy	0.5 inch	1 hour	0.17
1% Fiber	Heavy	1 inch	1 hour 40 minutes	0.18
1% Fiber	Heavy	1.5 inch	1 hour 55 minute	0.18
1.5% Fiber	Heavy	0.5 inch	50 minutes	0.08
1.5% Fiber	Heavy	1 inch	1 hour	0.17
1.5% Fiber	Heavy	1.5 inch	1 hour 15 minutes	0.19
0% Fiber	Fluffy	0.5 inch	50 minutes	0.11
0% Fiber	Fluffy	1 inch	1 hour 10 minutes	0.12
0% Fiber	Fluffy	1.5 inch	1 hour 15 minute	0.17
0.5% Fiber	Fluffy	0.5 inch	40 minutes	0.10
0.5% Fiber	Fluffy	1 inch	1 hour	0.13
0.5% Fiber	Fluffy	1.5 inch	1 hour 10 minutes	0.14
1% Fiber	Fluffy	0.5 inch	30 minutes	0.04
1% Fiber	Fluffy	1 inch	45 minutes	0.03
1% Fiber	Fluffy	1.5 inch	50 minutes	0.05
1.5% Fiber	Fluffy	0.5 inch	25 minutes	0.02
1.5% Fiber	Fluffy	1 inch	40 minutes	0.03
1.5% Fiber	Fluffy	1.5 inch	50 minutes	0.03

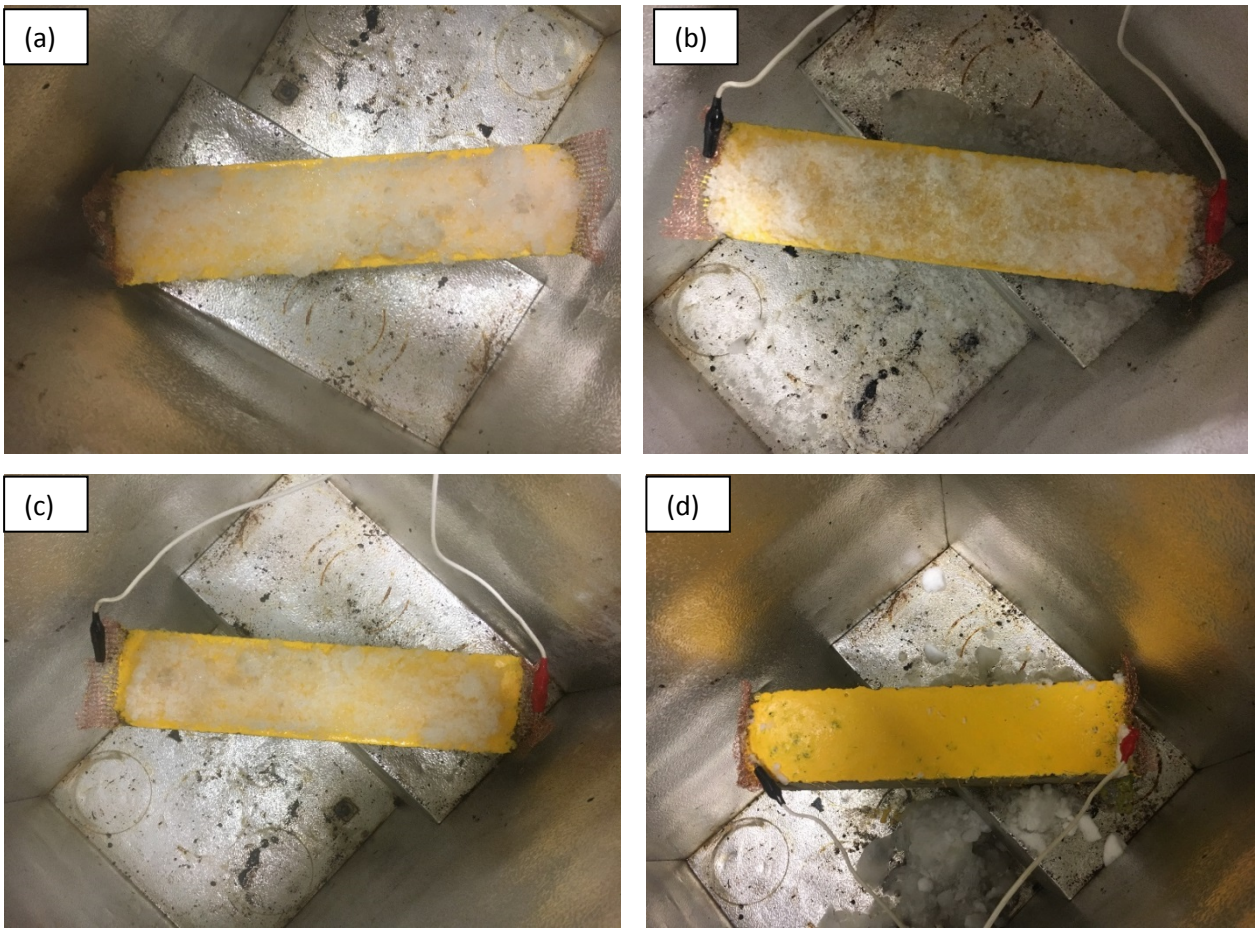

Figure 66 Melting process of Specimen with 1.5 % fiber content for 1 inch heavy snow at -15°C (a) Initial condition, (b) after 30 minutes, (c) after 1 hour, and (d) after 1 hour 10 minutes

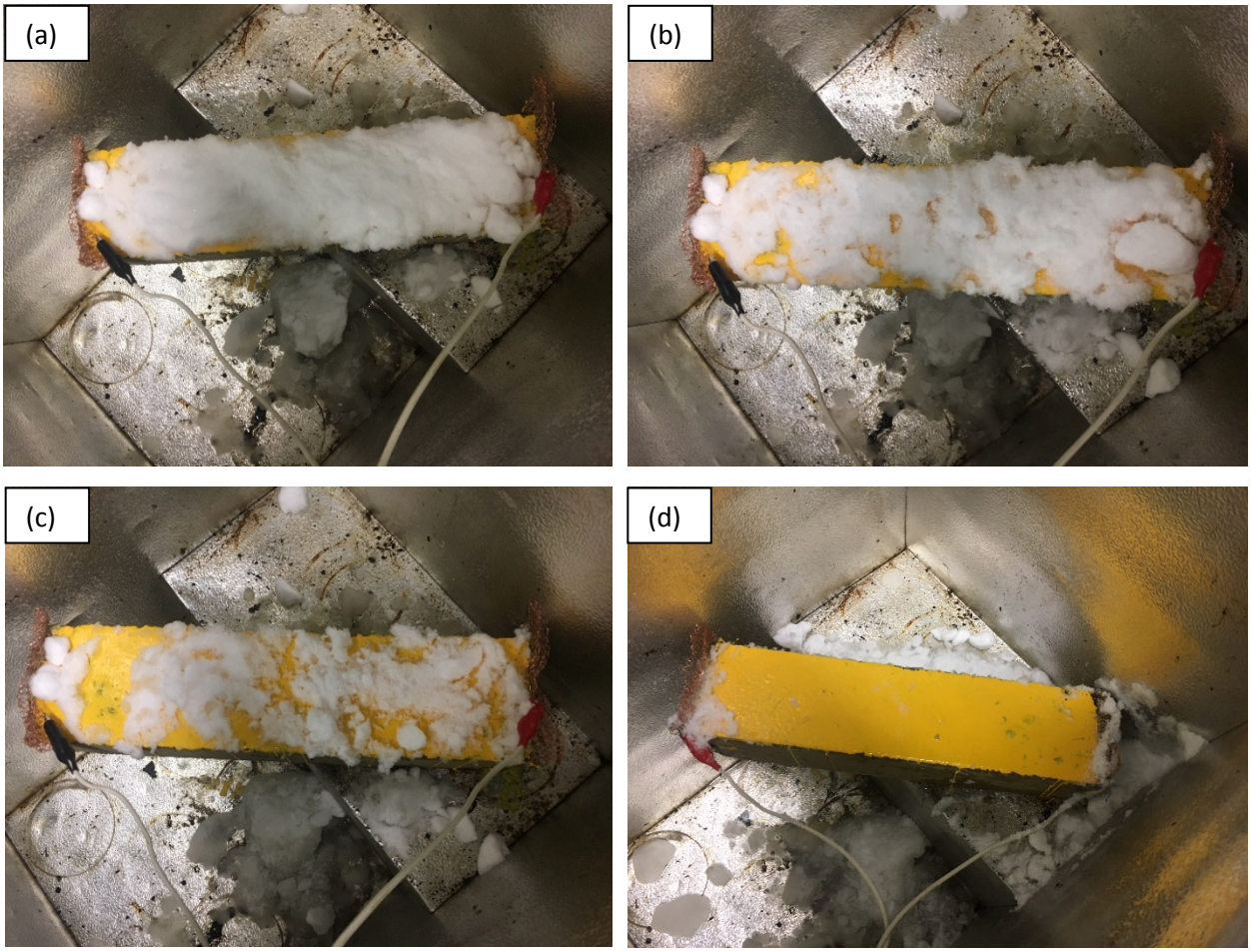

Figure 67 Melting process of Specimen with 1% fiber content for 1 inch fluffy snow at -15°C (a) Initial condition, (b) after 15 minutes, (c) after 30 minutes, and (d) after 1 hour 20 minutes

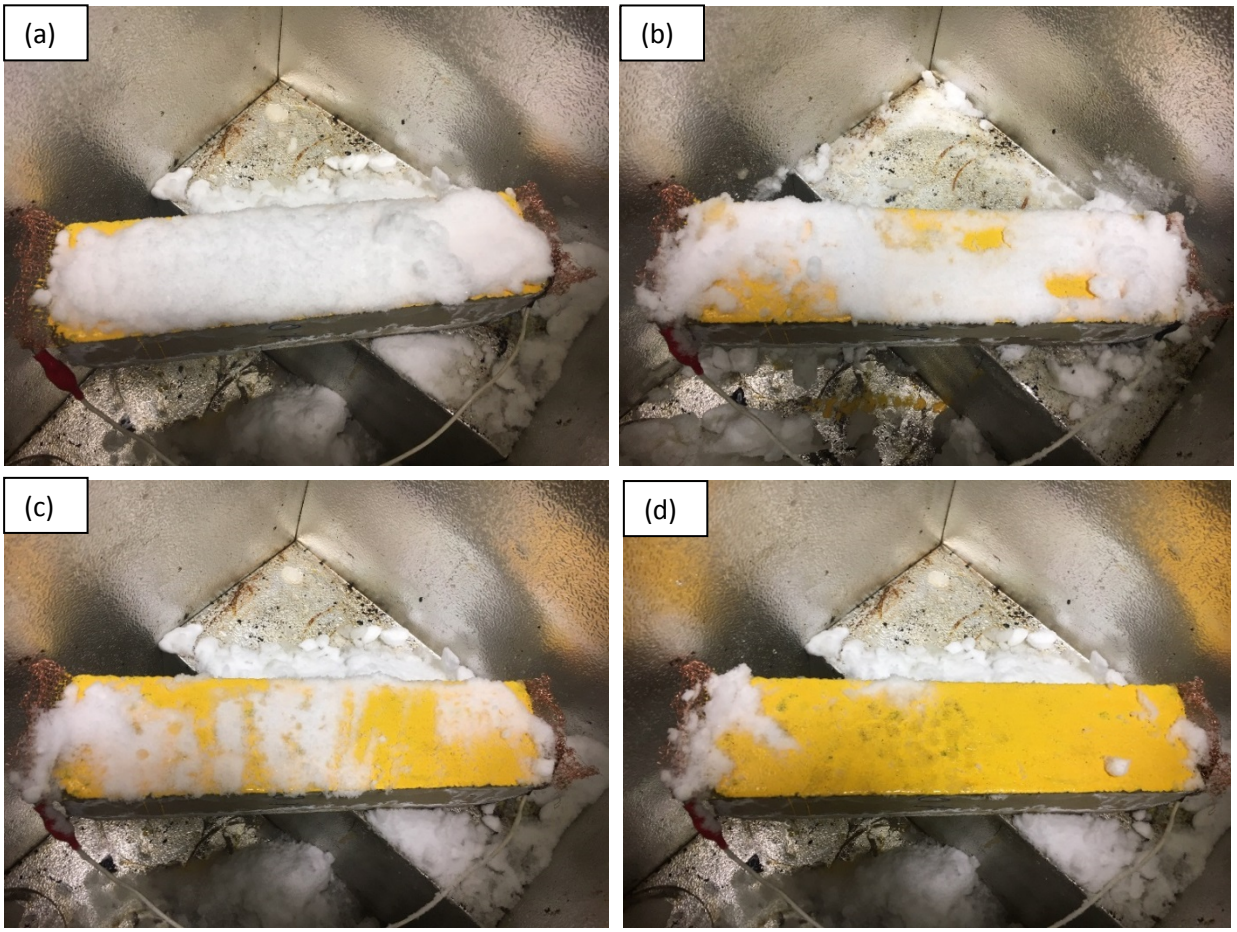

Figure 68 Melting process of Specimen with 1% fiber content for 1.5 inch fluffy snow at -20°C (a) Initial condition, (b) after 1 hour, (c) after 2 hours, and (d) after 2 hours 15 minutes

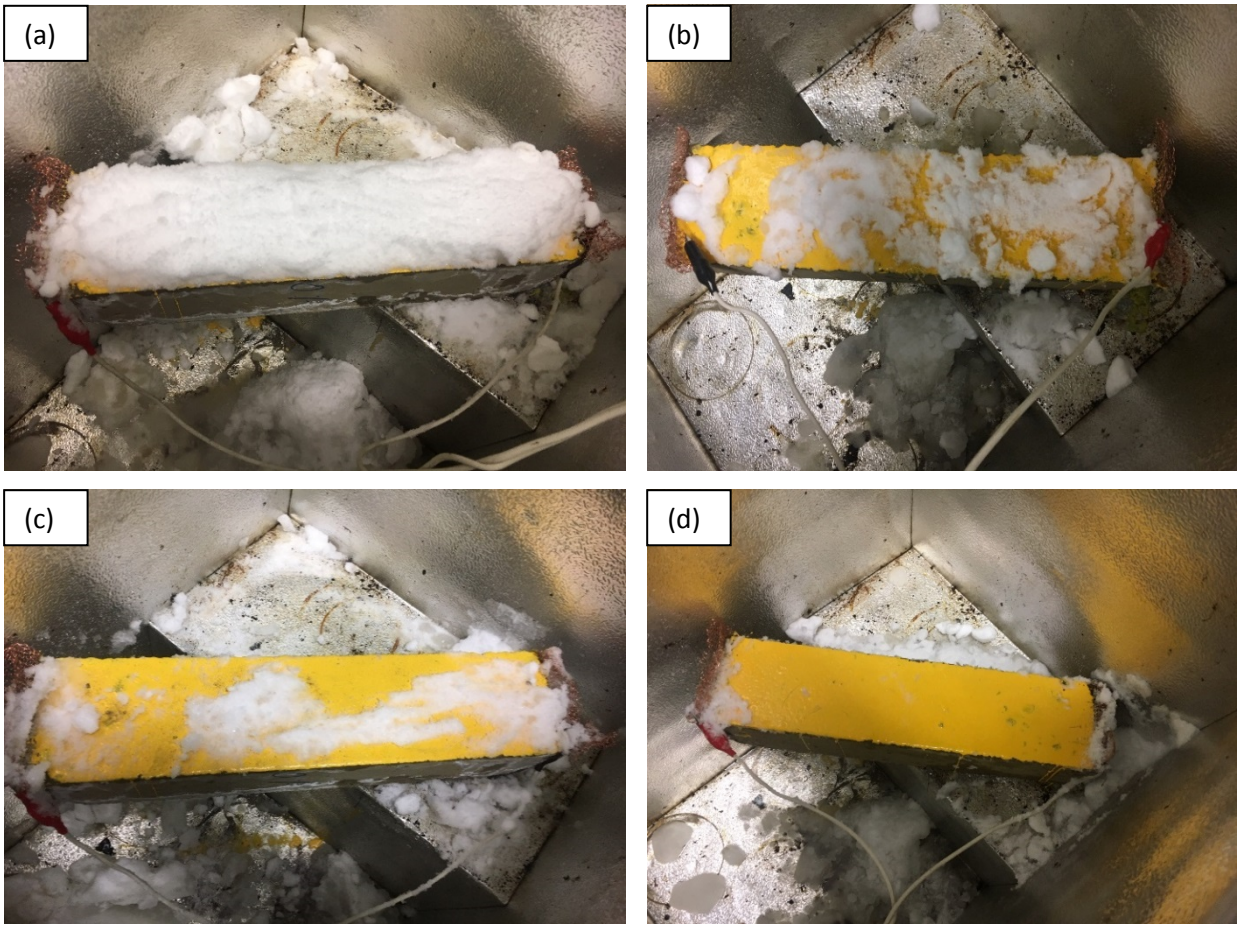

Figure 69 Melting process of Specimen with 1.5 % fiber content for 1.5 inch fluffy snow at -20°C (a) Initial condition, (b) after 40 minutes, (c) after 1 hour 20 minutes, and (d) after 1 hour 35 minutes

Chapter 11. Alternative Power Sources and Cost-effectiveness Analysis of the Suggested Snow-Proof Marking System

In a highway system, the possible power source includes the electrical energy. But there are other alternative power sources, such as solar energy. Currently there are many existing products in the market, such as solar panel powered stop signs and warning signs that could be directly adopted. The only modification of these products is rewired the connection to the pavement fly ash geopolymer concrete, instead of the traffic lights. This option will be called the off-the-shelf option. The second option is to modify the existing off-the-shelf product and optimize its energy harvesting and storage capacity. Considering the more power needed for melting ice and snow in a long distance, a new architecture of the solar panel powered power conversion and storage system is suggested in Figure 70. In Figure 70, a customized DC-DC Converter connecting the solar panel and the battery pack for the solar power maximizes power point tracking and battery charging purposes. Due to the time constraint and the budget, the design of this option has been completed, but implementation will need additional support.

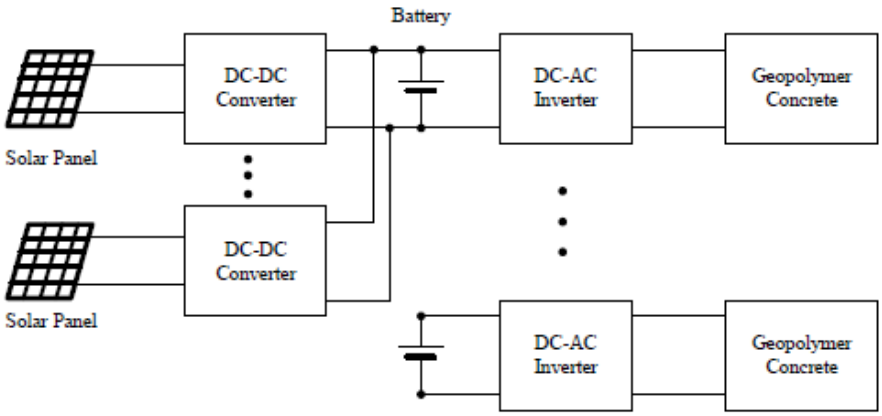

Figure 70 Customized Power Conversion and Storage System through Solar Panels

A life-cost analysis is also performed. The cost includes initial costs, operating costs, system maintenance costs and salvage values. Life-cost analysis starts with the project size, material costs, construction labor costs, and operational costs. But the benefits are obvious and include the accidents and traffic delay reduced. A detailed cost-effectiveness analysis is shown in Table 9.

Table 9 Cost-Effectiveness Analysis Per 100 Feet Markings

Estimate of project size

	amount	units	
Expected numbers of marking lines	4.00		(A)
Average finished length	304.8*100	mm	(B_1)
Average finished width	152.4	mm	(B_2)

Average finished depth	304.8	mm	(B_3)
Expected total volume of finished marking patches [(B_1 × B_2 × B_3 × A) ÷ 10^9]	5.66	m^3	(C)

MATERIAL COSTS (e.g., cold mix, cement, aggregate, sand, bonding agent, joint bond breaker, curing agent, etc.)

Material 1 = fly ash			
Material 1 Purchase Cost	0.00	$/___	(D_1)
Expected Material 1 needs	0.00	___	(E_1)
Material 1 Shipping cost	0.00	$	(F_1)
Total Material 1 Cost [(D_1 × E_1) + F_1]	0.00	$	(G_1)
Material 2 = _Alkaline solution			
Material 2 Purchase Cost	3.55	$/ lb	(D_2)
Expected Material 2 needs	837.76	Lb	(E_2)
Material 1 Shipping cost	22.82	$	(F_2)
Total Material 2 Cost [(D_2 × E_2) + F_2]	2995.47	$	(G_2)
Material 3 = Aggregate and sand			
Material 3 Purchase Cost	0.084	$/lb	(D_3)
Expected Material 3 needs	8432.67	lb	(E_3)
Material 3 Shipping cost	79.00	$	(F_3)
Total Material 3 Cost [(D_3 × E_3) + F_3]	787.34	$	(G_3)
Material 4 = Steel fiber (1%)			
Material 4 Purchase Cost	2.38	$/lb___	(D_4)
Expected Material 4 needs	363.76	lb	(E_4)
Material 4 Shipping cost	0.00	$	(F_4)
Total Material 4 Cost [(D_4 × E_4) + F_4]	865.31	$	(G_4)

LABOR COSTS

	amount	units	
Number in Repair Crew	3		(H)
Average Daily Wage per Person	120	$/day	(I)
Number in Traffic Control Crew	1		(J)
Average Daily Wage per Person	120	$/day	(K)

Supervisor Daily Wage	200	$/day	(L)

EQUIPMENT COSTS

Material Truck	20	$/day	(M)
Traffic Control Truck and Signs	150	$/day	(N)
Patch Preparation Equipment (e.g., concrete saw, jackhammer, milling machine, water blaster)	225	$/day	(O_1)
	60	$/day	(O_2)
Cleaning Equipment (e.g., sandblaster, air blaster)	350	$/day	(P_1)
	0	$/day	(P_2)
Mixing Equipment (e.g., mortar mixer, Jiffy mixer)	35	$/day	(Q_1)
	0	$/day	(Q_2)
Consolidation/Compaction Equipment (e.g., pencil vibrator, vibrating screed, vibratory roller)	20	$/day	(R)
Extra Equipment Truck	0	$/day	(S)
Miscellaneous Equipment (e.g., spray-injection machine, joint sealing equipment, etc.)	0	$/day	(T_1)
	0	$/day	(T_2)

SUMMARY COSTS

	amount	units	
Total Material Cost (G1 + G2 + G3 + G4 + ….)	4648.12	$	(U)
Total Daily Labor Cost [(H × I) + (J × K) + L)]	680	$/day	(V)
Total Equipment Cost			

[M + N + (O1 + O2 + …) + (P1 + P2 + …) + (Q1 + Q2 + …) + R + S + (T1 + T2 + ….)]	860	$/day	(W)
User Daily Costs	26.5	$/day	(X)
Average Daily Productivity	1	Marking line/ day	(Y)
Estimated Number of Days for Marking Layout Operation (A/Y)	4	days	(Z)
Total Marking Layout Operation Cost [U + {Z × (V+ W + X)}]	10,914.12	$	(AA)
Expected Mean Life for New Marking Lines[1] (Duration may vary)	80.1	months	(BB)
Time to Pavement Rehabilitation	120	months	(CC)
Effective Markings Cost over time [AA × (CC/BB)]	16,350.74	$	(DD)

[1] Until expected mean life values have been determined, agency experience should be applied.

Chapter 12. Conclusions and Future Research Needs

12.1 Project conclusions

The objective of the project is to develop a snow-proof marking system that could be implemented in field. Through a systematic set of experiments, a patch of viable mixes have been found and reached the desired performance, which can be listed as

1) Tests of ten different mixes of geopolymer mortar with steel fiber were conducted. From our testing we found that, the steel fiber helps to increase the overall stiffness and strength of the mixes; however it also depends upon molar ratio of alkaline activator. Among the ten mixes only mix 2 has reached to 3ksi in compression strength at 28 days.
2) Because only mix 2 reaches to 3 ksi in compression strength at 28 days, we decided to use the same molar ratio of alkaline activator from mix 2 and vary the percentage of steel fiber and curing condition. From this testing we found that we can achieve the desired strength i.e. 3 ksi by cured at elevated temperature and we have also found that if we use 1.5% of steel fiber we don't need to do elevated temperature curing.
3) Compressive strengths of the geopolymer concrete were measured using three different percentages of fibers as we did on mortar. Elevated temperature curing was also used for the comparison purpose. The result shows that the compressive strength of the geopolymer concrete increases with increase in fiber content and temperature of curing. Since we used elevated temperature curing just for the comparison purpose, it has been found that the ambient curing of the geopolymer concrete is enough to achieve the required amount of the strength.
4) We have calculated the resistivity of all the mixes used for strength measurement (given in Table 2). We found that addition of the steel fiber helps to increase conductivity and from the result we found we can also conclude that increase in curing temperature will reduce the conductivity of geopolymer mortar.
5) The resistivity measurement of concrete cylinders with similar three different percentages of fiber content and four different curing conditions was carried out. The result shows that the resistivity of geopolymer concrete cylinders is higher as compared to that of the mortar cubes. It has been also found that the resistivity increases with increase in curing temperature and decreases with increase in fiber content into the mix.
6) The freeze and thaw test was carried out for the geopolymer concrete beam specimens with four different percentages (0%, 0.5%, 1% and 1.5%) of steel fibers. It has been found that the relative dynamic modulus of elasticity reduces slightly more at the first 100 cycles and keeps almost constant thereafter. The modulus of elasticity was found to be reduced more in the case of without steel fiber content than the specimens with steel fibers. The mass loss percentage of the specimens at each 30 cycles was measured which shows that there is less than 0.3% of mass loss in the case of specimen without fiber at the end of 240 cycles. Within the comparison between the fiber percentages into the specimen, we can conclude that the mass loss percentage gets decreased with increase in steel fiber into the mix.

7) From pull-off adhesion tests of paint on the geopolymer concrete with different percentage of steel fibers and their comparisons with paint on ordinary Portland concrete with the same percentage of steel fibers, we can conclude that the bond strength between concrete and paint enhances with increment in percentage of fiber in the concrete. The overall bond strength of OPC concrete with epoxy based paint is slightly more as compared to that of the geopolymer based concrete. However, in the case of geopolymer concrete, the pull-off tests failed the specimens in concrete, which shows that the bond strength between the NDDOT permitted epoxy based paint and the new geopolymer concrete is adequate.
8) From maturity test of the cylindrical geopolymer concrete specimens, all four different percentages of fiber were included for the comparison purpose. It was found that the geopolymer concrete w/o steel fibers can achieve desired amount of compressive strength (3 ksi) in less than 6 hours. The maturity test of the geopolymer concrete beam specimen was conducted using the maturity meter to get the real time temperature change .vs. flexural strength. It was found that the flexural strength of the concrete increased with the increase of fiber percentage; while the time to reach the desired flexural strength was reduced with increase of fiber percentage. For the suggested mix, 350 psi of flexural strength was reached in between 7 to 14 days of curing.
9) Air content test of the fresh geopolymer concrete was conducted per ASTM 321. The air content of the fresh geopolymer concrete was found to be 0.8%.
10) Conductivity test of geopolymer concrete with man-made cracks has been carried out. Two different cracks were prepared, i.e. longitudinal and transverse cracks with $1/3^{rd}$ of the specimen depth. Different percentages of steel fiber and different curing condition were applied. The result shows that the conductivity of the specimen with longitudinal crack is more as compared to the transverse crack. It shows that the resistivity of specimen with longitudinal crack is 1.5 to 2 times more as compared to healthy specimen whereas the resistivity of specimen with transverse crack is 1.7 to 2.5 times more as compared to the healthy specimen.
11) The melting test shows that the time required to melt the heavy snow (with higher density) is higher and it requires more energy. As we have seen on conductivity test, the conductivity of the specimen increase with increase in fiber percentage into the specimen, which correspondingly reflects in the shortened time taken to melt the same amount of snow. The specimen without fiber took 55 minutes to melt only 0.5 inch of light snow whereas the specimen with 1.5% fiber content melted 1.5 inch of the snow in the same time. It has been also found that, when the surrounding temperature is low, the energy and time needed for melting snow also increase.
12) A cost-effectiveness analysis is also performed. The total cost for a 4-lines 100ft pavement marking using the new geoploymer concrete is around $16,350.74. Considering the accidents and traffic delays reduced, the suggested steel fiber reinforced geopolymer will be a viable solution for traffic marking revealing.

With systematic strength, electrical conductivity, and snow melting experiments, it has been concluded that the fly ash based geopolymer concrete has a very good strength to resist the compressive and flexural load, and shows excellent freeze and thaw resistance capacity. The fly

ash based mortar and concrete also show a very good electric conductivity properties, which could be applied as a pavement material with the self-snow melting capacity. The bond strength between epoxy based paint and GPC is a little weaker than the bond between OPC and the marking paint. But failure modes and bond strength values show that the bond between GPC and marking paints fulfills the pavement marking qualification requirements. And finally, the melting test shows that the fly ash concrete has capacity of melting snow in a very fast rate with reasonable amount of energy. Based on the research outcome, it is recommended to implement the research outcomes in field.

12.2 Future research needs

While research outcomes exceed our expectations, implementation in field will bring in additional variables and need more research work. The research team foresees the key issues lie in the following aspects:

(1) Effect of marking patching sizes on the long-term overall performance of pavements.
(2) Cost effectiveness of extending the conductive steel fiber reinforced geopolymer concrete to the whole pavement surface.
(3) Wear resistance of the suggested steel fiber reinforced geopolymer concrete under traffic.
(4) Effect of steel fiber reinforcement on traffic safety.

The research team anticipates these issues could be solved in the Phase II of this research and recommends NDDOT to continue supporting it.

References:

[1] Yehia, S., Tuan, C. Y., Ferdon, D., & Chen, B. (2016). Conductive concrete overlay for bridge deck deicing: Mixture proportioning, optimization, and properties. American Concrete Institute, 97(2), 172-181.

[2] Sun, M., Mu, X., Wang, X., Huo, Z., & Li, Z. (2008). Experimental studies on the indoor electrical floor heating system with carbon black mortar slabs. Energy and Buildings, 40(6), 1094-1100.

[3] Baldwin, K. (1998). Electrically conductive concrete: Properties and potential. Construction Canada, 98(1), 28-29.

[4] Feng, J.-h., Li, H., Ji, X.-y., Chang, C., & Koay, Y. (2009). Development of self-heating concrete using carbon nano-fiber paper. Proc. SPIE 7292, Sensors and Smart Structures Technologies for Civil, Mechanical, and Aerospace Systems 2009.

[5] Chung, D. (2002). Electrical conduction behavior of cement-matrix composites. Journal of Materials Engineering and Performance, 11(2), 194-204.

[6] Davidovits, J. (1994). Properties of geopolymer cements. First International Conference on Alkaline Cements and Concretes, (pp. 131-149). Kiev.

[7] Davidovits, J., & Davidovics, M. (1988). Geopolymer: Room-temperature ceramic matrix for composites. Ceramic Engineering and Science Proceedings, 9(7-8), 835-842.

[8] Palomo, A., & Lopez dela Fuente, J. I. (2003). Alkali-activated cementitious materials: Alternative matrices for the immobilisation of hazardous wastes:Part I. Stabilisation of boron. Cement and Concrete Research, 33(2), 281-288.

[9] Saravanan, G., Jeyasehar, C., & Kandasamy, S. (2013). Fly ash based geopolymer concrete - A state of the art review. Journal of Engineering Science & Technology Review, 25-32.

[10] Du, L., Lukefahr, E., & Naranjo, A. (2013). Texas Department of Transportation fly ash database and the development of chemical composition-based fly ash Alkali-Silica reaction durability index. Journal of Materials in Civil Engineering, 25(1), 70-77.

[11] Chindaprasirt, P., Silva, P. D., Sagoe-Crentsil, K. and Hanjitsuwan, S.. Effect of SiO2 and Al_2O_3 on the setting and hardening of highcalcium fly ash-based geopolymer systems, Journal of Materials Science, 2012, 47(12), pp 4876–4883

[12] Hanjitsuwan, S., Chindaprasirt, P. and Pimraksa, K. Electrical conductivity and dielectric property of fly ash geopolymer pastes. International Journal of Minerals, Metallurgy, and Materials, 2011, 18(1), pp 94–99

[13] McCarter, W.J., Starrs, G. and Chrisp, T.M.. Electrical conductivity, diffusion, and permeability of Portland cement-based mortars. Cement and Concrete Research, 2000, 30(9), pp 1395-1400

[14] Ramujee, K and Potharaju, M. Develeopment of mix design for low calcium based geopolymer concrete in low, medium and heigher grades-Indian scenario. Journal of Civil Engineering and Technology, 2013, 1(1), pp 15-25

[15] Mustafa Al Bakri, A.M., Kamarudin, H., Nizar, Khairul, Bnhussain, M., Zarina Y., and Rafiza, A.R. Correlation between Na2SiO3/NaOH ratio and fly ash/alkaline activator ratio to the strength of geopolymer. Advanced Materials Research, 2012, 341, pp 189-193

[16] ASTM Standard C109. (2016). Standard Test Method for Compressive Strength of Hydraulic Cement Mortars (Using 2-in. or [50-mm] Cube Specimens). West Conshohocken, PA: ASTM International. doi:10.1520/C0109_C0109M-16
[17] ASTM Standard C192. (2015). Standard Practice for Making and Curing Concrete Specimens in the Laboratory. West Conshohocken, PA: ASTM International. doi:10.1520/C0192_C0192M-15
[18] Davidovits, J. Structural characterization of geopolymeric materials with x-ray diffractometry and mass NMR spectroscopy. Geopolymer, 1988, 149-166.
[19] Davidovits, J. Chemistry of geopolymeric systems, terminology. Proceedings of the Second International Conference on Geopolymer '99, 1999, pp 9-39. Saubt-Quentin, France.
[20] Hardjito, D., Rangan, B.V. (2005). Development and properties of low calcium fly ash based geopolymer concrete. Research Report of Curtin University, Australia.
[21] Silva, P. and Sagoe-Crenstil, K. The effect of Al_2O_3 and SiO_2 on setting and hardening of Na_2O-Al_2O_3-SiO_2-H_2O Geopolymer Systems. Journal of Australia Ceramic Society, 2008. 44(1), pp 39-46
[22] Kim, K., Shim, J., Yang, S., A Study on the Control Method of Hydration Heat in Double-T Beam Concrete Bridge, Res. Rep. 98-67-50, Korea Highway, Korea, 1998.
[23] Akita, H., Fujiwara, T. and Ozaka, Y. “A practical procedure for the analysis of moisture transfer within concrete due to drying.” Mag. Concrete Res., 1997, 49(179), pp 129–137.
[24] Bakharev, T., Sanjayan, J.G., Cheng, Y.B. Effect of admixtures on properties of alkali-activated slag concrete Cement and Concrete Reserach, 2000, 30(9), pp 1367-1374.
[25] Cengiz, D. A., Cahit, B., Özlem, C., Okan, K. Influence of activator on the strength and drying shrinkage of alkali-activated slag mortar, Construction Building Materials, 2009, 23(1), pp 548-555.
[26] Fernando, P-T., João, C-G., Said, J. Alkali-activated binders: a review. Part 2. About materials and binders manufacture, Construction Building Materials, 2008. 22(7), pp 315-1322.
[27] Sun, P.J., Wu, H.C. Chemical and freeze–thaw resistance of fly ash-based inorganic mortars, Fuel,111, pp 740-745
[28] Palomo, A., Grutzeck, M.W., Blanco, M.T. Alkali-activated fly ashes: a cement for the future. Cement Concrete Research, 1999, 29(8), pp 1323-1329
[29] Li, Z., Ding, Z., Zhang, Y. Development of sustainable cementitious materials. K. Wang (Ed.), International Workshop on Sustainable Development and Concrete Technology, 2004, pp 55-76, Beijing, China.
[30] ASTM C1074-17 Standard Practice for Estimating Concrete Strength by the Maturity Method, ASTM International, West Conshohocken, PA, 2017, https://doi.org/10.1520/C1074-17
[31] ASTM D4541-17 Standard Test Method for Pull-Off Strength of Coatings Using Portable Adhesion Testers, ASTM International, West Conshohocken, PA, 2017, https://doi.org/10.1520/D4541-17

[32] ASTM D7234-12 Standard Test Method for Pull-Off Adhesion Strength of Coatings on Concrete Using Portable Pull-Off Adhesion Testers, ASTM International, West Conshohocken, PA, 2012, https://doi.org/10.1520/D7234-12
[33] Sadowski, Ł. and Hoła, J. New nondestructive way of identifying the values of pull-off adhesion between concrete layers in floors, Journal of Civil Engineering and Management, 2014, 20(4), pp 561-569, DOI: 10.3846/13923730.2014.897642
[34] Cleland, D. J., Adrian, E. L. "The pull-off test for concrete patch repairs." Proceedings of the Institution of Civil Engineers: Structures and Buildings. 1997, 122(4), pp 451-460
[35] Carino, N. J. "The maturity method: theory and application." Cement, concrete and aggregates, 1984, 6(2), pp 61-73.
[36] Guo, C. J. "Maturity of concrete: method for predicting early-stage strength." Materials Journal, 1989, 86(4), pp 341-353.
[37] ASTM C231/C231M-17a Standard Test Method for Air Content of Freshly Mixed Concrete by the Pressure Method, ASTM International, West Conshohocken, PA, 2017